Development of solid polymer electrolytes for applications in all solid state energy storage devices with high energy density and improved safety

Thesis submitted to
Cochin University of Science and Technology
in partial fulfillment of the requirements
for the award of the degree of
Doctor of Philosophy

By

Jinisha B

Department of Physics
Cochin University of Science and Technology
Cochin-682 022, Kerala, India

January 2019

Development of solid polymer electrolytes for applications in all solid state energy storage devices with high energy density and improved safety

Ph.D. thesis in the field of Materials Science

Author

Jinisha B
Division for Research in Advanced Materials
Department of Physics
Cochin University of Science and Technology
Cochin-682 022, Kerala, India
E-mail: jinishabhaskar@gmail.com

Supervising Guide

Dr. S. Jayalekshmi
Emeritus Professor
Division for Research in Advanced Materials
Department of Physics
Cochin University of Science and Technology
Cochin-682 022, Kerala, India
E-mail: jayalekshmi@cusat.ac.in

January 2019

Department of Physics
Cochin University of Science and Technology
Kochi - 682022, Kerala, India

Dr. S. Jayalekshmi
Emeritus Professor

Certificate

Certified that the thesis entitled **"Development of solid polymer electrolytes for applications in all solid state energy storage devices with high energy density and improved safety"** submitted by **Mrs. Jinisha B.** in partial fulfilment of the requirements for the award of the degree of Doctor of Philosophy in Physics to Cochin University of Science and Technology, is an authentic and bonafide record of the original research work carried out by her under my supervision at the Division for Research in Advanced Materials Laboratory of the Department of Physics. Further, the results embodied in this thesis, in full or part, have not been submitted previously for the award of any other degree. All the relevant corrections and modifications suggested by the audience during the pre-synopsis seminar and recommended by the Doctoral Committee have been incorporated in the thesis.

Cochin - 22
Date:

Dr. S. Jayalekshmi
(Supervising Guide)

Declaration

I hereby declare that the work presented in the thesis entitled "**Development of solid polymer electrolytes for applications in all solid state energy storage devices with high energy density and improved safety**" is based on the original research work done by me under the guidance of Dr. S. Jayalekshmi, Emeritus Professor, Department of Physics, Cochin University of Science and Technology, Cochin-22, India and no part of the thesis has been included in any other thesis submitted previously for the award of any degree.

Cochin - 22 **Jinisha B.**
January 2019

Acknowledgement

It is my pleasure and privilege to record my deep sense of gratitude to all who have contributed to the accomplishment of this thesis work.

I owe my deepest gratitude to my supervising teacher Dr. S Jayalekshmi, Emeritus Professor, and former Head of the Department of Physics, Cochin University of Science and Technology, Kochi, for giving me an opportunity to conduct the research work under her distinguished guidance. Without her unparalleled vision, constant inspiration and guidance, meticulous supervision and protective endearment, the timely completion of the research work would not have been possible. I thank her for being such a great role model.

I am extremely thankful to Prof. .Junaid Bushiri,, Head of the Department of Physics, Cochin University of Science and Technology and the former Heads of the Department for providing me all the necessary facilities for carrying out the research work and extending constant help and encouragement.

I express my deep gratitude to Dr. M.K Jayaraj, Professor, Department of Physics, CUSAT and the Doctoral committee member of the Ph.D. programme for his support,help and constant encouragement. I take this opportunity to thank Dr. M.R. Anantharaman, Emeritus Professor of the Department of Physics for his advice and valuable comments related to the work and equipping me with the basics of research during my M.Phil course. I express my deep sense of gratitude to all the former Professors of the Department of Physics, CUSAT for their timely help and the support extended during my research work.

I express my sincere thanks to the office staff, library staff, laboratory assistants and other non-teaching staff of the Department of Physics, CUSAT, for their constant help and support.

I greatly appreciate and acknowledge Dr.AnilKumar K M, Assistant Professor, Department of Physics, M.S.M College, Kayamkulam for his constant motivation and immense support and for having stood by me in almost every instance where I required help from a knowledgeable expert, especially while dealing with the instruments in the laboratory.

I express my deep sense of gratitude to Dr V S Pradeep, DST-INSPIRE Faculty, Department of Physics, CUSAT for offering valuable information and constant help throughout my research work and during the preparation of the PhD thesis by sparing considerable amount of his valuable time.

I express my sincere gratitude to Mr. Manoj M, Mr Abhilash A , Mr Joseph John, Dr Anand P.B, Dr. Sabira K , Dr. Saheeda P, Mrs Renjini R Mohan, Miss. Merin K Wilson, Mrs. Soumya Ravi and other alumni from the Division for Research in Advanced Materials (DREAM lab) laboratory of the Department of Physics, CUSAT for their help and constant support.

I express my sincere thanks to OED laboratory friends, Department of Physics, CUSAT for their help to acquire different experimental data. I take this opportunity to thank all the research scholars of the Department of Physics, CUSAT for their encouragement and support. I express my sincere gratitude to STIC, CUSAT for helping me with the analysis of different types of samples.

I am extremely grateful to my roommate Mrs.Vineetha P K, for her care and support during the entire research career at CUSAT. I express my thanks to all my seniors, juniors and hostel mates for their help and care.

Words are insufficient to express my gratitude to my parents for their affection, constant encouragement, endless support and their prayers for all the endeavours in my life and especially in the research career. I take this opportunity to thank my brothers and their wives for their love and care during the period of my research work. Also I am thankful to my father, mother and brother in laws, for their continuous support and prayers for the timely completion of the work. The patience, love, unconditional care and support of my husband and our daughter are the main backbones for the satisfactory completion of the research work.

Above all, I thank God Almighty for showering blessings upon me and giving positive energy and patience for the satisfactory completion of the research work.

Jinisha B

Preface

Development of sustainable and clean energy sources and the associated technologies is currently having high priority to reduce the impact of fossil fuels on our ecosystem. Renewable energy sources are highly dependent on the time of day and local weather conditions. Efficient methods for energy harvesting, conversion and storage need to be developed in order to efficiently utilize the intermittent, renewable energy sources. Batteries, electrochemical supercapacitors and fuel cells are all recognized as the most important electrochemical energy storage/conversion devices. These storage devices find widespread applications in consumer electronics ranging from mobile phones, laptops, digital cameras, emergency doors and hybrid vehicles.

There has been an ever increasing and urgent demand for environmental friendly high-power energy resources to meet the requirements of portable electronic devices and for the development of hybrid electric vehicles. Extensive research is being carried out for the development of next generation electrode and electrolyte materials with superior electrochemical energy storage properties. The main objective of the work presented in the thesis is the development of solid polymer electrolytes with appreciable ionic conductivity for designing all solid state Li ion and Na ion cells capable of giving safe and stable operation at room temperature and higher temperatures. Gel polymer electrolytes based on redox mediators, endowed with high ionic conductivity and excellent electrochemical performance characteristics are also expected to be developed for realizing solid state supercapacitors with high power density.

The term electrolyte in batteries refers to an ion- conducting solution comprising of a salt in a mixture of organic solvents. Stability of the electrolyte is an important factor determining the irreversible capacity loss by means of passive film formation due to electrolyte decomposition at the surfaces of the electrodes. The anticipated characteristics of good electrolyte materials encompass high ionic conductivity, excellent chemically stability, large window of electrochemical stability, non-toxic nature, low cost and environment friendliness. Conventionally used electrolytes in lithium ion cells are liquid electrolytes having quite high ionic conductivity in the range of 10^{-3} to 10^{-2} S cm^{-1} along with good surface contact area

for the electrodes. However, the issues related to the possibility of electrolyte leakage, narrow range of operation temperature and limited potential window range put limitations on the use of liquid electrolytes. The possible electrolyte leakage can lead to internal short circuiting problems, raising many safety concerns. The use of liquid electrolytes also makes it mandatory to have robust sealing for the whole device. These limitations of liquid electrolyte usage call for approaches towards identifying suitable materials to serve as solid electrolytes with the ultimate aim of realizing all solid state energy storage devices with improved safety and simplicity in the device architecture. Among the solid electrolytes, gel-type polymer electrolytes (GPEs) and solid polymer electrolytes (SPEs) are being extensively investigated to serve as solid electrolyte materials, owing to the meritorious characteristics they are endowed with. The thesis entitled **"Development of solid polymer electrolytes for applications in all solid state energy storage devices with high energy density and improved safety"** is a complete report of the experiments conducted on the lithium and sodium based cells and the supercapacitors in order to attain higher harmony between the energy density and the power density.

The thesis is divided into seven chapters. The first chapter gives a brief introduction to the present day energy scenario, the need for the development of renewable energy sources and the associated energy storage systems and evolves into emphasising the significance of solid state energy storage systems as the next generation storage systems for the efficient and safe storage of the energy generated from renewable power sources. The following chapters are dedicated to the studies on the development of three different types of solid polymer electrolyte films for applications in all solid state rechargeable batteries and a gel polymer electrolyte film for realizing solid state supercapacitors with high power density and good cycling stability. One of the chapters, in particular deals with the assembling of all solid state lithium ion half cells using eco- friendly cathode active materials and the developed solid polymer electrolyte film serving both as the separator and the electrolyte.

The details of the development of the solid polymer electrolyte (SPE) films based on the polymer blend of PEO and PVdF and treated with lithium nitrate as the Li source, using solution casting technique from the focal theme of the second

chapter. The SPE films are found to be transparent, flexible and freestanding and the crystalline nature of the films gets lowered with the increase in the amount of lithium nitrate added. These films are electrochemically characterized using cyclic voltammetry and electrochemical impedance spectroscopy techniques. The SPE films obtained are found to have quite impressive electrochemical properties, expected for good solid electrolytes.

The attempts carried out to develop SPE films with much higher Li ion conductivity close to that of the liquid electrolytes and having good electrochemical stability, are detailed in the third chapter. Here, the only difference from the synthesis route adopted in the previous case is that, instead of PVdF, PVP is used to make the polymer blend with the semi-crystalline and rigid polymer, PEO. The polymer PVP, owing to its amorphous nature is expected to improve the flexible nature of the PEO-PVP blend system, which in turn can facilitate better Li ion transport through the resulting SPE film. The PEO-PVP-$LiNO_3$ based SPE films are also obtained as free standing and flexible films. These films are subjected to detailed structural, thermal and electrochemical characterisations. However, there is a limit for the increase in the lithium nitrate concentration, beyond which, the concentration increase is found to affect the quality of the films formed. The most fascinating feature of these SPE films is the observation of room temperature Li ion conductivity around 1.13×10^{-3} S cm^{-1} in these films, which is quite close to that of liquid electrolytes. The most significant result of the whole research work is the identification of the PEO-PVP-$LiNO_3$ based SPE film with quite remarkable electrochemical features for applications as one of the most promising solid polymer electrolyte films.

The fourth chapter deals with the practical realization of solid state Li ion half cells using $LiFePO_4$ and $LiNiMnO_4$ as the cathode active materials, Li foil as anode and the PEO-PVP-$LiNO_3$ based SPE film serving both as the solid electrolyte and the separator. The cathode active materials are subjected to detailed structural and morphological characterization. The electrochemical performance of the solid state Li ion half cells is assessed in terms of specific capacity and cycling stability. This work is an initiative towards realizing all solid state Li ion cells and more investigations to understand the interfacial effects between the solid electrolyte and the electrodes are necessary to achieve better results.

The work presented in chapter five highlights the realization of the Na ion conducting solid polymer electrolyte (SPE) films, based on the polymer blend of PEO and the plasticizers , ethylene carbonate (EC) and propylene carbonate (PC) and treated with $NaNO_3$ salt and modified with the addition of the nano-filler material, Al_2O_3. The SPE films obtained using the simple solution casting technique are found to be free standing, flexible and transparent. The enhanced amorphous nature of the SPE films facilitates easier ion transport which in turn leads to high Na ion conductivity. The most striking result of the present work is concerned with the superb effect of the Al_2O_3 filler, in enhancing the ionic conductivity of the SPE films. These results highlight the application prospects of the SPE films in the design of all solid state Na ion cells, capable of stable operation at temperatures well above room temperature.

The studies on the solid-state supercapacitor, developed with activated carbon as electrodes and the redox mediated, polyvinyl alcohol (PVA)--potassium hydroxide(KOH)--hydroquinone (HQ) based gel polymer electrolyte (GPE) as the separator and the electrolyte form the central theme of chapter six. Presence of the redox mediator 'HQ' in the GPE film is found to improve the electrochemical performance of the assembled supercapacitor. From the electrochemical analysis, it can be concluded that the presence of the redox mediator HQ in the GPE can significantly influence the electrochemical performance of the solid-state supercapacitor by improving the ionic conductivity and the pseudo-capacitance behaviour. Redox mediators offer excellent prospects for improving the performance of energy storage devices and the GPE films of the present study can be used for the development of solid supercapacitors with high capacitance, high power density, excellent cycle life and good safety standards.

The salient features of the work presented in the thesis are summarized in the concluding chapter. The important results are highlighted and the inferences drawn are explained with logical reasoning. The prospects for future investigations, based on the present results, are also emphasized in this chapter.

Contents

Chapter **1 Introduction ----------1**

1.1 Introduction ---------- 1

1.2 Electrochemical cells and batteries ---------- 6

1.2.1 Electrochemical operation of a cell ------- 7

1.3 Lithium ion battery----------10

1.3.1 Working of Lithium ion battery ----------11

14 Sodium ion battery----------13

1.5 Supercapacitors----------14

1.5.1 Electric double-layer capacitors (EDLCs) ----------15

1.5.2 Pseudocapacitor----------16

1.5.3 Hybrid capacitor ----------17

1.6 Electrolytes----------18

1.6.1 Liquid electrolytes----------19

1.6.2 Gel polymer electrolytes (GPEs)-------21

1.6.3 Solid polymer electrolytes (SPEs) -----21

1.6.4 Composite polymer electrolytes--------23

1.7 Definitions ----------24

1.8 Objectives of the present work----------25

1.9 References----------27

Chapter **2 Poly (ethylene oxide) and poly (vinylidene fluoride) based solid polymer electrolytes for applications in Li ion cells---------- 35**

2.1 Introduction ----------35

2.2 Experimental details ----------38

2.2.1 Materials ----------38

2.2.2 Growth of solid polymer electrolyte films ----------38
2.2.3 Characterization studies ----------39
2.2.3.1 Structural, morphological and thermal characterization ---------- 39
2.2.3.2 Electrochemical characterization---40
2.3 Results and Discussion ----------41
2.3.1 XRD Analysis ----------41
2.3.2 FTIR spectroscopic analysis ----------44
2.3.3 FE-SEM Analysis ----------46
2.3.4 Thermal characterization ----------48
2.3.4.1 Thermo gravimetric analysis ----- 48
2.3.5 A C Conductivity studies ----------49
2.3.5.1 Impedance analysis---------- 49
2.3.5.2 Thermal activation energy measurement---------- 51
2.3.6 Ion transport number measurement ----53
2.3.7 Electrochemical stability ----------54
2.4 Conclusions ----------55
2.5 References----------56

Chapter **3 Development of solid polymer electrolyte films with enhanced ionic conductivity, based on lithium enriched poly (ethylene oxide) (PEO)/ poly (vinyl pyrrolidone) (PVP) blend polymer ------ 63**

3.1 Introduction ----------64
3.2 Experimental----------66
3.2.1 Materials ----------66
3.2.2 Synthesis of PEO/PVP/$LiNO_3$ based solid polymer electrolyte ----------67

3.2.3 Characterization ----------68
3.2.3.1 X-Ray diffraction, FTIR spectroscopy, FE-SEM and thermal analysis---------- 68
3.2.3.2 Electrochemical analysis---------- 70
3.3 Results and discussion----------71
3.3.1 XRD analysis----------71
3.3.2 FTIR spectroscopy studies ----------73
3.3.3 FE-SEM analysis ----------76
3.3.4 Thermal characterization ----------77
3.3.4.1 Thermo-gravimetric analysis----- 77
3.3.4.2 Differential scanning calorimetric studies---------- 79
3.3.5 A C Conductivity studies----------81
3.3.5.1 Impedance analysis---------- 81
3.3.5.2 Temperature dependence of ionic conductivity ---------- 83
3.3.5.3 Thermal activation energy measurement---------- 84
3.3.6 Ion transport number and transference number measurement ----------86
3.3.7 Electrochemical stability studies -------88
3.4 Conclusions ----------90
3.5 References----------91

Chapter **4 Realizing all solid state Li ion cells using solid polymer electrolyte films----------101**

4.1 Introduction ---------- 101
4.2 Experimental details ---------- 104
4.2.1 Materials and methods ---------- 104
4.2.2 Synthesis of $LiFePO_4$ cathode material---------- 104

4.2.3 Synthesis of $LiNi_{0.5}Mn_{1.5}O_4$ cathode material ---------- 105
4.2.4 Electrode making ---------- 106
4.2.5 Characterization ---------- 107
4.3 Results and Discussion ---------- 108
4.3.1 XRD Analysis ---------- 108
4.3.2 The FE-SEM analysis ---------- 109
4.3.3 Cyclic voltammetry studies ---------- 111
4.3.4 Galvanostatic charge discharge studies ---------- 113
4.4 Conclusions ---------- 116
4.5 References ---------- 116

Chapter **5 Poly (ethylene oxide) based, solid polymer electrolyte films for applications in sodium ion cells ---------- 123**

5.1 Introduction ---------- 123
5.2 Experimental ---------- 127
5.2.1 Materials ---------- 127
5.2.2 Synthesis details ---------- 127
5.2.3 Characterization ---------- 128
5.3 Results and Discussions ---------- 129
5.3.1 XRD Analysis ---------- 129
5.3.2 FTIR spectroscopy studies ---------- 131
5.3.3 FE-SEM analysis ---------- 132
5.3.4 Thermal characterization ---------- 134
5.3.4.1 Thermo gravimetric analysis - 134
5.3.5 A C Conductivity studies ---------- 135
5.3.5.1 Impedance analysis ---------- 135

5.3.5.2 Thermal activation energy measurement ---------- 138
5.3.6 Transport number measurement ------ 139
5.3.7 Electrochemical Stability ---------- 141
5.4 Conclusions ---------- 141
5.5 References ---------- 142

Chapter **6 Solid-state supercapacitor with impressive performance characteristics, assembled using redox mediated gel polymer electrolyte ---------- 151**

6.1 Introduction ---------- 152
6.2 Experimental details ---------- 157
6.2.1 Materials ---------- 157
6.2.2 Synthesis of the gel polymer electrolyte ---------- 157
6.2.3 Electrode making ---------- 158
6.2.4 Supercapacitor assembly ---------- 158
6.2.5 Characterization ---------- 159
6.2.5.1 Structural characterization ------ 159
6.2.5.2 Electrochemical Analysis ------- 159
6.3 Results and Discussions ---------- 160
6.3.1 XRD Analysis ---------- 160
6.3.2 FTIR spectroscopy studies ---------- 161
6.3.3 Thermal characterization ---------- 163
6.3.3.1 Thermo gravimetric analysis ----- 163
6.3.4 Ionic conductivity studies ---------- 164
6.3.5 Cyclic voltammetry studies ---------- 165
6.3.6 Cyclic voltammetry of assembled Supercapacitors ---------- 166

6.3.7 Galvanostatic charge/discharge (GCD) studies of the assembled supercapacitor ---------- 168

6.3.8 Electrode specific capacitance-current density plot and Ragone plot ---------- 170

6.3.9 Cycle-life testing ---------- 171

6.3.10 Self discharge ---------- 172

6.4 Conclusions ---------- **174**

6.5 References ---------- 175

Chapter **7 Summary, conclusions and scope for further studies ----------183**

7.1 Summary and conclusions ---------- 183

7.2 Future prospects ---------- 188

Journal Publications

[1] **Jinisha B**, Anilkumar K M, Manoj M, Pradeep V. S, S. Jayalekshmi, Development of a novel type of solid polymer electrolyte for solid state lithium battery applications based on lithium enriched poly (ethylene oxide) (PEO)/ poly (vinyl pyrrolidone) (PVP) blend polymer, Electrochimica Acta, 235 (2017) 210–222.

[2] **B. Jinisha**, K. M. Anilkumar, M. Manoj, A. Abhilash, V. S. Pradeep, S. Jayalekshmi, Poly (ethylene oxide) (PEO)-based, sodium ion-conducting, solid polymer electrolyte films, dispersed with Al2O3 filler, for applications in sodium ion cells, Ionics, October 2017, doi.org/10.1007/s11581-017-2332-2.

[3] K.M. Anilkumar, **B. Jinisha**, M. Manoj, S. Jayalekshmi, Poly(ethylene oxide) (PEO) – Poly(vinyl pyrrolidone) (PVP) blend polymer based solid electrolyte membranes for developing solid state magnesium ion cells, European Polymer Journal, 89 (2017) 249–262.

[4] K.M. Anilkumar, **B. Jinisha**, M. Manoj, Pradeep V. S, S. Jayalekshmi, Layered sulfur/PEDOT:PSS nano composite electrodes for lithium sulfur cell applications, Applied Surface Science 442 (2018) 556–564.

[5] Anilkumar K M, Manoj M, **Jinisha B**, Pradeep V. S, S. Jayalekshmi Mn3O4/reduced graphene oxide nanocomposite electrodes with tailored morphology for high power supercapacitor applications, Electrochimica Acta 236 (2017) 424–433.

[6] M. Manoj, K.M. Anilkumar, **B. Jinisha**, S. Jayalekshmi Polyaniline–Graphene Oxide based ordered nanocomposite electrodes for high-performance supercapacitor applications, June 2017, DOI 10.1007/s10854-017-7292-9.

[7] C. Muhamed Ashraf, K. M. Anilkumar, **B. Jinisha**, M. Manoj, V. S. Pradeep, S. Jayalekshmi, AcidWashed, Steam Activated, Coconut Shell Derived Carbon for High Power Supercapacitor Applications, Journal of The Electrochemical Society, 165 (5) A900-A909 (2018).

[8] Manoj M , Jasna M , Anilkumar K M , Abhilash A, **Jinisha B** , Pradeep V S , S Jayalekshmi, Sulfur-polyaniline coated mesoporous carbon composite in combination with carbon nanotubes interlayer as a superior cathode assembly for high capacity lithium-sulfur cells, Applied Surface Science 458 (2018) 751–761.

[9] M. Manoj, C. Muhamed Ashraf, M. Jasna, K.M. Anilkumar, **B. Jinisha**, V.S. Pradeep, S. Jayalekshmi, Biomass-derived, activated carbon-sulfur composite cathode with a bifunctional interlayer of functionalized carbon nanotubes for lithium-sulfur cells, Journal of Colloid and Interface Science 535 (2019) 287–299.

Conference Proceedings

[1] **Jinisha B**, Anil Kumar K M, Manoj M , S Jayalekshmi, "Lithium enriched solid polymer blend electrolytes based on poly (vinyl pyrrolidone) for energy storage application", Proceedings of National Conference on Carbon Materials (NCCM) 2015,IIC, New Delhi, India, November 26 - 28, 2015.

[2] **Jinisha B**, Anil Kumar K M, Manoj M , S Jayalekshmi, "Lithium enriched solid polymer blend electrolytes based on poly (vinyl pyrrolidone) using different lithium salts for energy storage applications", Proceedings of the International Conference on Materials for the Millennium (MATCON 2016), Dept. of Applied Chemistry, Cochin University of Science and Technology, Cochin 22, Kerala, January 14-16, 2016.

[3] **Jinisha B**, Anilkumar K M, S Jayalekshmi, "Studies on a prospective polymer blend electrolyte material for developing pollution free solid state Li-ion cells" Proceedings of 28th The Kerala Science Congress, Calicut University, Malappuram, 28-30 January, 2016.

[4] **Jinisha B**, Anil Kumar K M, Manoj M , S Jayalekshmi, Polyethylene oxide (PEO) / polyvinyl alcohol (PVA) complexed with lithium perchlorate (LiClO4) as a prospective material for making solid polymer electrolyte films, International Conference on Smart Engineering Materials ICSEM-2016, RV college of Engineering, Bangalore.

[5] **Jinisha B**, Anil Kumar K M, Manoj M, S Jayalekshmi, On the prospects of developing high voltage lithium ion cells using solid polymer electrolyte films, International Conference on Advanced Materials (SCICON-2016) 19-21 December, Amritha University, Coimbatore.

[6] **Jinisha B**, V.S. Pradeep, Anilkumar K M, Manoj M, S. JayalekshmiFe2O3/Graphene oxide based anode materials with solid polymer electrolytes for Li-ion storage applications, International Conference on Advances in Functional Materials(IC-AFM) January 6-8, 2017, Anna University, Chennai.

[7] **Jinisha B**, AnilKumar K M, Manoj M, Abhilash A, Pradeep V S, Jayalekshmi S, Poly (ethylene oxide) (PEO) based, novel sodium ion conducting, solid polymer electrolytes dispersed with Al2O3 nanoparticles for sodium ion battery applications, 1st World Conference on Solid Electrolytes for Advanced Applications: Garnets and Competitors, ("WCSEAA-1"), September 6-7, 2017.Pondicherry University, Pondicherry.

[8] Anilkumar K M, **Jinisha B**, Manoj M, S Jayalekshmi, "Will Mg-ion cells serve as substitute for Li-ion cells ?" Proceedings of IC CAST, 2015, BHU-Varanasi, August 7-9.

[9] Anilkumar K M, **Jinisha B**, Manoj M , S Jayalekshmi, "MWNT/ GO/ Grahene- Nickel doped Mn3O4 composite electrode material for supercapacitor application", Proceedings of National Conference on Carbon Materials (NCCM) 2015,IIC, New Delhi, India, November 26 - 28, 2015.

[10] Anil Kumar K M, **Jinisha B**, Manoj M , S Jayalekshmi, "Flexible Solid Electrolyte Sheets for Lithium ion cells", International conference on energy harvesting, storage and conversion (IC-EEE) 2015, Cochin University of Science and Technology, Cochin 22, Kerala. February 5-7, 2015.

[11] Anilkumar K M, **Jinisha B**, S Jayalekshmi, "On the development of new polymer blend electrolyte for realizing eco friendly all solid state Mg-ion cells " , Proceedings of 28th The Kerala Science Congress, Calicut University Campus, Malappuram, 28-30 January, 2016.

[12] Abhilash A, **Jinisha B**, Pradeep V S, S Jayalekshmi, Influence of SiO2 Nano filler on ionic conductivity and mechanical properties of PEO: PMMA: PEG: LiClO4 based solid polymer electrolyte films, International Conference On Crystal Ball Vision On Science & Engineering For Societal Upliftment, August 7-8, 2017, CSIR-NIO, Goa, India.

[13] Anilkumar K M, Manoj M, **Jinisha B** , Pradeep V S , S Jayalekshmi, Mn3O4 / Reduced Graphene Oxide Composite Anode material for high energy density lithium ion battery applications, International Conference On Crystal Ball Vision On Science & Engineering For Societal Upliftment, CSIR-NIO, Goa, India.

[14] Manoj M, Anilkumar K M, **Jinisha B**, S Jayalekshmi, "Polyaniline graphene oxide composite electrode materials for supercapacitor applications," Proceedings of National Conference On Carbon Materials (NCCM) 2015,IIC, New Delhi, India, November 26 - 28, 2015.

[15] Manoj M, Anilkumar K M, **Jinisha B**, S Jayalekshmi, "Polyaniline -Zinc oxide composite as a prospective electrode material for developing ecofriendly supercapacitors", Proceedings of 28th The Kerala Science Congress, Calicut University Campus, Malappuram, 28-30 January, 2016.

Chapter **1**

Introduction

The work presented in the thesis is focused on the development of solid polymer electrolytes for rechargeable energy storage devices such as batteries and supercapacitors. Recent developments in the field of energy storage devices and their impact on the betterment of existing appliances are addressed in detail. Current investigations cover the relevance of different materials for electrode and electrolyte applications. The introduction chapter gives an overview of existing developments in energy harvesting and storage systems. The motivation and objectives of the presented work serve as the main attractions of this chapter.

1.1 Introduction

Nowadays, the aggravating energy and environmental issues related to the use of fossil fuels, environmental pollution and global warming are ringing alarm bells, even to the survival of human society. It is high time to resort to renewable energy sources with the associated requirements of efficient energy storage and conversion materials and devices. Conventional energy production depends heavily on fossil fuels, such as coal, crude oil, and natural gas as primary energy source to power most of the electronic appliances. However, energy production from fossil fuels is associated with toxic emissions and this has a devastating impact on human health and the natural environment. The challenges related to the generation of pollution free renewable energy

and its storage can be addressed in many ways. Energy generated from sustainable sources, such as the sun and the wind can be stored by converting them to appropriate forms like electricity or fuel [1]. Due to the abundant natural fuel reserves of sun and wind, energy can be harvested using novel power conversion devices and many promising approaches are already in practice for solar and wind energy harvesting and storage. Energy available from sources like sunlight and wind faces limitations due to its interim availability as sun does not shine during night and wind doesn't blow on demand. For an efficient use of sustainable energy sources, techniques based on fuel cells, solar cells and water splitting are of most concern [2-4] and energy storage systems such as batteries play a key role to have an efficient back up of the harvested energy. Considering the sporadic nature of our renewable energy sources, it is important to develop environmentally benign, cost effective, and efficient energy storage systems to ensure that the generated energy is properly stored and made available upon demand.

Modern civilization is becoming increasingly dependent on portable power sources for continuous internet access and for working with people across the world [5]. The developments in portable energy storage technologies are facing limitations to meet the needs of rapid advancements in electronic devices [6]. Power generation using fossil fuels is causing damage to the environment due to the emission of large amounts of CO_2 [7,8]. In addition, natural reserves of fossil fuels are limited and not sustainable regardless of governmental policies or the fluctuation in price and supply. Concept of generating clean energy mainly includes three steps: production and conversion of energy from

sustainable sources such as sun, wind, mechanical vibration, and waste heat, followed by electrochemical energy storage in batteries, hydrogen, and biofuels. Efficient management of stored energy is important and this can be achieved by developing smart buildings and use of efficient lighting systems as presented in figure 1 [9-10]

Figure 1: The energy utilization chain. Efficient harvest, storage, and management are the three essential segments to energy consumption in modern society [5,11].

In major energy storage devices, such as fuel cells, batteries, and electrochemical capacitors, the energy is stored in the form of chemical potential and can be converted in to electrical energy when connected to a load [12-13]. Batteries can be classified in to primary and secondary batteries. Primary batteries can only be used once, whereas secondary storage batteries can be repeatedly charged and discharged, making them the most popular and efficient storage systems. Rechargeable batteries

are widely used in portable electronic devices such as laptop computers and mobile phones as efficient, portable power sources. To meet the future demand, methods of making cost effective, energy efficient and light-weight portable batteries need more attention.

In the evaluation of the performance of electrochemical energy storage devices, the energy density and power density are the two most important parameters, besides the charge-discharge cycling stability. The relationship between these two important parameters can be expressed by the Ragone plot [12, 14] as shown in figure 2.

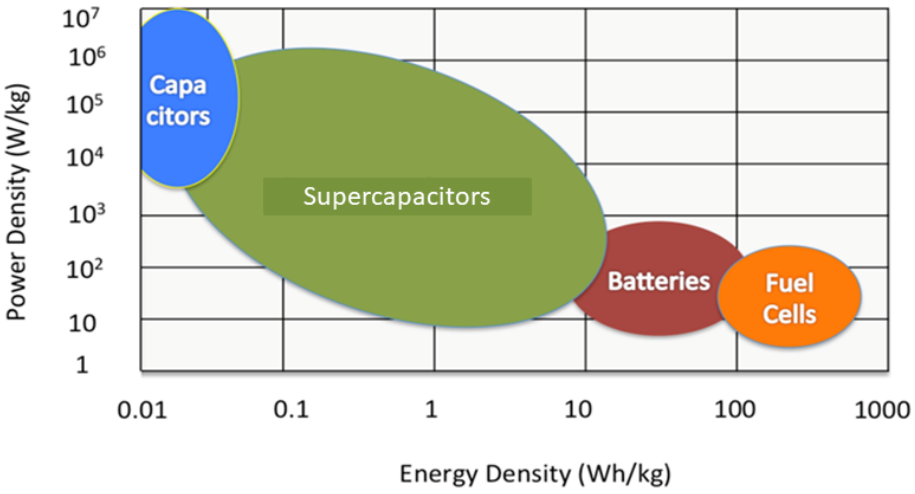

Figure 2: Ragone plot of energy density versus power density for various energy storage devices

Electrochemical energy storage systems mainly consist of batteries and supercapacitors. In batteries, electrical energy is stored and released by conversion of chemical energy via redox reactions at the anode and cathode [12] and in supercapacitors, exchange of electrical energy (charge–discharge cycling) is mainly via electrostatic, capacitive

interactions. Batteries constitute the most promising type of devices for energy storage purposes owing to their high energy density and cycling stability. Rechargeable batteries have the advantage of higher energy density due to discharging at a steady, flat rate until being almost exhausted, at which point energy drop-off increases the pace as shown in figure 3. On the other hand, high power density devices are mainly constituted by supercapacitors, capable of storing and releasing energy at much faster rates.

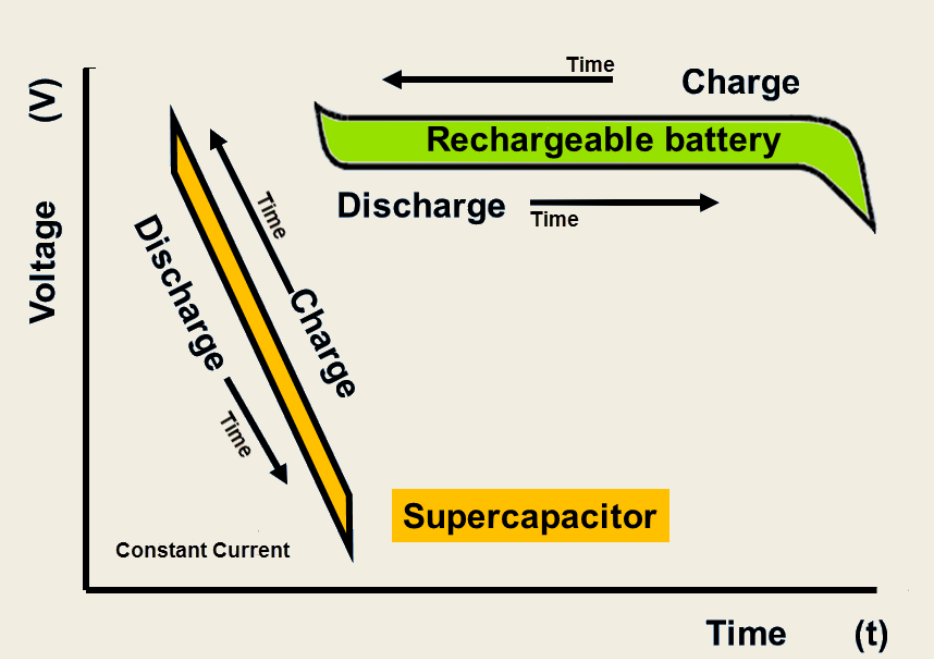

Figure 3: Supercapacitors can be charged and discharged rapidly. Batteries get discharged at a steady, flat rate, until almost exhausted, at which point energy drop-off increases pace.

1.2 Electrochemical cells and batteries

A cell is the basic electrochemical unit providing the source of electrical energy by direct conversion of chemical energy. Main components of a cell consist of an assembly of electrodes, separators and electrolyte. A battery consists of one or more of these electrochemical cells connected in series or parallel, or both, depending on the desired output voltage and capacity [12]. Electrodes are mainly classified in to anodes and cathodes. Anode (negative electrode) is oxidized during the electrochemical reaction by releasing electrons to the external circuit and the cathode (positive electrode) accepts electrons from the external circuit and is reduced during the electrochemical reaction. The electrolyte (the ionic conductor) provides the medium for transfer of charge, as ions, inside the cell between the anode and the cathode. Role of separator is to avoid the internal contact between cathode and anode to avoid a short circuit. An ideal separator should be electrically insulating and ionically conducting.

Electrochemical cells and batteries are recognized as primary (nonrechargeable) [15] or secondary (rechargeable) [16], depending on their capability of being electrically recharged to be used for multiple times. Primary batteries are not capable of being effectively recharged electrically and, hence, are discarded after single use. Primary cells in which the electrolyte is contained by an absorbent or separator material (there is no free or liquid electrolyte) are also known as ‘‘dry cells.’’ Primary batteries are usually inexpensive, lightweight energy sources

finding applications in devices such as photographic equipment, toys and memory backup. Secondary batteries can be used for multiple times owing to the fact that, they can be effectively recharged after every use to their original condition by passing current through them in the opposite direction to that of the discharge current. They belong to most widely used storage devices for electric energy and are known also as ‘‘storage batteries’’ or ‘‘accumulators’’. Their applications range from portable electronic devices to automotive and aircraft systems, hybrid electric vehicles and stationary energy storage (SES) systems for electric utility load levelling.

1.2.1 Electrochemical operation of a cell

During discharge of the cell, when the cell is connected to an external load, electrons flow from the anode, which is oxidized, through the external load to the cathode, where the electrons are accepted and the cathode material is reduced. Completion of electric circuit is only through the electrolyte by the flow of anions (negative ions) and cations (positive ions) to the anode and cathode, respectively which is depicted in figure 4 [17]. Assuming a metal as the anode material and a cathode material such as chlorine (Cl_2), the discharge reaction can be written as,

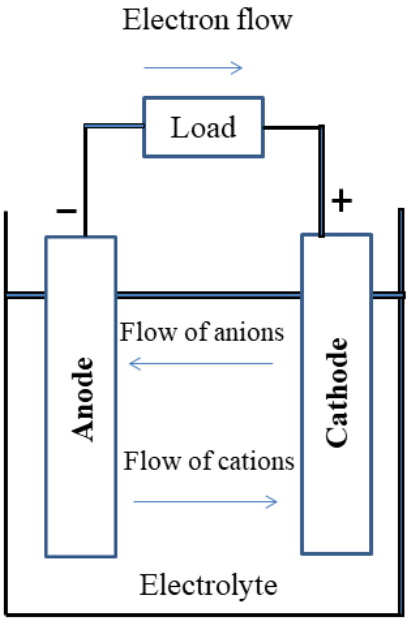

Figure 4: Electrochemical operation of a cell (discharge).

Negative electrode: anodic reaction (oxidation, loss of electrons)

$$Zn \rightarrow Zn^{2+} + 2e$$

Positive electrode: cathodic reaction (reduction, gain of electrons)

$$Cl_2 + 2e \rightarrow 2Cl^-$$

Overall reaction (discharge):

$$Zn + Cl_2 \rightarrow Zn^{2+} + 2Cl^-(ZnCl_2)$$

During the recharge of a rechargeable or storage cell, the current flow is reversed and oxidation takes place at the positive electrode and reduction at the negative electrode, as shown in figure 5. As the anode is, by definition, the electrode at which oxidation occurs and the cathode the one where reduction takes place, the positive electrode is now the

anode and the negative electrode, the cathode. In the example of the Zn/Cl_2 cell, the reaction on charge can be written as follows:

Negative electrode: cathodic reaction (reduction, gain of electrons)

$$Zn^{2+} + 2e \rightarrow Zn$$

Positive electrode: anodic reaction (oxidation, loss of electrons)

$$2Cl^- \rightarrow Cl_2 + 2e$$

Overall reaction (charge):

$$Zn^{2+} + 2Cl^- \rightarrow Zn + Cl_2$$

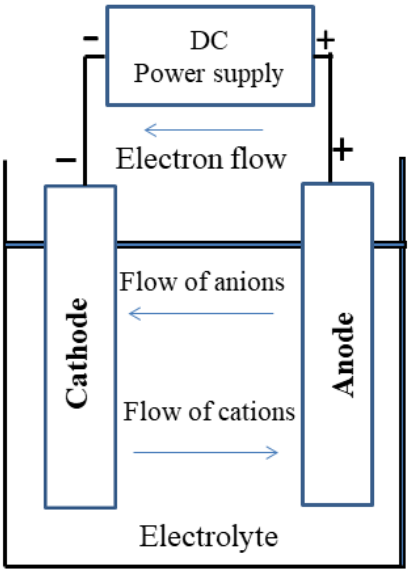

Figure 5: Electrochemical operation of a cell (charge).

The development of advanced materials for the next-generation rechargeable ion batteries is critical for understanding of material behaviour under complex electrochemical environment [18]. Nowadays,

considerable attention has been paid to battery technology for overcoming global energy and environmental concerns. Because of the safety problems, the use of inflammable organic solutions as electrolytes prevents the realization of large-scale batteries. An attractive alternative approach to focus on overcoming these safety issues is the development of all solid-state lithium ion cells. In many studies, considerable efforts have been devoted to develop solid polymer electrolytes with high lithium ion conductivity to overcome these safety problems [19]. In addition to lithium ion cells, attempts are being carried out to develop all solid state sodium ion cells because of the abundant nature of sodium on the earth's crust. Much attention has also been focused on the development of solid state supercapacitors since they have the ability to meet the requirements of end users in many applications especially where one needs high power density and desirable energy density [20].

1.3 Lithium ion cells

Lithium ion cells are currently the most widely used power sources in portable electronic applications owing to the high storage capacity, high energy density and excellent cycling stability, they offer. The cells with non-aqueous electrolytes, lithiated carbon anodes and $LiCoO_2$ cathodes are first commercialised by Sony in 1991 [21]. They have outstanding properties in comparison with conventional secondary batteries such as nickel / cadmium, nickel / metal hydride and lead-acid batteries. Main advantages of Li ion cells are,

1) High operating voltage,

2) High energy density (both gravimetric and volumetric),

3) Low self-discharge rate (less than 10% per month),

4) Absence of memory effect,

5) Operation over a wide temperature range.

Attempts have been carried out incessantly to improve further the performance of Li ion cells, which boost them into the most suitable power sources for portable devices like cellular phones and notebook computers. Pictures of basic battery types are shown in figure 6.

Figure 6: Pictures of basic battery types

1.3.1 Working of lithium ion cells

The lithium ion cell consists of two electrodes, the anode, of an insertion compound like graphite and the cathode of a lithium metal oxide and, an electrolyte [22], as shown in figure 7. There is also a separator, which prevents physical contact between the anode and the cathode.

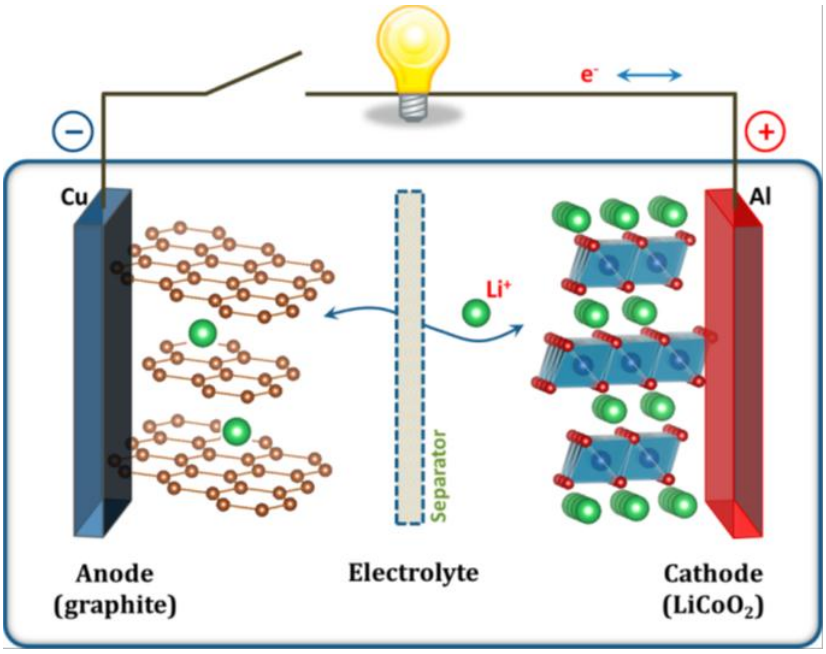

Figure 7: Schematic illustration of the first Li ion cell ($LiCoO_2/Li^+$ electrolyte/graphite) [23].

During charging/discharging of the cell, electrodes allow lithium ions to move in and out of their structures with a process called insertion (intercalation) or extraction (deintercalation), respectively. During discharge, the lithium ions move from the anode to the cathode through the electrolyte while the electrons flow through the external circuit in the same direction. When the cell is being charged, the reverse process occurs with the lithium ions and electrons moving back into the anode in a net higher energy state. The electrodes are separated by a microporous separator film which is made up of polyethylene or polypropylene and soaked with the electrolyte [24]. Electrolytes provide a conductive medium for lithium ions to move between the electrodes. The capacity, specific energy, voltage and energy density are governed by the

properties of bulk electrode materials. The cycle life is mostly dependent on the quality and stability of the diverse interfaces present.

1.4 Sodium ion cells

The limited availability and increasing cost of lithium with worldwide commercialization are posing challenges for the widespread use of Li based electrochemical cells. It is a difficult task to identify new approaches as replacements for the well-established Li-ion technology.

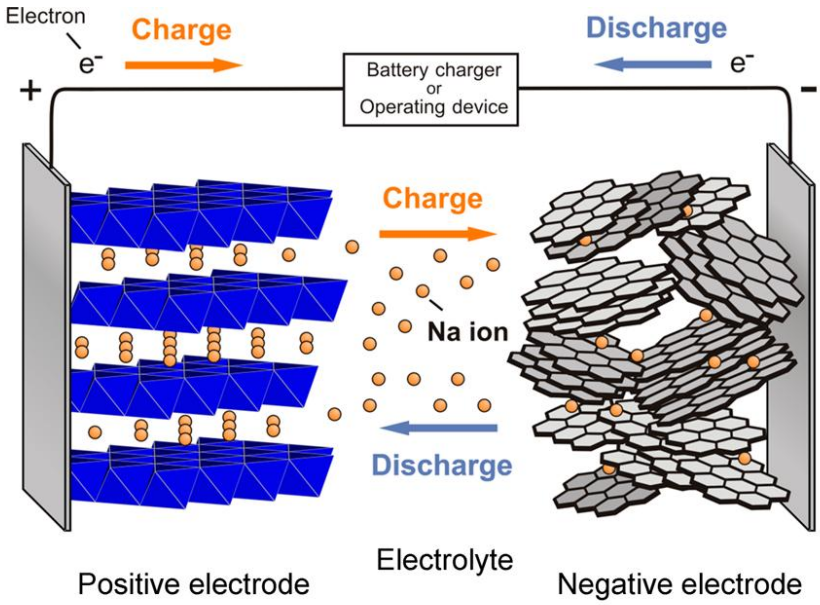

Figure 8: Schematic illustration of Na-ion cell

Currently, the possibilities of developing sodium as a supplement to lithium for future energy storage applications are being pursued, considering the high electrochemical reduction potential E^0 (Na^+/Na= -2.71V), [25,26] of sodium, the possibility of intercalation in both the cathode and anode materials along with its earth abundance, low cost and

non-toxic nature. In contrast to lithium, sodium resources are unlimited everywhere, and sodium is one of the most abundant elements in the earth's crust. Due to the material abundance and standard electrode potential properties, sodium is an appropriate alternative to lithium [27]. Additionally, sodium is the second-lightest and smallest alkali metal next to lithium and sodium ion cells are considered as potential alternatives to lithium ion cells. Working Li-ion cells and sodium ion cells shares the same principles for energy storage applications. Schematic illustration of Na-ion cells is given in figure 8. Electrochemical intercalation chemistry similar to that of lithium makes this element strategic in the innovative research of energy storage systems.

1.5 Supercapacitors

Compared to batteries, supercapacitors are devices capable of managing high power rates [28]. They have attracted considerable attention because of their long cycle life and high power density [14, 29]. They are potential candidates to meet the growing power demands of energy storage systems due to the high power capability and relatively large energy density compared to conventional capacitors. They are widely used in industrial power and energy management systems, consumer electronics and memory back-up systems [30].

Depending on the basis of the energy storage mechanism or cell configuration, supercapacitors can be classified into electric double-layer capacitors (EDLCs), pseudo-capacitors, and hybrid capacitors. All these types of supercapacitors can function simultaneously depending on the nature of the electrode materials used for their making.

1.5.1 Electric double-layer capacitors (EDLCs)

In EDLCs, the capacitance is generated via a non-faradaic process due to the formation of an electrochemical double layer at the electrode-electrolyte interface [31]. Electrodes for EDLCs are usually based on highly porous carbon materials [32,33,34] like activated carbons which serve as ideal materials for the rapid storing and release of energy [35]. Wide availability, low cost, good electrical conductivity, and high surface area are the main advantages of porous carbon materials.

During charging of a supercapacitor, the electrons are forced to go through the external circuit from the positive electrode to the negative electrode. The cations within the electrolyte concentrate in the negative electrode and anions in the positive electrode forming an electric double layer that compensates the external charge unbalance. During discharging, electrons travel through the external circuit from the negative electrode to the positive electrode, and both types of ions in the pores become mixed again until the cell is discharged [28].The process is schematically depicted in figure 9.

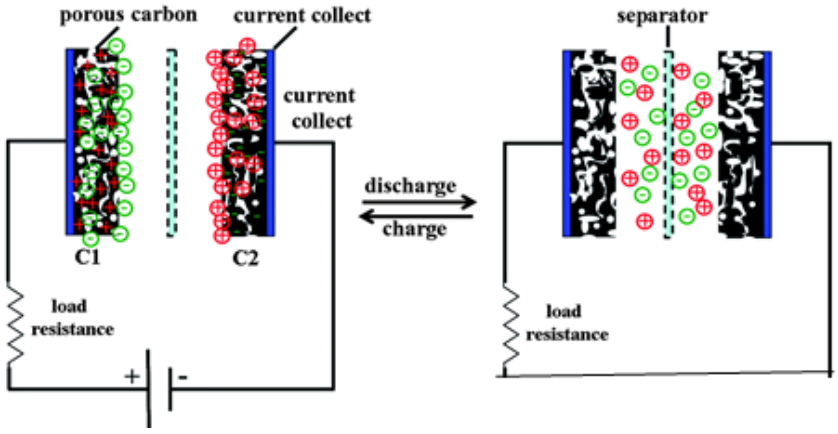

Figure 9: Schematic illustration of working of electric double layer capacitor

Advantages of EDLCs are as follows:

- ✓ Longer cycle life

  Without any reduction in its storage capacity, an EDLC can be charged and discharged for more than a million times. It can be used in combination with a battery to increase the battery life.

- ✓ Lighter and safer

  They are generally light in weight and do not have harmful metals inside and are environmental friendly.

- ✓ Faster charging times

  They store energy by the movement of ions, and in situations requiring rapid energy, they form a much better choice.

- ✓ Fast Release

  They release the stored charge much faster than rechargeable cells.

They are used in electric motor cycles, cell phones, digital cameras, radio control cars and video projectors.

1.5.2 Pseudo-capacitor

In pseudo-capacitors, the capacitance is generated from fast faradaic processes due to charge transfer reactions between the electrode and the electrolyte ions [31]. Conducting polymers, metal oxides and functionalized porous carbon based electrodes are mainly used for pseudo-capacitive charge storage. These materials can acquire much

higher specific capacitance, compared to EDLCs, with the charge storage mechanism relying on fast redox reactions occurring on the electrode surfaces [28]. In pseudo-capacitive electrodes, different charge storage mechanisms can be distinguished based on redox reactions of transition metal oxides, intercalation pseudo-capacitance and reversible electrochemical doping and de-doping in conducting polymers [36]. Faradic processes occurring together with EDL charge storage increase the specific capacitance of the electrode. The advantages of pseudo capacitors over the EDLCs are their high capacitance, which is 10–100 times higher than that of an EDLC and the possibility of obtaining higher energy densities. However, the power performance of a pseudo-capacitor is usually lower than that of EDLCs, due to the slower Faradaic processes involved.

1.5.3 Hybrid capacitors

The EDLCs offer good power performance and cyclic stability while the pseudo-capacitors offer better specific capacitance. In hybrid capacitors, both the electrical double-layer (EDL) and the pseudo-capacitance (faradaic mechanisms) are responsible for energy storage process. Hybrid systems with correct electrode combination can increase the cell voltage, which in turn leads to an enhancement in power and energy densities [37]. Usually, the faradaic electrode gives rise to an increase of energy density and capacitance at the cost of cyclic stability, which is the main problem of hybrid devices compared to EDLCs.

1.6 Electrolytes

Electrolytes play a key role in transporting the positive ions between the cathode and the anode. During charging, electrolytes promote the movement of ions from the cathode to the anode and in the reverse direction, during discharge. The ions are electrically charged atoms that have lost or gained electrons during reactions. The electrolyte of a battery consists of soluble salts, acids or other bases in liquid, gel and solid forms. Lead acid battery uses sulfuric acid as the electrolyte where as in nickel-cadmium (NiCd) and nickel-metal-hydride (NiMH) batteries, the electrolyte is an alkaline solution of potassium hydroxide. Lithium ion cells use liquid, gel or solid polymer electrolytes. Schematic representation of conventional and all solid state cell is given in figure 10.

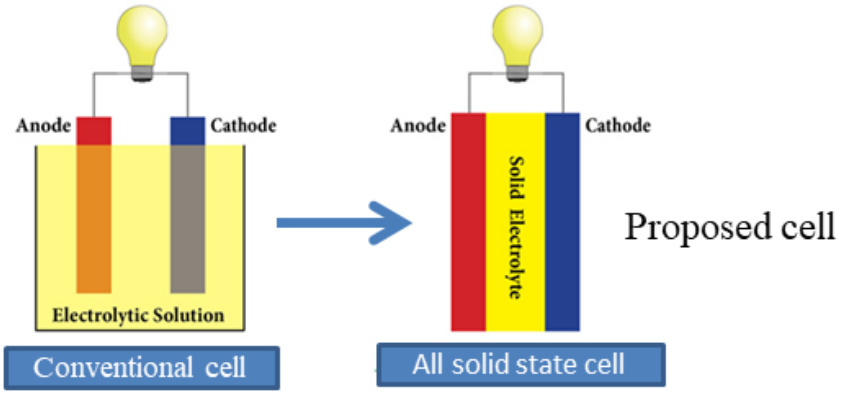

Figure 10: Schematic representation of conventional and all solid state cell

Electrolytes have important role in deciding the energy density and safety level of supercapacitors. For charge storage in supercapacitors, the aqueous, organic and ionic liquid electrolytes are commonly used. To overcome the leakage, internal shorting and

corrosion issues of the liquid electrolytes, current research is focussing on the introduction of solid or quasi-solid electrolytes which can enhance the safety aspects of supercapacitors [38]. Solid electrolytes based electrochemical energy storage devices have high application prospects in portable electronics, micro-electronics, wearable electronics and especially flexible electronics. High ionic conductivity, wide potential window, wide operating temperature range, low cost, high chemical and electrochemical stability and environment friendly nature are some of the mandatory characteristics of ideal electrolytes. Each electrolyte has its own advantages and shortcomings.

Properties of ideal electrolytes can be listed as follows:

- ❖ Good ionic conductors (facile ion transport)
- ❖ Electronic insulators (to avoid self-discharge)
- ❖ Chemically inert (no reactions with other cell components)
- ❖ Large window of electrochemical stability
- ❖ Non-toxic and cost effective
- ❖ Environmentally friendly / bio-degradable

1.6.1 Liquid electrolytes

Current energy storage systems have solid electrodes, separated by liquid electrolytes. Due to the high ionic conductivities in the range of 10^{-3} -10^{-2} S cm^{-1} and good contacts with electrodes, liquid electrolytes have played essential roles in electrochemical energy storage devices for several decades. They are mainly categorized in to liquid

organic electrolytes which are electrolyte salts dissolved in organic solvents, liquid inorganic electrolytes and ionic liquids. Important properties of liquid electrolytes are high ionic conductivity, good dissociation of electrolyte salt in electrolyte solvents, low viscosity, high Li^+ transport number, ability to stay as liquids over a wide temperature range, chemical stability towards all cell components, electrochemical stability over wide potential range and high thermal stability.

Safety issue is the main drawback of liquid electrolytes in energy storage devices. They are flammable and internal cell pressure caused by overheating will lead to explosion. With liquid electrolytes, robust sealing of the device is mandatory to avoid leakage problems and generally, the sealing is expensive. Liquid electrolytes get easily subjected to internal shorting and leakage problems and will involve in combustible reactions at the electrode surfaces.

The cathode and anode are the building blocks of a battery and these two electrodes are isolated by a separator. The separator is moistened with liquid electrolyte and forms a catalyst that promotes the movement of ions and must be permeable and porous. The ions pass freely between the electrodes through the separator, which is an isolator with no electrical conductivity. Separators are made of rubber, glass fiber mat, cellulose and polyethylene. Commercially available Li-ion cells use polyolefin as the separator which has excellent mechanical properties, good chemical stability and is cost effective. Regarding lithium ion cells with high energy density, safety is one of the prime issues to be addressed which makes solid polymer electrolytes (SPEs) ,

serving as both the separator and the electrolyte, the highly sought after ones to replace the potentially dangerous liquid electrolytes [39].

1.6.2 Gel polymer electrolytes (GPEs)

Gel polymer electrolytes (GPEs) can function not only as electrolytes but as separators as well and have attracted increasing attention. Due to the ease of processability of polymers, adjustable shapes and high flexibility, the GPEs can endow the energy storage devices with features promising for portable and wearable electronics [40]. Among the various electrolytes for the electrochemical energy storage devices, GPEs have come up as the most desirable alternatives and significant progress has been made in their applications in lithium-ion cells, supercapacitors (SCs), sodium-ion cells, lithium–sulfur cells and fuel cells. Typical polymer components used to synthesize GPEs are poly (vinyl alcohol) (PVA), poly (vinylidene fluoride) (PVdF), poly (acrylonitrile) (PAN) and poly (methylmetacrylate) (PMMA).

1.6.3 Solid polymer electrolytes (SPEs)

Solid polymer electrolytes are solvent-free electrolytes providing opportunities to tackle the safety issue and prohibit the growth of lithium dendrites. The SPEs based on polymers have high application prospects in the next-generation lithium ion cells and other energy storage devices. However, the ionic conductivity of solid polymer electrolytes have to be further improved for applications in commercial batteries. Attempts are being carried out to design strategies for improving their ionic conductivity and understanding the mechanisms of lithium transport.

Since the SPEs are free of liquid solvents, the interface properties towards electrodes differ from those of classical organic liquid electrolytes. The SPEs can be grown as free-standing, stable, flexible films without any electrolyte leakage and internal shorting issues. There is no need for any separator, since the SPEs can serve as both the electrolyte and the separator. Typical host polymers used to synthesize SPEs are poly (ethylene oxide) (PEO) and poly (propylene oxide) (PPO). They can simplify the cell design and improve the safety and durability of the cells

The semicrystalline, rigid polymer PEO polymer is capable of forming complexes with alkali metal salts, exhibiting good room temperature ionic conductivity and PEO based materials are at the centre stage of lithium electrolyte research for more than a decade [41,42]. The ion conduction in PEO and other similar polyether based media mainly occur in the amorphous phases. The ion conductors are closely associated with certain local structural relaxations related to the glass transition of the polymers. A model describes a microscopic sequence in which lithium ions are coordinated by the ether oxygen atoms on the segments of the polymeric chain. Long-range net displacement of lithium ions results due to the continuous segmental rearrangement accompanied by the gradual replacement of the ligands in the solvation sheath of lithium ions, as shown in figure 11.

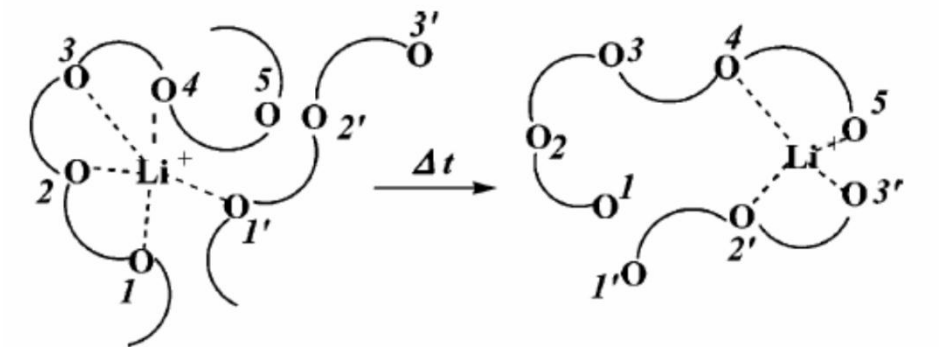

Figure 11: Schematic illustration of lithium ion transport in polyether media [42]

Due to chain entanglement of the polymer host and the local segmental motion of the polymer, these polymer-salt complexes may exhibit mechanical properties. The glass transition temperature (Tg) of the polymer, which to a great extent determines the mechanical strength and hence processability of the polymer material is another important parameter.

1.6.4 Composite polymer electrolytes

In certain case of SPEs, such as complexes between PEO and metal salts, higher ionic conductivities are reported at temperatures above the transition from the crystalline to the amorphous phase [43]. To improve the morphological characteristics and the ionic conductivity of the solid polymer electrolytes, the addition of inert fillers to the electrolyte appears to be quite useful. The filler provides a support matrix for the conductive amorphous polymer complex, and it retains a complete solid structure even at high temperatures.

Addition of nano-sized inorganic components such as ceramic filler materials can act as plasticizers to further improve the electrolyte properties.

Some of the common examples for ceramic additives are Al_2O_3, TiO_2 and SiO_2. The advantageous aspects of composite polymer electrolytes include significant enhancement of conductivity, improvement of interfacial stabilities with anode and cathode, improvement of mechanical stability, suppression of polymer chain motion and decreasing anion transport, introduction of grain boundaries with high defect concentration which allow fast ion transport and good interaction between filler and electrolyte salt resulting in higher degree of dissociation.

1.7 Definitions

The following definitions are used during the course of discussions on rechargeable cells and electrochemical capacitors.

- Open circuit voltage (OCV) - Voltage across the terminals of a cell when no external current flows. It is usually close to the thermodynamic voltage of the system.
- Closed circuit voltage (CCV) - Voltage of a cell, when the device is giving current into the external circuit (operating voltage).
- Discharge is the operation in which the cell delivers electrical energy to an external load.
- Charge is the operation in which the cell is restored to its original charged condition by reversal of current flow.
- Active mass is the material that generates electrical current by means of a chemical reaction within the cell.

- ❖ Internal resistance or impedance is the resistance or impedance that a cell offers to current flow.
- ❖ Capacity or capacitance represents specific energy in ampere-hours (Ah) or Farads (F).
- ❖ A load defines the current that is drawn from the cell.
- ❖ Energy density is the total electrical energy obtained from unit mass of the active material of the cell. It defines cell capacity in weight, expressed as Wh kg^{-1}.
- ❖ Power density is the power provided by unit mass of the active material of the cell and is expressed in W kg^{-1}
- ❖ The C-rate specifies the speed at which the cell can be charged or discharged and expressed in h^{-1}.

1.8 Objectives of the present work

The current studies are mainly focused on identifying the suitable solid polymer electrolyte materials for realizing the Li-ion and Na-ion rechargeable cells and high power supercapacitors. The objectives of the present work can be summarized and listed as follows.

- ➢ To investigate the ionic conducting properties and the electrochemical characteristics of the free standing and flexible solid polymer electrolyte (SPE) films grown by treating the polymer blend of poly (ethylene oxide) (PEO) and poly (vinylidene fluoride) (PVdF) with the lithium salt, lithium nitrate ($LiNO_3$). The application prospects of these SPE films for developing solid state Li ion cells will be assessed.

- To develop a promising SPE film with room temperature lithium ion conductivity in the range of 10^{-3} S cm^{-1} based on poly ethylene oxide (PEO) and poly (vinyl pyrrolidone) (PVP) and treated with lithium nitrate ($LiNO_3$) as the lithium source. Detailed studies on the structural aspects, the impedance characteristics and the electrochemical behaviour of these flexible SPE films will be carried out to assess their prospective applications in energy storage devices.

- Investigations to practically accomplish the assembling of two different types of all solid state Li ion half cells for 3.2 V and 5 V using the eco-friendly materials $LiFePO_4$ and $LiNiMnO_4$ as the cathode active materials respectively, lithium foil as the anode and the developed SPE film with the highest Li ion conductivity serving as both the solid electrolyte and the separator. Detailed investigations will be carried out on the electrochemical performance of the assembled, solid state Li ion cells using cyclic voltammetry and charge-discharge studies to assess the charge storage capacity and the cycling stability of these cells.

- The development of solid polymer electrolyte (SPE) films with high ionic conductivity suitable for the realisation of all solid state Na ion cells, forms another prime objective of the present investigations. The sodium ion conducting SPE films are obtained by the solution casting technique using the blend solution of poly (ethylene oxide) (PEO) with ethylene carbonate (EC) and propylene carbonate (PC) and treated with sodium

nitrate as the sodium source. The suitability of the addition of nanostructured Al_2O_3, as the filler material to enhance the room temperature, Na ion conductivity of these SPE films will be studied in detail.

- To assemble a solid-state supercapacitor with high power density and capacitance, using the redox mediated gel polymer as the electrolyte and separator and activated carbon as the electrodes. The gel polymer electrolyte (GPE) film is based on poly (vinyl alcohol) (PVA) - potassium hydroxide (KOH)- hydroquinone (HQ) combination and obtained using solution casting technique. The assembled, solid- state supercapacitors will be subjected to detailed electrochemical characterization.

1.9 References

[1] Nasir Mahmood, Chenzhen Zhang, Han Yin and Yanglong Hou, Graphene-based nanocomposites for energy storage and conversion in lithium batteries, supercapacitors and fuel cells, J. Mater. Chem. A, 2014, 2, 15–32.

[2] X. Liu, F. Wang and Q. Wang, Phys. Chem. Chem. Phys., 2012, 14, 7894–7911.

[3] Z.-Y. Shih, A. P. Periasamy, P.-C. Hsu and H.-T. Chang, Appl. Catal., B, 2013, 132–133, 363–369.

[4] J. Hou, Z. Liu and P. Zhang, J. Power Sources, 2013, 224, 139– 144.

[5] Chaofeng Liu, Zachary G. Neale and Guozhong Cao, Understanding electrochemical potentials of cathode materials in rechargeable batteries, Materials Today Volume 19, Number 2 March 2016.

[6] John B. Goodenough and Youngsik Kim, Challenges for Rechargeable Li Batteries, Chem. Mater. 2010, 22, 587–603 587.

[7] Xiang Yin, WenyingChen, JiyongEom, LeonE.Clarke, SonH.Kim, PralitL.Patel, Sha Yu, G.PageKyle, China's transportationenergyconsumptionandCO2 emissions froma global perspective, Energy Policy82(2015)233–248.

[8] K. Kalyanasundaram, M. Gratzel, Themed issue: nanomaterials for energy conversion and storage, J. Mater. Chem., 2012, 22, 24190.

[9] Qifeng Zhang, Evan Uchaker, Stephanie L. Candelaria, Guozhong Cao, Nanomaterials for energy conversion and storage, Chem. Soc. Rev., 2013, 42, 3127.

[10] G.M. Shafiullah, Amanullah M.T.Oo, A.B.M. ShawkatAli, Peter Wolfs, Potential challenges of integrating large-scale wind energy into the power grid–A review, Renewable and Sustainable Energy Reviews 20 (2013) 306–321.

[11] Santosh Kumar, Ms. Shubhangi Satdeve, Mr. Yash A. Zode, Energy: Rechargeable Batteries and Sustainable Development, International Journal of Engineering Technology Science and Research, ISSN 2394 – 3386 Volume 5, Issue 2, February 2018.

[12] Martin Winter, Ralph J. Brodd, What Are Batteries, Fuel Cells, and Supercapacitors?, Chem. Rev. 2004, 104, 4245-4269.

[13] Patrice Simon, Yury Gogotsi, Materials for electrochemical capacitors, nature materials, 7, 2008, 320-329

[14] Li Li Zhang, X. S. Zhao, Carbon-based materials as supercapacitor electrodes, Chem. Soc. Rev., 2009, 38, 2520–2531.

[15] Rizanaliah Kasim, Abdul Rahim Abdullah, Nur Asmiza Selamat, Muhammad Sufyan Safwan Mohamad Basir and Mohd Zulkifli Ramli, Nickel-Cadmium battery analysis using spectrogram, ARPN Journal of Engineering and Applied Sciences, vol. 11, no. 6, 2016, ISSN 1819-6608.

[16] Qi Li, Juner Chen, Lei Fan, Xueqian Kong, Yingying Lu, Progress in electrolytes for rechargeable Li-based batteries and beyond, Green Energy & Environment 1 (2016) 18-42.

[17] David Linden, Thomas B. Reddy, Handbook of Batteries, Copyright @ 2002, 1999, 1994, 1972 by The McGraw-Hill Companies.

[18] Yifei Yuan, Khalil Amine, Jun Lu, Reza Shahbazian-Yassar, Understanding materials challenges for rechargeable ion batteries with in situ transmission electron microscopy, Nature Communications, 2017, DOI: 10.1038/ncomms15806.

[19] Masanobu Nakayama, Shinta Wada, Shigeki Kuroki, Masayuki Nogami, Factors affecting cyclic durability of all-solid-state lithium polymer batteries using poly(ethylene oxide)-based solid polymer electrolytes, Energy Environ. Sci., 2010, 3, 1995–2002, DOI: 10.1039/c0ee00266f.

[20] S. T. Senthilkumar, R. Kalai Selvan, J. S. Melo, Redox additive/active electrolytes: a novel approach to enhance the performance of supercapacitors, J. Mater. Chem. A, 2013, 1, 12386.

[21] T. Minami, M. Tatsumisago, M. Wakihara, C. Iwakura, S. Kohjiya, I. Tanaka, Solid State Ionics for Batteries, ISBN 4-431-24974-5 Springer-Verlag Tokyo Berlin Heidelberg New York, 2005.

[22] Lizhen Long, Shuanjin Wang, Min Xiao and Yuezhong Meng, Polymer electrolytes for lithium polymer batteries, J. Mater. Chem. A, 2016, 4, 10038.

[23] John B. Goodenough, Kyu-Sung Park, The Li-Ion Rechargeable Battery: A Perspective, J. Am. Chem. Soc. 2013, 135, 1167−1176.

[24] M. Rosa Palacin, Recent advances in rechargeable battery materials: a chemist's perspective, Chem. Soc. Rev., 2009, 38, 2565–2575.

[25] Veronica Palomares, Montse Casas-Cabanas, Elizabeth Castillo-Martinez, Man H. Han, Teofilo Rojo, Update on Na-based battery materials. A growing research path, Energy Environ. Sci., 2013, 6, 2312.

[26] Dipan Kundu, Elahe Talaie, Victor Duffort, and Linda F. Nazar, The Emerging Chemistry of Sodium Ion Batteries for Electrochemical Energy Storage, Angew. Chem. Int. Ed. 2015, 54, 3431 – 3448.

[27] Naoaki Yabuuchi, Kei Kubota, Mouad Dahbi, Shinichi Komaba, Research Development on Sodium-Ion Batteries, Chem. Rev. 2014, 114, 11636−11682.

[28] [28] Ander Gonzalez, Eider Goikolea, Jon Andoni Barrena, Roman Mysyk, Review on supercapacitors: Technologies and materials, Renewable and Sustainable Energy Reviews 58 (2016) 1189–1206.

[29] Andrew Burke, Ultracapacitors: why, how, and where is the technology, Journal of Power Sources, 91, (2000), 37–50.

[30] J. R. Miller and A. F. Burke, Electrochemical Capacitors: Challenges and Opportunities for Real-World Applications, Electrochem. Soc. Interface Spring, 2008, 17, 53.

[31] S. T. Senthilkumar, R. Kalai Selvan, J. S. Melo, Redox additive /active electrolytes: a novel approach to enhance the performance of supercapacitors, J. Mater. Chem. A, 2013, 1, 12386.

[32] Silvia Roldan, Zoraida Gonzalez, Clara Blanco, Marcos Granda, Rosa Menendez, Ricardo Santamaria, Redox-active electrolyte for carbon nanotube-based electric double layer capacitors, Electrochimica Acta 56 (2011) 3401–3405.

[33] Anilkumar K M, Manoj M, Jinisha B, Pradeep V S, S. Jayalekshmi, Mn3O4/reduced graphene oxide nanocomposite electrodes with tailored morphology for high power supercapacitor applications, Electrochimica Acta 236 (2017) 424–433.

[34] Cheng Zhong, Yida Deng, Wenbin Hu, Jinli Qiao, Lei Zhang, Jiujun Zhang, A review of electrolyte materials and compositions for electrochemical supercapacitors, Chem. Soc. Rev., 2015, 44, 7484.

[35] Jingsong Huang, Bobby G. Sumpter, Vincent Meunier, Theoretical Model for Nanoporous Carbon Supercapacitors, Angew. Chem. Int. Ed. 2008, 47, 520 –524.

[36] Guoping Wang, Lei Zhang, Jiujun Zhang, A review of electrode materials for electrochemical supercapacitors, Chem. Soc. Rev., 2012, 41, 797–828.

[37] Zaharaddeen S. Iro, C. Subramani, S.S. Dash, A Brief Review on Electrode Materials for Supercapacitor, Int. J. Electrochem. Sci., 11 (2016) 10628 – 10643, doi: 10.20964/2016.12.50

[38] Haijun Yu, Jihuai Wu, Leqing Fan, Kaiqing Xu, Xin Zhong, Youzhen Lin, Jianming Lin, Improvement of the performance for quasi-solid-state supercapacitor by using PVA–KOH–KI polymer gel electrolyte, Electrochimica Acta 56 (2011) 6881– 6886.

[39] Jinisha B, Anilkumar K M, Manoj M, Pradeep V.S, Jayalekshmi S, Development of a novel type of solid polymer electrolyte for solid state lithium battery applications based on lithium enriched poly (ethylene oxide) (PEO)/poly (vinyl pyrrolidone) (PVP) blend polymer, Electrochimica Acta 235 (2017) 210–222.

[40] Xunliang Cheng, Jian Pan, Yang Zhao, Meng Liao, and Huisheng Peng, Gel Polymer Electrolytes for Electrochemical Energy Storage, Adv. Energy Mater. 2018, 8, 1702184.

[41] Zhigang Xue, Dan He, Xiaolin Xie, Poly(ethylene oxide)-based electrolytes for lithium ion batteries, J. Mater. Chem. A, 2015, 3, 19218.

[42] Kang Xu, Nonaqueous Liquid Electrolytes for Lithium-Based Rechargeable Batteries, Chem. Rev. 2004, 104, 4303-4417.

[43] F. Capuano, F. Croce, B. Scrosati, Composite Polymer Electrolytes, doi: 10.1149/1.2085900, J. Electrochem. Soc. 1991, Volume 138, Issue 7, Pages 1918-1922.

Chapter 2

Poly (ethylene oxide) and poly (vinylidene fluoride) based solid polymer electrolyte films for applications in Li ion cells

Solid polymer electrolyte (SPE) films based on poly (ethylene oxide) (PEO), poly (vinylidene fluoride) (PVdF) and lithium nitrate ($LiNO_3$) are grown by solution casting technique. These films are flexible, free-standing and transparent. The maximum ionic conductivity of these SPEs is around 8.245 $x10^{-5}$ S cm^{-1} for optimum concentration of the lithium salt. The PEO-PVdF-$LiNO_3$ based SPE films have excellent thermal stability, ideal ion transport number and good electrochemical properties, suitable for applications in all solid state lithium ion cells.

2.1 Introduction

Solid polymer electrolytes (SPEs) are currently being extensively investigated to assess their numerous application prospects in lithium ion cells, supercapacitors, fuel cells and sensors [1,2]. Lithium ion cells are in strong demand in day to day life owing to the high energy density and the excellent energy storage capacity offered for applications in portable electronic devices, power supplies and hybrid electric vehicles [3]. The research on Li ion cells has recently been intensified in identifying novel materials to serve as solid electrolytes. The use of liquid electrolytes in conventional Li ion cells has many inherent difficulties. The possibility

of electrolyte leakage and the associated short circuiting and fire hazards make it mandatory to have robust sealing for the cells. This makes the cell design more complicated especially for bigger ones. These limitations can be totally avoided if the liquid electrolytes can be replaced by suitable solid ones. The solid electrolytes when used can serve both as the electrolyte and the separator, thus eliminating the need for using distinct separator material. Their use in Li in cells makes the cell design compact and simple and guarantees the overall safety of the cells. Among solid electrolytes, solid polymer electrolytes (SPEs) have attracted much research attention for applications in energy storage devices especially due to their flexible nature and the possibility of growing them as free standing films and membranes [4,5].

Generally high molecular weight, dielectric polymers like poly (ethylene oxide) (PEO), seem to be the most suitable hosts for the synthesis of SPEs. [6]. High mechanical and chemical stability of PEO is quite attractive for a variety of applications. It can easily solvate a wide variety of salts. At room temperature it is a semi-crystalline polymer consisting of both crystalline and amorphous phases phase. This multiphase nature of PEO is considered as a major problem in many practical situations, especially requiring high ionic conductivity.

In PEO, the ionic conduction has been shown to take place mainly in the amorphous phase. For achieving better ionic conduction, one of the main criteria is to improve the polymer chain mobility through the suppression of the crystallinity of the polymer chain. The most viable way to increase the amorphous phase of PEO is to blend it

with other suitable polymers, which will improve the ionic conductivity and the dimensional stability of the resulting polymer electrolytes [7,8].

Designing and development of new polymeric materials with different application prospects are the driving factors of polymer blending technique [9, 10]. Many polymers are suitable for making good blends with PEO. In the present work, poly (vinylidene fluoride) (PVdF) is used as the polymer to make the blend with PEO to reduce the crystallinity and enhance the ionic conduction. Due to the excellent electrochemical stability, good compatibility with PEO and high dielectric constant around 8.4 [11], PVdF is specially selected to synthesize PEO-based electrolytes [12,13,14]. It has a strong electron withdrawing group, (-CF_2-) in the back bone of the polymer chain which can facilitate better intermolecular interactions.

The present work is aimed to check the compatibility of the lithium salt, $LiNO_3$ with the PEO-PVdF polymer blend and the solvation of the lithium salt by the polymer blend to yield flexible solid polymer electrolyte films, suitable for applications in all solid state Li ion cells. Lithium nitrate can be handled under ambient conditions and polymer systems treated with $LiNO_3$ have already been identified to be of much application prospects as biodegradable polymers. The structural aspects and the complex formation of the synthesized SPE films are established from X-ray diffraction (XRD), Fourier Transform Infra-Red Spectroscopy (FTIR), and Field Emission Scanning Electron Microscopy (FESEM) analysis. Thermo-gravimetric analysis (TGA) is used to assess the thermal stability of the synthesized SPE films. The

ionic conductivity of the films at different temperatures is measured using the impedance analyzer. The total ion transport number of the SPE films is estimated using Wagner's dc polarization method. Linear sweep and cyclic voltammetry studies of the SPEs are carried out to understand the electrochemical activity.

2.2 Experimental details

2.2.1 Materials

The poly (ethylene oxide) (PEO: bought from Aldrich), poly (vinylidene fluoride) (PVdF; bought from Sigma-Aldrich, India) and lithium nitrate ($LiNO_3$; obtained from Sigma-Aldrich, India) were used as received. The solvent, dimethyl formamide (DMF) was obtained from Alpha Chemicals, India, and was used as received.

2.2.2 Growth of solid polymer electrolyte films

Fixed concentrations of PEO (70 %) and PVdF (30%) were dissolved in dimethyl formamide (DMF) with continuous stirring to get the PEO-PVdF polymer blend solution. Different weight percentages of the lithium salt, $LiNO_3$ (4, 6, 8 and 10) were added to the solution and stirred vigorously for 12 hours. The resulting solution was poured onto a teflon petri-dish for drying under vacuum for 24 hours at 50 °C. After the complete evaporation of the solvent, the SPE films were peeled out from the petri-dish. In order to avoid moisture absorption, the flexible, freestanding and transparent SPE films were stored in an evacuated desiccator. Flexibility and transparency of the films indicate the

favourable compatibility of the components in the composite electrolyte. The photograph of the SPE films is shown in figure 1.

Figure 1: Transparent, flexible and freestanding SPE film

2.2.3 Characterization studies

2.2.3.1 Structural, morphological and thermal characterization

X-ray diffraction (XRD) and Fourier transform Infra-Red Spectroscopy (FTIR) techniques were used to study the structural features of the SPE films. The XRD analysis was carried out using Rigaku Max C diffractometer with Ni filtered Cu Kα radiation of 1.54 Å at 30 KV and 20 mA at a scanning rate of 5° per minute from 10° to 50°. The FTIR spectroscopic studies were done using the FTIR spectrophotometer, SHIMADSU in the range of 400–4000 cm^{-1}. Scanning electron microscopy (SEM) was used to analyse the surface morphology of the SPE films using Carl Zeiss Sigma FESEM instrument. Thermal characterizations were done by thermo-gravimetric

analysis (TGA) using the Perkin Elmer STA 6000 machine in the temperature range from room temperature to 700 °C under controlled nitrogen atmosphere.

2.2.3.2 Electrochemical characterization

The ionic conductivity of the solid polymer electrolyte films was measured using AC impedance analysis, employing the HP4192A impedance analyser with an electrochemical cell (Swagelok cell) consisting of the SPE film being sandwiched between two blocks of stainless steel (SS) electrodes. The ionic conductivity is calculated using the following equation.

$$\sigma = \frac{t}{R_b A} \text{ ---------- (1)}$$

where R_b is the bulk resistance obtained from the complex AC impedance plot, A the area of the SPE film and t the thickness of the film [15].

The temperature dependence of the ionic conductivity of the SPE films was studied in the temperature range from 300 K to 340 K. The slope of the linear fit of the resulting Arrhenius plot gives the thermal activation energy of the films. The Arrhenius plot contains linear variation in log σ against 1000/T which suggests a thermally activated process represented by

$$\sigma = \sigma_0 \exp(-\frac{E_a}{kT}) \text{ ---------- (2)}$$

where σ_0, is a constant, T stands for the absolute temperature, Ea is the thermal activation energy and k, the Boltzmann constant [7].

The total ionic transport number, t_{ion} of the SPE films was measured using Wagner's DC polarization method. Applying a fixed d.c. voltage (0.5 V) across the SS/SPE film /SS structure, where SS, the stainless steel, acts as the blocking electrode, the equation for t_{ion} is,

$$t_{ion} = (i_T - i_e)/i_T \text{ ---------- (3)}$$

where i_T is the total current and i_e the residual current [16].

Cyclic voltammetry (CV) and linear sweep voltammetry (LSV) studies were carried out using Biologic SP 300 unit to investigate the electrochemical properties and fix the stability window of the SPE films. The CV technique is the most common one to obtain preliminary information about an electrochemical process. This technique is used to analyse the rate of current generation against a range of the applied voltage. One of the most general applications is the LSV technique, where the potential is linearly scanned over time in either the negative or the positive direction.

2.3 Results and Discussion

2.3.1 XRD Analysis

The influence of lithium salt concentration in PEO- PVdF polymer blend is analysed using XRD studies and the plots are shown in figure 2. Crystalline peak of $LiNO_3$ at $2\theta = 35.59°$ [9] is quite clear in the XRD pattern shown in figure 2. The characteristic peaks of PEO are found at $2\theta = 18.11°$ and 22.31° which confirm its semi-crystalline nature [7]. The peaks at 18.4° and 20.07° correspond to the characteristic ones of PVdF. The crystallinity of the polymer blend decreases with the

addition of $LiNO_3$ at various weight percentages of 4, 6, 8 and 10, denoted by A,B,C and D respectively in the figure. The presence of the lithium salt induces a significant disorder in the polymer blend structure as evident from the XRD patterns. The lithium salt gets completely dissolved in the polymer blend and the corresponding crystalline peak is absent in the XRD pattern of the PEO-PVdF-$LiNO_3$ system or the SPE. This implies the better miscibility of the polymer blend and the lithium salt. The miscibility is referred to as the ability to be mixed at molecular levels in order to achieve good interaction between the functional groups of the polymers and the lithium salt. Excellent miscibility often results in the generation of newer systems with enriched properties [17]. The XRD patterns reveal that the peaks of the PEO-PVdF-$LiNO_3$ based SPEs are mainly the ones corresponding to PEO and PVdF, but with much less intensity, implying decreased crystallinity of the SPEs with increase in the concentration of the lithium salt, as evident from the patterns A to D in figure 2. The decrease in the crystalline nature results in enhanced ion diffusion through the SPEs with higher ionic conductivity. The flexible backbones associated with amorphous polymers help to attain high ionic mobility. On adding $LiNO_3$ to the polymer blend the 10wt% sample D has more amorphous than that of others. Upon the addition of salt to the blend suggesting a decrease in the degree of crystallinity of the complexes and intensity of all crystalline peaks of PEO and PVdF are decreases gradually. The lithium salt will disrupt the semi-crystalline structure of the film is the reason for this decreased crystallinity. The reduction of the crystalline phase of polymer chains is due to the dissolution of $LiNO_3$ in the

polymer blend and the interaction between PEO-PVdF polymer matrix and $LiNO_3$ leads to a decrease in the intermolecular interaction among the polymer chains [18]. The intensity of the XRD peaks corresponding to PEO and PVdF in the SPEs decreases gradually with the addition of the lithium salt to the polymer blend matrix and the maximum intensity reduction is observed for 10 weight %of $LiNO_3$. Further increase in the lithium salt concentration is found to affect the quality of the SPE films.

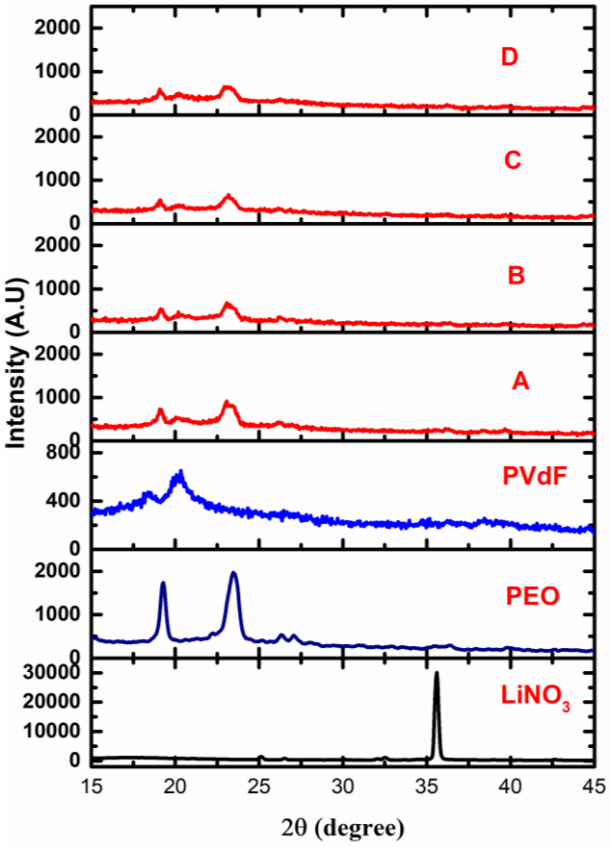

Figure 2: The XRD patterns of pure $LiNO_3$, pure PEO, pure PVdF and the SPE films represented by A to D, corresponding to 4,6,8 and 10 weight % of $LiNO_3$ in the polymer blend.

2.3.2 FTIR spectroscopic analysis

The FTIR transmittance spectra of pure PEO, PVdF, $LiNO_3$ and the SPEs with various $LiNO_3$ concentrations are shown in figure 3. The presence of ether oxygen group of PEO is observed at 1799 cm^{-1} which is a small intensity peak [9]. The peak at 1100 cm^{-1} is assigned to the C-O-C stretching mode of pure PEO. The vibrational bands of PEO at 1236, 1282, 1342 and 1480 cm^{-1} correspond to CH_2 symmetric twisting, asymmetric CH_2 twisting, CH_2 bending and C-H bending of CH_2, respectively [9,11]. The strong peak at 845 cm^{-1} is the anti-symmetric stretching vibration of the CH_2 group and the one at 947 cm^{-1} is attributed to C-O stretching vibration. The absorption peak of PVdF at 1402 cm^{-1} is assigned to the C–F stretching vibration [11, 19]. The vibrational bands at 1175 and 1216, cm^{-1} correspond to the stretching frequencies of CF_2 and C–F, respectively and the mode at 874 cm^{-1} is ascribed to the vinylidene ($-C=CH_2$) group vibration. [20]. The crystalline and amorphous phases of PVdF are represented as the peaks at 1067 and 828 cm^{-1} [21] respectively. The absorption bands of $LiNO_3$ at 1051,1384 and 827 cm^{-1} are attributed to the symmetric stretching mode, asymmetric stretching mode and the out of plane deformation mode of NO_3^- ions respectively [9].

On the addition of $LiNO_3$ to the PEO-PVdF blend, significant changes are observed for the characteristic vibrational peaks of PEO and PVdF, as depicted in the spectra of the SPEs titled as A, B,C and D. These changes confirm the perfect miscibility through effective

intermolecular interactions between the polymers and the lithium salt. The intensity of the characteristic peaks of PEO and PVdF are found to get enhanced in the SPEs upon the increase in lithium salt concentration from 4 to 10 weight %, as seen in the spectra, A,B,C and D Subsequent to the incorporation of the lithium salt, the structure of PEO is completely distorted because the intensity of the peaks at 1100, 947 and 845 cm^{-1} of PEO gets enhanced in the SPEs due to the stretching of the helical confirmation of PEO [22]. The peak at 1067 cm^{-1} of PVdF vanishes from the spectra of the PEO-PVdF-$LiNO_3$ based SPEs indicating that PEO has blended well with PVdF and it is the crystalline peak that disappears. The effects of the Li salt incorporation on the vibrational modes of the PEO-PVdF polymer blend system are observed as the changes in the intensity of the peaks, broadening of the peaks and the shifting of the peaks to lower wave numbers. The FTIR spectroscopic studies support the formation of the PEO-PVdF-$LiNO_3$ based solid polymer electrolyte system with reduced crystallinity, enhanced amorphous nature and good flexibility.

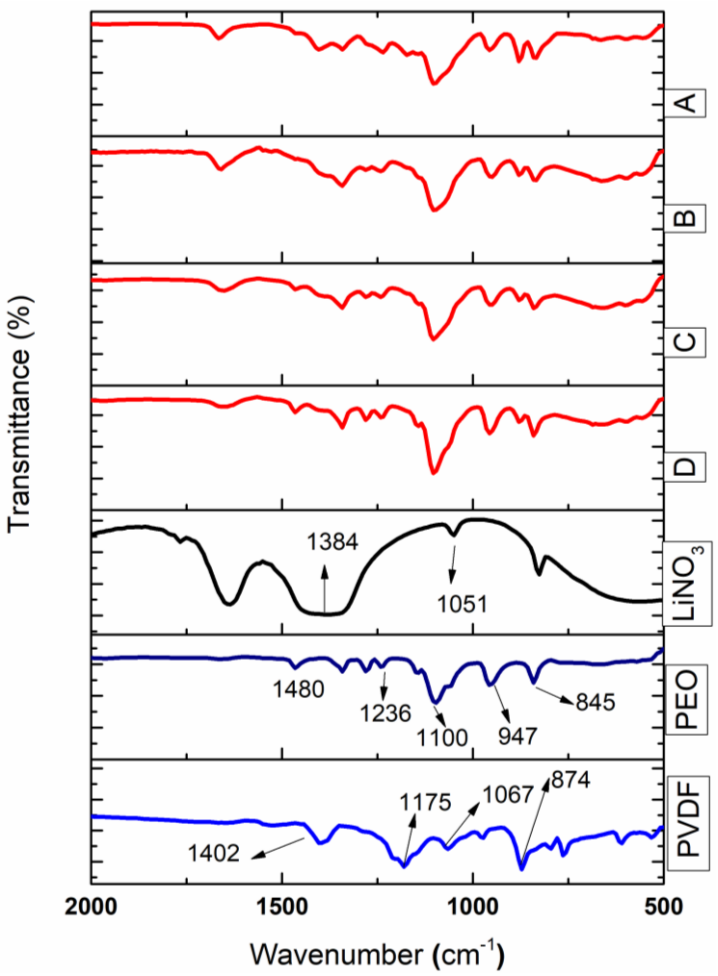

Figure 3: The FTIR spectra of (a) PVdF (b) PEO (c) $LiNO_3$ and the SPEs denoted by A,B,C and D corresponding to 4,6,8 and 10 weight % of $LiNO_3$ in the polymer blend

2.3.3 FE-SEM Analysis

The FE-SEM micrographs of PEO, PVdF, PEO-PVdF blend and PEO-PVdF-$LiNO_3$ based SPE sample D, corresponding to 10 weight percentage of $LiNO_3$ in the polymer blend are shown in figure 4. Due to the rigid nature of PEO, several micro cracks are seen on its rough micro structure, as shown in figure 4 (a) [9]. Micro porous membrane of PVdF

[23] is observed in figure 4(b). After the formation of the polymer blend PEO-PVdF, the micro cracks of PEO disappear and the polymer blend surface becomes more porous, smoother and flexible, as shown in figure 4 (c), due to the increase in the amorphous nature of the polymer blend [24]. On the addition of $LiNO_3$ salt to the polymer blend, in addition to retaining the smooth appearance of the blend, several micro pores are also formed, as seen from figure 4 (d). One of the desirable characteristics of the separator membranes used in rechargeable cells is the presence of such micro pores on the membrane surfaces [16]. The $LiNO_3$ salt in the PEO-PVdF polymer blend improves the flexibility and porosity of the PEO-PVdF- $LiNO_3$ based SPE membrane and consequently, the room temperature ionic conductivity also gets greatly enhanced due to the easy penetration of ions through the porous structure.

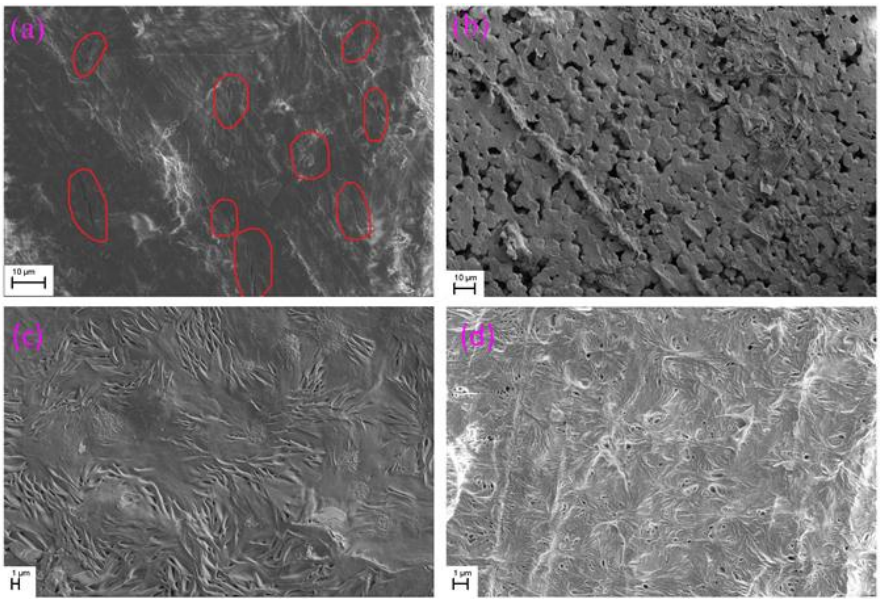

Figure 4: FE-SEM images of (a) PEO (b) PVdF (c) PEO- PVdF blend and (d) PEO- PVdF-$LiNO_3$ based SPE sample D.

2.3.4 Thermal characterization

2.3.4.1 Thermo gravimetric analysis

Thermal stability of the SPE film was studied using thermo-gravimetric analysis. The thermal curves of PEO, PVdF, PEO-PVdF blend film and the SPE film D (PEO-PVdF-10 weight % of $LiNO_3$) are shown in figure 5. The decomposition temperature of PEO and PVdF starts from 340 °C and 443 °C respectively. Therefore these two polymers are stable up-to those temperatures. After the temperature of 425 °C, PEO gets gradually decomposed and completely decayed at 730 °C. The polymer, PVdF has 68% weight loss at 502 °C and thereafter gets gradually decomposed. It is seen that the TG curve of PEO-PVdF blend shows a characteristic two step weight loss, with the first short peak at a temperature of 340 °C and the longer peak at 443 °C corresponding to the decomposition temperatures of PEO and PVdF respectively [12]. After the second weight loss, the PEO-PVdF blend gets gradually decomposed at the same temperature as that of PVdF, at 502 °C. There is an initial 11% weight loss observed at 85 °C for the SPE film due to the moisture content accumulated on the film surface during the process of sample loading [25]. After the initial weight loss, the SPE film is stable upto 334 °C and thereafter the second decomposition starts due to the degradation of the lithium salt. The thermal stability of the SPE film is slightly less than that of the polymer blend, due to the presence of the lithium salt [9]. The polymer blend with the lithium salt or the SPE film acquires higher flexibility and consequently shows comparatively lower degradation temperature. The

presence of the lithium salt makes the SPE film more flexible and porous, compared to the PEO-PVdF blend and brings about the observed reduction in the thermal stability [26]. In the TG curve of the SPE film, the plateau region between 85 °C and 334 °C indicates that the SPEs are stable in this temperature range and the presence of the lithium salt does not significantly affect the thermal stability.

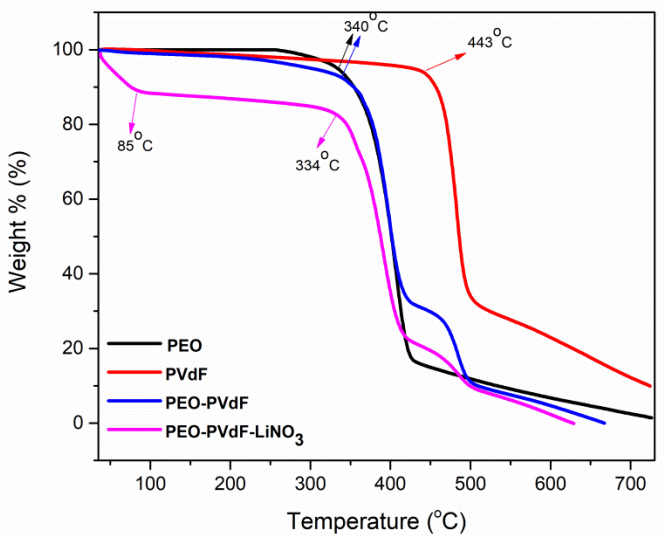

Figure 5: TG curves of PEO, PVdF, PEO-PVdF blend and the SPE film D (PEO-PVdF-10 weight % of $LiNO_3$)

2.3.5 A C Conductivity studies

2.3.5.1 Impedance analysis

The impedance analysis of the SPE films was carried out by sandwiching them between two stainless steel discs which act as blocking electrodes for Li^+ ions under an applied electric field. The room temperature impedance plots for the SPE films are shown in figure 6. Two well defined regions are observed in the complex impedance plots, with the semi-circular region in the high frequency range, related to the ionic

conduction process in the bulk of the electrolyte and the linear region at low frequency range, attributed to the effect of blocking electrodes [27]. The plot at low frequency region shows a straight line parallel to the imaginary axis. The intercept at the higher frequency side on the Z^{I} axis gives the bulk resistance R_b. The ionic conductivity of the four SPE films A,B,C and D is calculated as explained earlier, where the sample codes A to D refer to the PEO-PVdF polymer blend with 4, 6, 8 and 10 weight % of $LiNO_3$ added. Maximum ionic conductivity obtained is 8.245 $x10^{-5}$ S cm^{-1} for 10 weight % of lithium salt in the polymer blend matrix. The ionic conductivity values of the SPE films are tabulated in Table 1. It increases with increase in the concentration of the lithium salt in the SPEs as shown in figure 7. This increase in ionic conductivity can be related to the increase in the concentration of mobile charge carriers in the SPE films brought about by the enhancement in the flexibility and the porosity of the SPE films with the presence of the lithium salt [28].

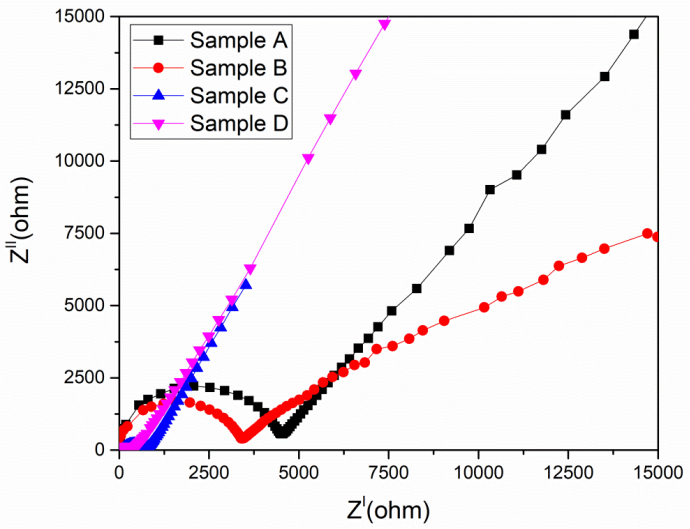

Figure 6: Room temperature complex impedance plots for SPE films of sample codes A to D

Table 1: Room temperature ionic conductivity of the SPE films

Sample Code	Weight Percentage of $LiNO_3$ (%)	Ionic conductivity (S cm^{-1})
A	4	5.07 $x10^{-6}$
B	6	7.025 $x10^{-6}$
C	8	3.49 $x10^{-5}$
D	10	8.245 $x10^{-5}$

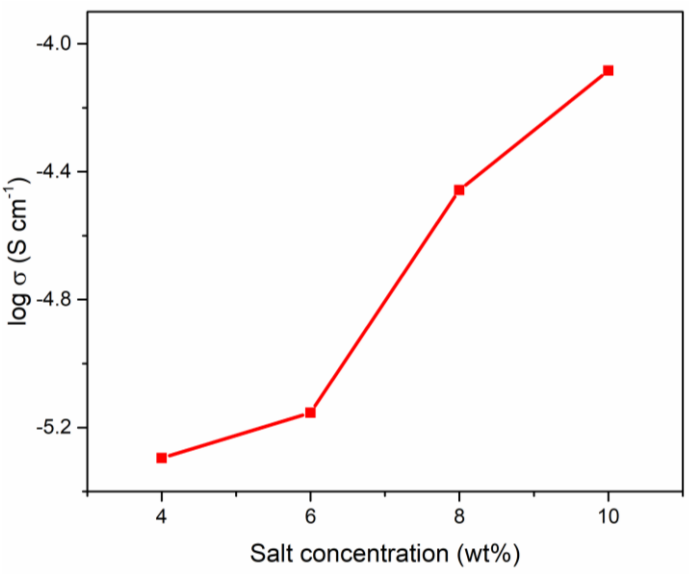

Figure 7: The variation of ionic conductivity of the SPE films with the concentrations of $LiNO_3$ in the polymer blend at room temperature.

2.3.5.2 Thermal activation energy measurement

The variation of ionic conductivity as a function of temperature in the range 300–340 K for the SPE films is shown in figure 8. With the increase in temperature, an enhancement in the magnitude of ionic conductivity is observed [9], mainly due to the increase in ionic mobility and the concentration of carrier ions. When the temperature is increased,

the polymers expand to produce free volume. Consequently the ionic mobility and the polymer segmental mobility [29] get enhanced, which in turn facilitate the increase in ionic conductivity. The plot given in figure 8 follows the Arrhenius behaviour throughout the temperature range. The activation energy calculated as explained earlier, for the sample D with the highest ionic conductivity is found to be 0.0815 eV. The energy required to provide the suitable conductive conditions for the smooth migration of the ions through the electrolyte is referred to as the activation energy [30,31]. The activation energy values for different SPE film samples are shown in Table 2. Among the SPE films, the sample D with the highest ionic conductivity has the smallest value of the activation energy which indicates the possibility of the smoother and easier migration of ions through this SPE film, compared to the other films.

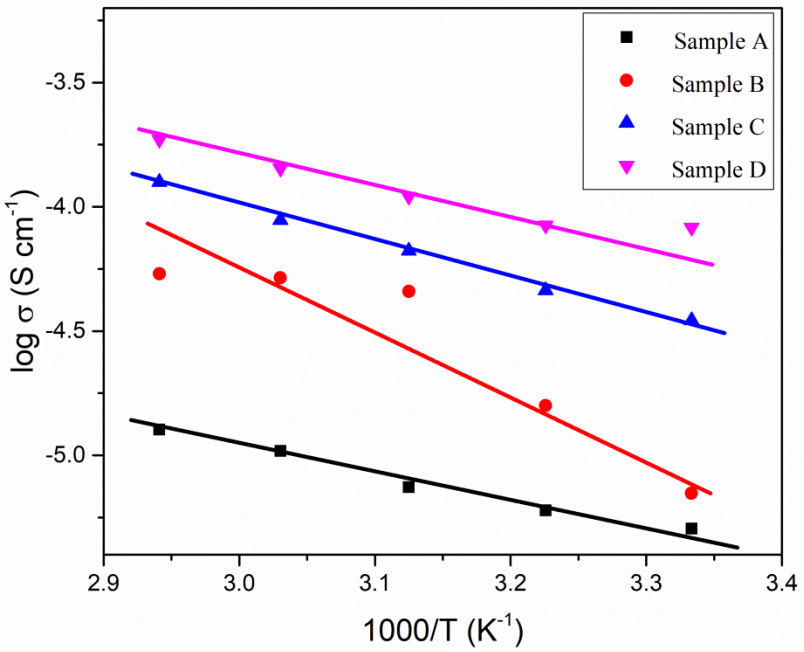

Figure 8: Arrhenius plots for SPE film samples

Table 2: Activation energy values of the SPE films.

Sample Code	Weight Percentage of $LiNO_3$ (%)	Activation energy (eV)
A	4	0.1
B	6	0.198
C	8	0.123
D	10	0.0815

2.3.6 Ion transport number measurement

The total ion transport number t_{ion} is obtained from the variation of current with time for the SPE films and the plot is given in figure 9. For the SPE film with the highest ionic conductivity, the value of t_{ion} obtained is 0.9942, which is close to the theoretical value, unity. It is evident that the conductivity of the SPE films is mainly ionic [9] and the electron influence is quite negligible.

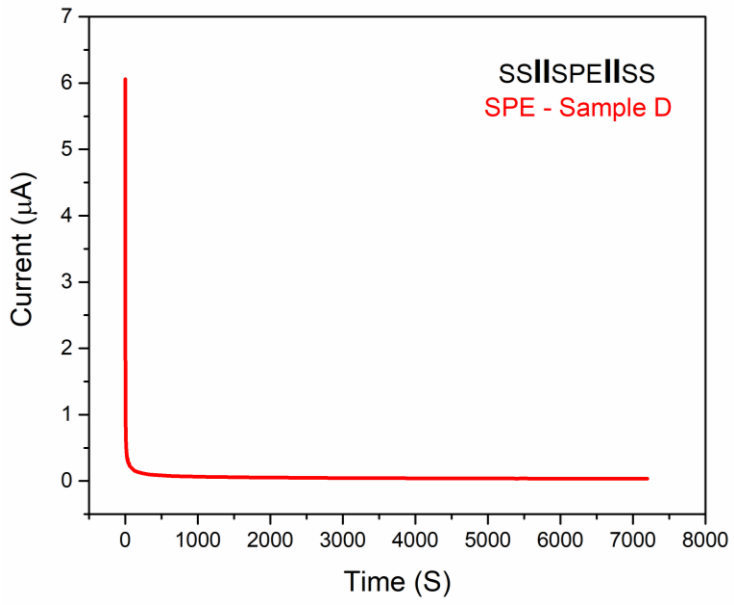

Figure 9: The variation of current with time of the SPE film sandwiched between two stainless steel (SS) blocking electrodes.

2.3.7 Electrochemical stability

Electrochemical stability window of the SPE films is assessed using linear sweep voltammetry technique (LSV) in the configuration of SS/SPE/Li (SS: stainless steel blocking electrode) Swagelok type cell [32] as shown in figure 10. The LSV studies are carried out at a scan rate of 5 mV s^{-1} within the potential window of 0 to 6 V (versus Li/Li^+). A rapid increase of current at around 4 V is observed indicating the anodic break down of the electrolyte film due to the decomposition of the electrolyte. The PEO- PVdF-$LiNO_3$ based solid electrolyte is stable up to at least 4 V versus Li/Li^+.

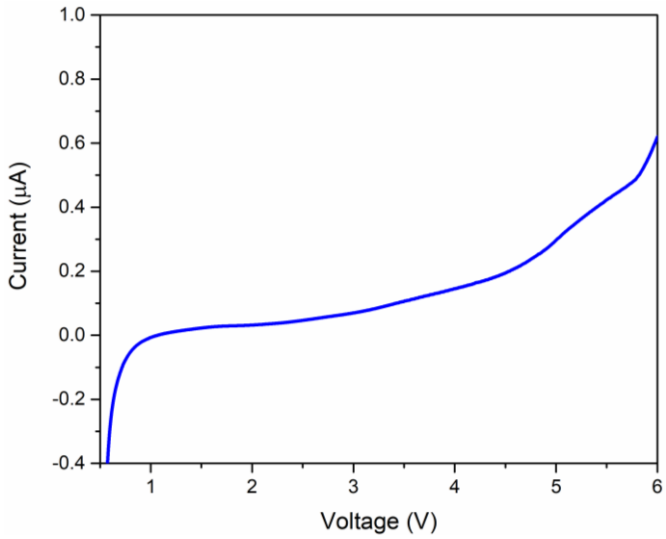

Figure 10: Linear sweep voltammetry of Li/SPE film D/SS

Cyclic voltammetry (CV) response of the SPE film D in SS||SPE||SS (SS: stainless steel blocking electrode) arrangement at a scan rate of 5 mV s^{-1} from 0 to 4 V is shown in figure 11. It is observed that the CV curves of three cycles present in the figure do not have any

distinct peaks up to 4V, which indicates that there is no electrolyte decomposition up to 4V. The electrochemical stability of the SPE film can be established by the reproducible and clear nature of the CV curves [16]. The stability window of the SPE film is found to be in the voltage range 0 to 4 V.

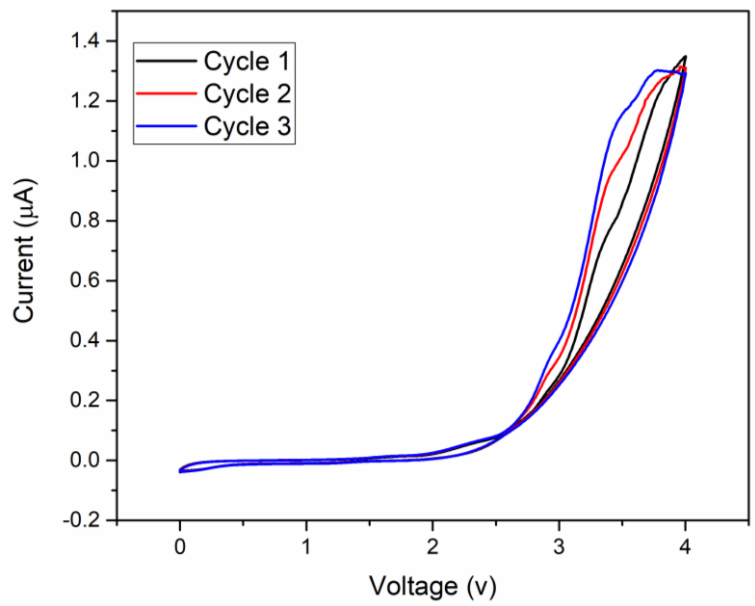

Figure 11: Cyclic voltammetry curves of the system, SS/SPE film D/SS

2.4 Conclusions

The work presented in this chapter introduces a simple and cost effective technique to grow flexible and free standing solid polymer electrolyte (SPE) films, using the polymer blend of PEO and PVdF as the host matrix and $LiNO_3$ as the lithium source, for applications in all solid state Li ion cells. As confirmed from the structural and morphological studies using the XRD, FTIR spectroscopy and FE-SEM

techniques, the addition of the lithium salt, $LiNO_3$ facilitates the enhancement of the amorphous nature, flexibility and the porosity of the resulting SPE films, which ultimately results in significant increase of the Li ion conductivity. Corresponding to the maximum concentration of $LiNO_3$ in the PEO-PVdF blend, the resulting SPE films show the maximum Li ion conductivity around 8.245 $x10^{-5}$ S/cm at room temperature. These SPE films have good thermal stability above 300 ^oC and excellent electrochemical stability up to 4 V. These parameters, combined with the flexible and porous nature of these SPE films are quite favourable for their applications as the solid electrolyte and the separator membrane in the design of all solid state Li ion cells, capable of operation at higher temperatures.

2.5 References

[1] K. Naveen Kumar, Misook Kang, K. Sivaiah, M. Ravi, Y. C. Ratnakaram, Enhanced electrical properties of polyethylene oxide (PEO)+ polyvinylpyrrolidone (PVP):Li+ blended polymer electrolyte films with addition of Ag nanofiller, Ionics, 2015, DOI 10.1007/s11581-015-1599-4

[2] Jun-Xia Li, Zhong-Xiang Du, Jian-Ge Wang, Tao Wang, Jun-Na Lv, Zinc and manganese coordination polymers constructed by a new coordination mode of 4,5-dicyanoimidazolate ligand: syntheses, crystal structures, fluorescent and magnetic properties. Inorganic Chemistry Communications 15 (2012) 243–247.

[3] John B. Goodenough, Kyu-Sung Park, The Li-Ion Rechargeable Battery: A Perspective, J. Am. Chem. Soc. 2013, 135, 1167−1176.

[4] Anand B. Puthirath, Sudeshna Patra, Shubhadeep Pal, Manoj M, P.B. Aravind, S. Jayalekshmi, Tharangattu N. Narayanan, Transparent Flexible Lithium Ion Conducting Solid Polymer Electrolyte, J. Mater. Chem. A, 2017, DOI: 10.1039/ C7TA02182H.

[5] Feng Wu, Ting Feng, Ying Bai, Chuan Wu, Lin Ye, Zengguo Feng, Preparation and characterization of solid polymer electrolytes based on PHEMO and PVDF-HFP, Solid State Ionics 180 (2009) 677–680.

[6] Xiang-Wu Zhang, Chunsheng Wang, A. John Appleby, Frank E. Little, Characteristics of lithium-ion-conducting composite polymer-glass secondary cell electrolytes, Journal of Power Sources 112 (2002) 209–215.

[7] B. Jinisha, K. M. Anilkumar, M. Manoj, A. Abhilash V. S. Pradeep, S. Jayalekshmi, Poly (ethylene oxide) (PEO)-based, sodium ion-conducting, solid polymer electrolyte films, dispersed with Al2O3 filler, for applications in sodium ion cells, Ionics (2017) https://doi.org/10.1007/s11581-017-2332-2

[8] Bo Liang, Siqi Tang, Qingbai Jiang, Chuangsheng Chen, Xu Chen, Shengliang Li, Xuehui Yan, Preparation and characterization of PEO-PMMA polymer composite electrolytes doped with nano-Al2O3, Electrochimica Acta 169 (2015) 334–341.

[9] Jinisha B, Anilkumar KM, Manoj M, Pradeep V.S, Jayalekshmi S, Development of a novel type of solid polymer electrolyte for solid state lithium battery applications based on lithium enriched poly (ethylene oxide) (PEO)/poly (vinyl pyrrolidone) (PVP) blend polymer, Electrochimica Acta 235 (2017) 210–222.

[10] K. Kesavan, C.M. Mathew, S. Rajendran, Lithium ion conduction and ionpolymer interaction in poly(vinyl pyrrolidone) based electrolytes blended with different plasticizers, Chinese Chem. Lett. 25 (2014) 1428–1434.

[11] R. Rathika, O. Padmaraj, S. Austin Suthanthiraraj, Electrical conductivity and dielectric relaxation behaviour of PEO/PVdF-based solid polymer blend electrolytes for zinc battery applications, Ionics (2018) 24:243–255.

[12] Raghavan Prasanth, Nageswaran Shubha, Huey Hoon Hng, Madhavi Srinivasan, Effect of poly(ethylene oxide) on ionic conductivity and electrochemical properties of poly(vinylidenefluoride) based polymer gel electrolytes prepared by electrospinning for lithium ion batteries, Journal of Power Sources 245 (2014) 283-291.

[13] Zhigang Xue, Dan He, Xiaolin Xie, Poly(ethylene oxide)-based electrolytes for lithiumion batteries, J. Mater. Chem. A, 2015, 3, 19218–19253.

[14] M. M. E. Jacob, S. R. S. Prabaharan and S. Radhakrishna, Effect of PEO addition on the electrolytic and thermal properties of PVDF-LiClO polymer electrolytes, Solid State Ionics 104 (1997) 267–276.

[15] H K Koduru, M T Iliev, K K Kondamareddy, D Karashanova, T Vlakhov, XZ Zhao, N Scaramuzza, Investigations on Poly (ethylene oxide) (PEO) – blend based solid polymer electrolytes for sodium ion batteries, IOP Publishing, Journal of Physics: Conference Series 764 (2016) 012006.

[16] K.M. Anilkumar, B. Jinisha, M. Manoj, S. Jayalekshmi, Poly (ethylene oxide) (PEO) – Poly(vinyl pyrrolidone) (PVP) blend polymer based solid electrolyte membranes for developing solid state magnesium ion cells, European Polymer Journal, 89 (2017) 249-262.

[17] P. Pradeepa, S. Edwinraj, G. Sowmya, J. Kalaiselvimary, M. Ramesh Prabhu, Optimization of hybrid polymer electrolytes with the effect of lithiumsalt concentration in PEO/PVdF-HFP blends, doi.org/10.1016/j.mseb.2015.11.009, Materials Science and Engineering B, 2015.

[18] S. Rajendran, O. Mahendran, Experimental Investigations on Plasticized PMMA/PVA Polymer Blend Electrolytes, Ionics 7 (2001) 463-468.

[19] J. Theerthagiri, R. A. Senthil, M. H. Buraidah, J. Madhavan, A. K. Arof, Effect of tetrabutylammonium iodide content on PVDF-PMMA polymer blend electrolytes for dye-sensitized solar cells, DOI 10.1007/s11581-015-1464-5, 2015, ionics.

[20] S. Rajendran, R. Kannan, O. Mahendran, An electrochemical investigation on PMMArPVdF blend-based polymer electrolytes, Materials Letters 49 (2001) 172–179.

[21] S. Ganesan, B. Muthuraaman, Vinod Mathew, M. Kumara Vadivel, P. Maruthamuthua, M. Ashokkumar, S. Austin Suthanthiraraj, Influence of 2,6 (N-pyrazolyl)isonicotinic acid on the photovoltaic properties of a dye-sensitized solar cell fabricated using poly(vinylidene fluoride) blended with poly(ethylene oxide) polymer electrolyte, Electrochimica Acta 56 (2011) 8811– 8817.

[22] K.N. Kumar, M.V. Reddy, L. Vijayalakshmi, Y.C. Ratnakaram, Synthesis and analysis of Fe3+, Co2+ and Ni2+: PEO + PVP blended polymer composite films for multifunctional polymer applications, Bull. Mater. Sci. 38 (2015) 1015–1023, http://dx.doi.org/10.1007/s12034-015-0925-9. \

[23] Jingyu Xi, Xinping Qiu, Jian Li, Xiaozhen Tang, Wentao Zhu, Liquan Chen, PVDF–PEO blends based microporous polymer electrolyte: Effect of PEO on pore configurations and ionic conductivity, Journal of Power Sources 157 (2006) 501–506.

[24] P.V. Braun, J. Cho, J.H. Pikul, W.P. King, H. Zhang, High power rechargeable batteries, Curr. Opin. Solid State Mater. Sci. 16 (2012) 186–198, http://dx.doi.org/ 10.1016/ j.cossms.2012.05.002.

[25] K. Kiran Kumar, M. Ravi, Y. Pavani, S. Bhavani, A.K. Sharma, V.V.R. Narasimha Rao, Investigations on PEO/ PVP/NaBr complexed polymer blend electrolytes for electrochemical cell applications, Journal of Membrane Science 454 (2014) 200–211.

[26] Ana F. Nogueira, M.A.S. Spinace, W.A. Gazotti, E.M. Girotto, Maco-A. De Paoli, Polyžethylene oxide-co-epichlorohydrin/ rNaI: a promising polymer electrolyte for photoelectrochemical cells, Solid State Ion. 140 (2001) 327–335.

[27] Lizhen Fan, Zhimin Dang, Ce-Wen Nan, Ming Li, Thermal, electrical and mechanical properties of plasticized polymer electrolytes based on PEO/P(VDF-HFP) blends, Electrochimica Acta 48 (2002) 205-209.

[28] C.S. Ramya, S. Selvasekarapandian, T. Savitha, G. Hirankumar, P.C. Angelo, Vibrational and impedance spectroscopic study on PVP-NH4SCN based polymer electrolytes, Physica B 393 (2007) 11–17, http://dx.doi.org/ 10.1016/j.physb.2006.11.021

[29] V. Aravindan, P. Vickraman, A novel gel electrolyte with lithium difluoro(oxalato)borate salt and Sb2O3 nanoparticles for lithium ion batteries, Solid State Sci. 9 (2007) 1069–1073, http://dx.doi.org/10.1016/j.solidstatesciences.2007.07.011.

[30] K.K. Kumar, Y. Pavani, M. Ravi, S. Bhavani, A.K. Sharma, V.V.R.N. Rao, Effect of complexation of NaCl salt with polymer blend (PEO/PVP) electrolytes on ionic conductivity and optical energy band gaps, AIP Conf. Proc. vol. 1391, 2011, pp. 641–644, , http://dx.doi.org/10.1063/1.3643635.

[31] A.A. Mohamad, N.S. Mohamed, M.Z.A. Yahya, R. Othman, S. Ramesh, Y. Alias, et al., Ionic conductivity studies of poly(vinyl alcohol) alkaline solid polymer electrolyte and its use in nickel-zinc cells, Solid State Ionics 156 (2003) 171–177.

[32] B. Liang, S. Tang, Q. Jiang, C. Chen, X. Chen, S. Li, et al., Preparation and characterization of PEO-PMMA polymer composite electrolytes doped with nano-Al2O3, Electrochim. Acta 169 (2015) 334–341.

Chapter 3

Development of solid polymer electrolyte films with enhanced ionic conductivity, based on lithium enriched poly (ethylene oxide) (PEO)/ poly (vinyl pyrrolidone) (PVP) blend polymer

In order to improve the room temperature ionic conductivity of the PEO based, Li ion conducting SPE films, developed as described in the previous chapter, the polymer PVdF is replaced by poly (vinyl pyrrolidone) (PVP) to make the polymer blend with PEO. The details of this modification and the studies on the PEO-PVP-$LiNO_3$ based SPE films are described in this chapter. Here, the only difference from the synthesis route explained in the previous chapter is that, instead of PVdF, PVP is used to make the polymer blend with the semi-crystalline and rigid polymer, PEO. The polymer PVP, owing to its amorphous nature is expected to improve the flexible nature of the PEO-PVP blend system, which in turn can facilitate better Li ion transport through the resulting SPE films. The highlight of the present work is that these SPE films exhibit room temperature ionic conductivity around 1.13×10^{-3} S cm^{-1} which is quite comparable to that of liquid electrolytes. Excellent thermal stability, flexibility and wide electrochemical stability window are the other meritorious aspects of these SPE films. They are of profound application prospects for realizing all solid state Li ion cells with excellent performance characteristics.

3.1 Introduction

Among the various energy storage systems, lithium ion cells are dominating as power sources for portable electronic applications owing to the advantageous aspects like high energy density, high output voltage, high storage capacity and long cycling stability [1-5]. Attempts are going on to utilize them in hybrid electric vehicles requiring higher energy density and improved safety features. Regarding high-energy density lithium ion cells, safety is one of the prime issues to be addressed which makes solid polymer electrolytes (SPEs) the highly sought after ones [6] to replace potentially dangerous liquid electrolytes.

The SPEs are considered to be highly safe in Li-ion cells, compared to liquid electrolytes, since they do not get easily subjected to internal shorting and leakage problems and will not involve in combustible reactions at the electrode surfaces. They are suitable to make safer, durable cells with comparatively simple designs [7, 8]. They are highly prospective for applications in electrochemical energy storage devices including rechargeable batteries and supercapacitors. [9-11].Solid state lithium ion cells utilize solid electrolytes instead of more traditional liquid or gel electrolyte materials [12]. Solvent free conditions, simple processing strategies and wide electrochemical stability windows are the major advantages of SPEs [13-15]. They can also act as separators in rechargeable cells [16], eliminating the necessity for using alternate separator materials, as explained earlier.

Polymer blending technique has been widely used in developing and designing new polymeric materials with a wide variety of

application prospects [17]. Suitable control of physical properties by compositional changes and the simplification of synthesis conditions are two main advantages of polymer blending. Since poly (ethylene oxide) (PEO) based electrolytes have good thermal and mechanical properties along with good interfacial stability when used with lithium metal, they have been widely studied and exploited as major components in solid polymer electrolytes[18]. The structure of PEO, containing ether-oxygen linkages at favourable inter atomic separation, facilitates segmental motion of the polymeric chain and there by promotes facile ionic conduction [19, 20]. The microstructure of PEO is a mixture of crystalline and amorphous phases which has significant influence on the ion transport properties as outlined earlier.

Electrochemical properties of PEO based systems have been significantly improved by tailoring the final polymer structure with the addition of other active materials. Poly (vinyl pyrrolidone) (PVP) has some unique properties which support its selection as the second polymer in the synthesis of polymer blend with PEO. Simple processing techniques, moderate electrical conductivity, good environmental stability and rich physics in charge transport mechanism are some of the favourable properties of PVP, when compared with similar polymers. Presence of the rigid pyrrolidone group in amorphous PVP helps to provide better ionic mobility in these systems. The carbonyl group (C=O) attached to the side chains of PVP helps in the formation of a number of complexes with different inorganic salts [21-24].

Treating with lithium salts is another important criterion to assess the application of SPE films in Li-ion cells. The ionic conducting properties of PEO, treated with different lithium salts like lithium perchlorate ($LiClO_4$), lithium bis(oxalato) borate ($LiB(C_2O_4)_2$) [11,13], lithium hexafluorophosphate ($LiPF_6$) [25], lithium hexafluoroarsenate ($LiAsF_6$) [26] and lithium tetrafluoroborate ($LiBF_4$) [27] have already been reported widely in literature. In the present study, lithium nitrate ($LiNO_3$) is selected as the Li source for effecting Li enrichment of the PEO/PVP polymer blend.. The present investigation is focused on assessing the suitability of the solid film obtained by the reaction of $LiNO_3$ with the blended polymer of PEO and PVP, as a solid polymer electrolyte in all solid state Li ion cells. The PEO/PVP polymer blend system has been investigated in detail as an active polymer blend [16, 17, 24,28,29]. There are not many studies based on $LiNO_3$ incorporated PEO/PVP polymer blend system for the development of flexible and freestanding SPE films. In the present work, the concentration of $LiNO_3$ in PEO/PVP blend polymer is optimized to get good quality SPE films with the desired characteristics for realizing all solid state Li ion cells.

3.2 Experimental

3.2.1 Materials

The polymer, PEO [(-CH_2CH_2O-) n], of average molecular weight 200,000, poly (vinyl pyrrolidone) (PVP) of average molecular weight 40000 and $LiNO_3$ were purchased from Sigma-Aldrich, India and used as received. The solvent methanol was purchased from Alpha

Chemicals, India. A solution mixing approach was used to synthesize the PEO/PVP/$LiNO_3$ based solid electrolyte with methanol as the solvent.

3.2.2 Synthesis of PEO/PVP/$LiNO_3$ based solid polymer electrolyte

The initial concentrations of PEO and PVP in the PEO/PVP blend were fixed to be approximately 90% and 10 % respectively. For a typical SPE sample with 5 weight % of the PEO/PVP blend as the concentration of the $LiNO_3$ salt, the total mass of the SPE would be 0.475 g out of which the mass of PEO would be 0.4 g, that of PVP, 0.05 g and that of $LiNO_3$, 0.025 g. The ratio of PEO/PVP was kept the same throughout the experiment since PVP acts as a binder to facilitate the incorporation of the lithium salt within the polymer blend matrix. The concentration of $LiNO_3$ in the SPE samples was varied from 5 weight% to 25 weight% of the total mass 0.45 g of the PEO/PVP blend. The polymers PEO and PVP were dissolved in methanol at room temperature, followed by adding the required amounts of $LiNO_3$ to the polymer blend. The quantity of $LiNO_3$ was adjusted to be 5,10,15,20 and 25 weight percentages of the polymer blend in the final product. The whole mixture was then stirred for 6 hours and the resulting solution was poured onto a well cleaned teflon petri-dish for drying. The solvent methanol was allowed to evaporate slowly at 60 $^{\circ}$C for 24 hours by keeping the petri dish in a vacuum oven. In the final step, free standing, flexible films of the solid electrolyte material were peeled off the petri-dish and stored in an evacuated desiccator to avoid moisture absorption and were used for further investigations. Schematic representation of the formation [30] of Li^+ ion incorporated blend polymer electrolyte film is given in figure 1.

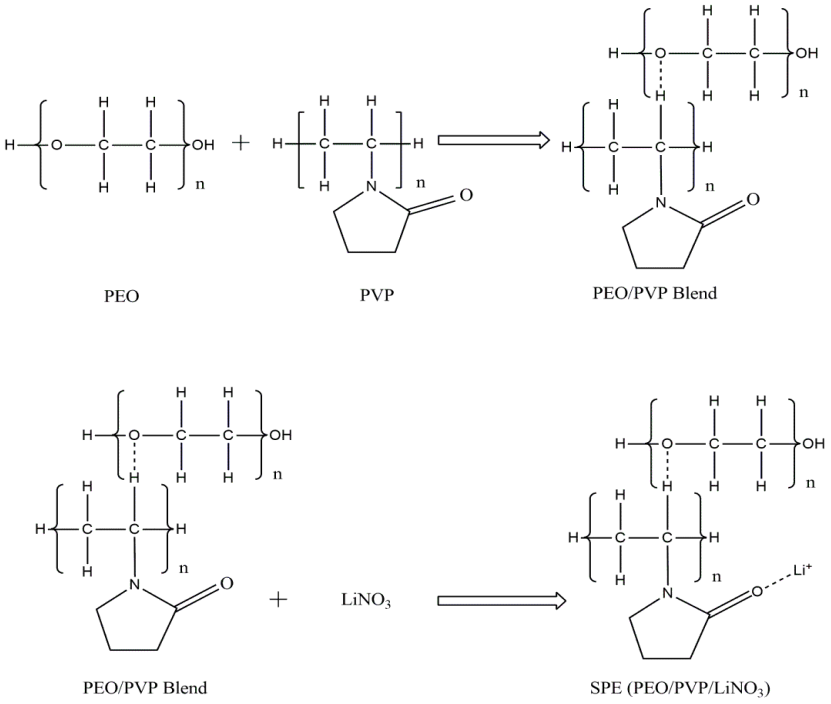

Figure 1: Schematic representation of the formation of Li^+ ion incorporated blend polymer electrolyte film.

3.2.3 Characterization

3.2.3.1 X-Ray diffraction, FTIR spectroscopy, FE-SEM and thermal analysis

Photograph of the freestanding and flexible SPE film is shown in figure 2. The structural aspects of the SPE films were investigated by XRD analysis with the help of a Rigaku Max C diffractometer with Ni filtered Cu Kα radiation of 1.54 A° at 30KV and 20 mA at a scanning rate of 5° per minute from 10° to 50°. The complex formation between the polymer blend and the lithium salt was confirmed by FTIR spectroscopic studies using the SHIMADSU spectrophotometer in the

range of 400–4000 cm^{-1}. Carl Zeiss Sigma FE-SEM instrument was used to study the surface morphology of the SPE films. Thermal stability of the films was studied by thermo-gravimetric analysis using the Perkin Elmer STA 6000 instrument in the temperature range from room temperature to 700 $^{\circ}$C under controlled nitrogen atmosphere. Differential scanning calorimetry (DSC) measurements were done for all the samples at a heating rate of 10 $^{\circ}$C min^{-1} from -90 $^{\circ}$C to 100 $^{\circ}$C under nitrogen atmosphere using the Mettler Toledo DSC 822E machine to find the glass transition temperature and assess the flexibility of polymer chains. Relative percentage of crystallinity was calculated using the equation,

$$\chi_c(\%) = \frac{\Delta H_m^{sample}}{\Delta H_m^0} \text{x}100\% \text{----------} \quad (1)$$

where, ΔH_m^{sample} is the experimentally obtained melting enthalpy and ΔH_m^0 the melting enthalpy for 100 % crystalline PEO, which is referred to as 213.7 J g^{-1}[31].

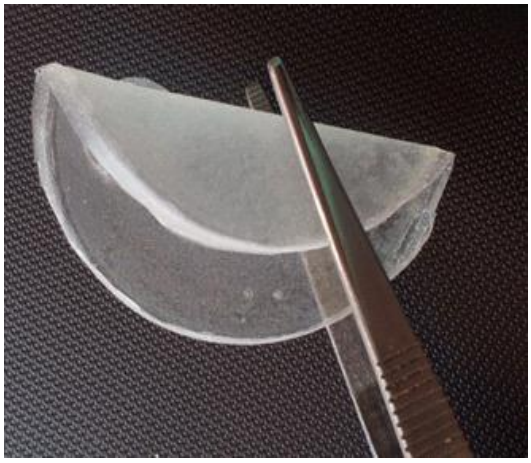

Figure 2: Free standing and flexible SPE film.

3.2.3.2 Electrochemical analysis

The ionic transport properties of the film samples were investigated using HP4192A impedance analyzer in the frequency range from 5 Hz to 1 MHz by sandwiching the SPE film across blocking electrodes made of stainless steel (SS) using Swagelok cells.

Ionic conductivity is calculated using the equation,

$$\sigma = \frac{t}{R_b A} \text{---------- (2)}$$

where t stands for the thickness of the SPE film, R_b is the bulk resistance obtained from the X-axis intercept of the complex AC impedance plot and A is the area of the SPE film [20].

The variation of ionic conductivity of the SPE film with temperature was studied in the temperature range from 288 K to 328 K. Low temperature measurements were carried out using ice. The thermal activation energy for ionic transport was calculated from the slope of the linear fit of the Arrhenius plot. The linear variation in log σ against 1000/T plot suggests a thermally activated process represented by

$$\sigma = \sigma_0 \exp(-E_a/kT) \text{---------- (3)}$$

where σ_0, the pre-exponential factor is a constant and E_a is the thermal activation energy. The parameter T stands for the absolute temperature and k for the Boltzmann constant as explained in the previous chapter

Wagner's DC polarization method was used to calculate the total ionic transport number, t_{ion},as mentioned earlier. By applying a fixed d.c.

voltage (0.5 V) across the specimen with structure SS/ film sample/SS, where SS stands for stainless steel which acts as the blocking electrode, the dc current developed was observed as a function of time. The following equation gives the value of t_{ion},

$$t_{ion}=(i_T-i_e)/i_T \text{ ---------- (4)}$$

Here i_T is the total current and i_e the residual current. The Li-ion transference number was calculated using Evans and Vincent method [32]. Symmetrical cells, with configuration Li/SPE film/Li, using lithium metal electrodes in Swagelok type arrangement were assembled in an argon filled glove box. The details of the transference number calculation are given in the next section.

Linear sweep and cyclic voltammetry characteristics of the SPE films were obtained using Biologic SP 300 unit.

3.3 Results and discussion

3.3.1 XRD analysis

The X-ray diffraction data of pure $LiNO_3$, PEO, PVP and the PEO/PVP blend, complexed with $LiNO_3$ (SPE films) are shown in figure 3. The sample codes A1, A2, A3, A4 and A5 stand for the SPE films with 5,10,15,20 and 25 weight percentages of $LiNO_3$ respectively. The XRD pattern of $LiNO_3$ depicted in figure 3 (a) has an intense peak at $2\theta = 35.59^\circ$ indicating the high extent of crystallinity of the ionic salt. The semi crystalline nature of PEO is evident from the appearance of broad peaks at $2\theta = 18.11^\circ$ and 22.31°, as depicted in figure 3(b), which are the characteristic peaks of PEO. The amorphous nature of pure PVP is clear

from the XRD pattern shown in figure 3(c). The XRD patterns of the SPEs with different weight percentages (5,10,15,20, and 25) of $LiNO_3$ are shown in figures 3(d)–(h). The thorough dispersion of lithium nitrate in the polymer blend matrix can be ascertained from the absence of lithium nitrate peaks in the XRD patterns shown in figures 3 (d)-(h). Absence of XRD peaks representing $LiNO_3$ in the final product confirms the complete dissociation of $LiNO_3$ salt into Li^+ and NO_3^- ions in the blended polymer system. Addition of $LiNO_3$ to the PEO/PVP blend results in the reduction of its crystalline nature and in the final XRD pattern, only those peaks representing the semi-crystalline nature of PEO appear. The relative intensity of the peaks corresponding to PEO is found to be decreasing with the addition of $LiNO_3$ up to 15 weight %, as evidenced from figures 3(d)-(f). Crystallinity of PEO is found to be minimum for the sample A3 having a composition of 15 weight % of $LiNO_3$. When the concentration of $LiNO_3$ is increased above 15 weight %, the crystallinity of SPE films gets slightly increased as shown in figures 3 (g) and (h). Maximum ionic conductivity is observed for the SPE films, having the concentration of 15 weight % of $LiNO_3$. With further increase in the concentration of $LiNO_3$, ionic aggregation takes place which results in the decrease of ionic mobility and ionic conductivity. Rather than contributing towards ionic conductivity, the Li^+ and NO_3^- ions of the additional $LiNO_3$, interact with the polymer back bone of PEO and improve the order/alignment of PEO structure. This results in the observed small increase in the intensity of the characteristic peaks of PEO with the increase in the $LiNO_3$ concentration beyond 15 weight %.

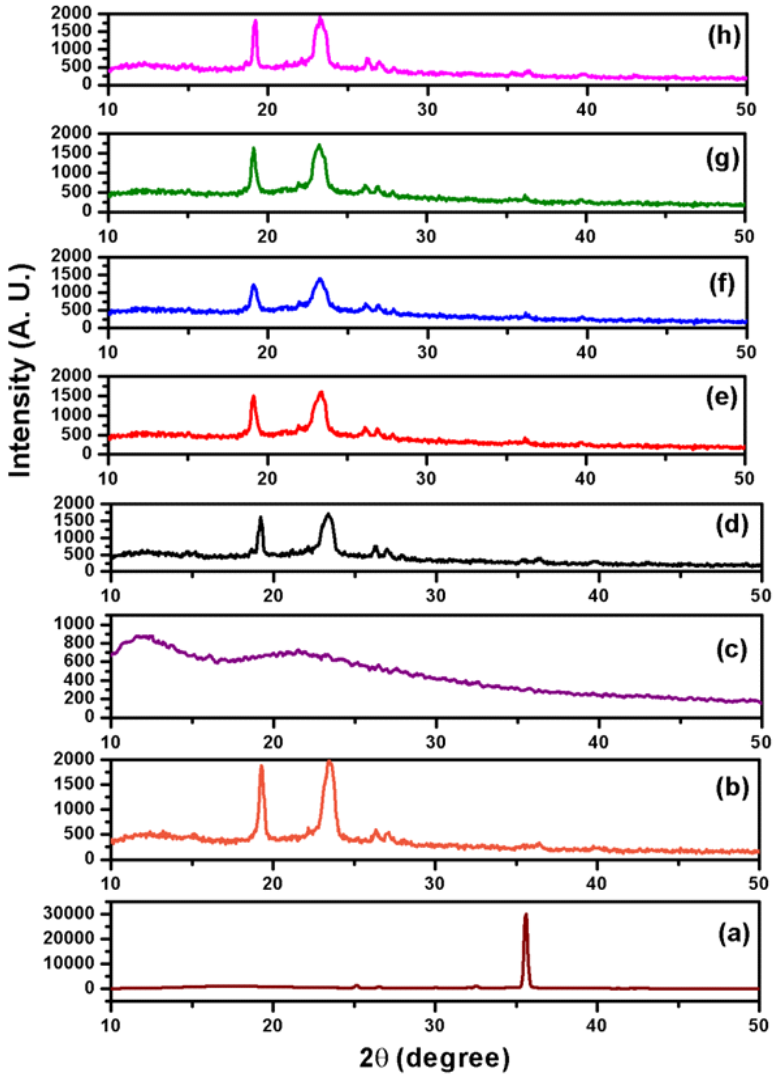

Figure 3: XRD patterns of **(a)** pure $LiNO_3$ **(b)** PEO **(c)** PVP and **(d)-(h)** SPE films - [(d)-(h) correspond to sample codes (A1-A5) respectively]

3.3.2 FTIR spectroscopy studies

The FTIR transmittance spectra of pure $LiNO_3$, PEO, PVP and SPE films are shown in figure 4. In the spectrum of pure $LiNO_3$ shown

in figure 4(a), a strong absorption band is observed at 1384 cm^{-1} corresponding to asymmetric stretching mode of NO_3^- ions. The bands at 1051 and 827 cm^{-1} are ascribed to the symmetric stretching mode and out of plane deformation mode of NO_3^- ions respectively [33].

The vibrational bands of PEO are depicted in figure 4 (b). The CH_2 bending and asymmetric twisting vibrations are observed at 1342 cm^{-1} and 1282 cm^{-1} respectively for pure PEO. The band at 1236 cm^{-1} is attributed to CH_2 symmetric twisting vibration [16]. Strong anti-symmetric stretching vibrations of the CH_2 group [7] give rise to the peak at 845 cm^{-1}. The C–O stretching vibration contributes towards the peak at 947 cm^{-1}. At 1799 cm^{-1}, a small intensity peak is observed, which corresponds to the presence of ether oxygen group of PEO [17]. The band at 2900 cm^{-1} corresponds to C-H stretching of PVP as shown in figure 4(c). Absorption peak at 1452 cm^{-1} is attributed to CH_2 wagging mode of PVP and those at 1650 cm^{-1} and 1234 cm^{-1} respectively are assigned to C=O stretching and C-N stretching modes of PVP. Due to the increase in basicity of C=O group, the spectral perturbation of the carbonyl band in PVP becomes more pronounced [34]. The carbonyl group in PVP interacts with Li^+ ions of $LiNO_3$, which leads to the disruption of crystallization of the complex and consequently the amorphous nature of the complex increases. The vibrational bands of $LiNO_3$ are found to disappear completely in all of the SPE films which confirms the complete dissolution of $LiNO_3$ in the PEO/PVP blend. Characteristic peak positions of PEO and PVP are

found to get slightly shifted with the variation of the amount of the lithium salt in different film samples, as shown in Table 1. With increase in the amount of $LiNO_3$ beyond 15 weight %, the width of the vibrational bands decreases [16] corresponding to a decrease in the amorphous nature of the SPEs.

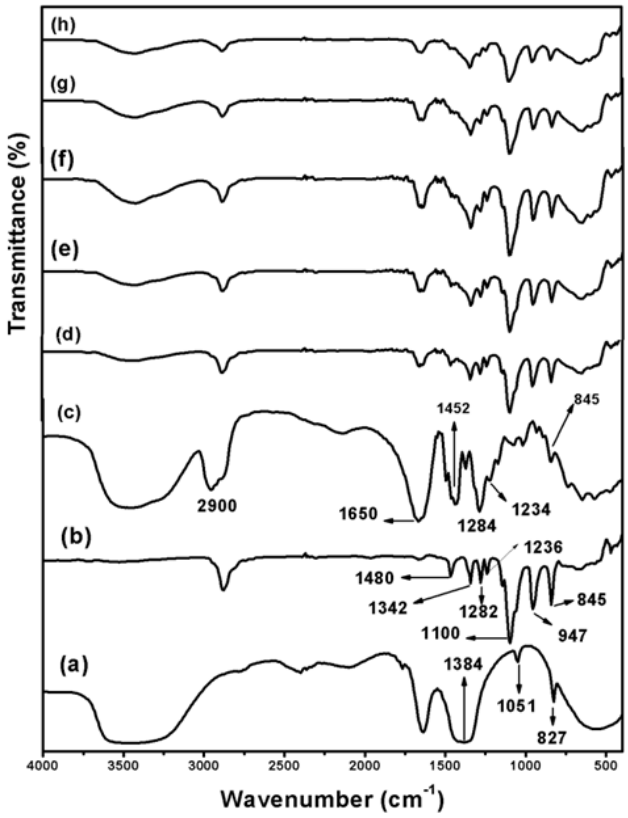

Figure 4: FTIR spectra of **(a)** pure $LiNO_3$ **(b)** PEO **(c)** PVP and **(d)-(h)** SPE films [(d)-(h) correspond to sample codes (A1-A5) respectively]

Table 1: FTIR spectral data of PEO, PVP and SPE films [16, 35]

Band assignments	Wavenumber (cm^{-1})						
	PEO	PVP	SPE films				
	(b)	(c)	(d) A1	(e) A2	(f) A3	(g) A4	(h) A5
Symmetric C-H stretching	-	2900	2891	2882	2885	2881	2882
C=O stretching	-	1650	1649	1650	1650	1648	1648
C-H bending of CH_2	1480	-	1485	1483	1483	1482	1483
CH_2 wagging	-	1452	1445	1458	1449	1457	1459
CH_2 bending	1342	-	1348	1349	1340	1345	1349
Asymmetric CH_2 twisting	1282	1284	1280	1283	1285	1282	1284
CH_2 symmetric twisting	1236	-	1236	1240	1248	1245	1243
C-N stretching	-	1234	1223	1228	1222	1223	1220
Symmetric and asymmetric C-O-C stretching (Amorphous peak)	1100	-	1097	1105	1096	1098	1101
C-O stretching vibration with some CH_2 asymmetric rocking motion	947	-	954	953	954	959	957
CH_2 rocking in PVP and with some C-O stretching in PEO	845	845	846	838	847	845	839

3.3.3 FE-SEM analysis

The FE- SEM images of PEO, PEO/PVP blend and SPE film A3 [PEO/PVP/15weight % of $LiNO_3$] are shown in figure 5. The image of PEO shows several micro-cracks on the sample surface [34] as shown in figure 5(a). The surface roughness is related to the crystalline phase of PEO [35,36]. The image of PEO/PVP blend shown in figure 5(b) indicates a more porous surface morphology compared to PEO. On the addition of lithium salt to the polymer blend PEO/PVP, the surface morphology becomes more smoothened which represents the lowering of PEO crystallinity as shown in figure 5 (c). This lowering of crystallinity leads to the enhanced amorphous nature of the SPE films, which is established from the XRD and FTIR analysis. The enhancement in the porous nature of the PEO/PVP polymer blend and the

PEO/PVP/$LiNO_3$ based SPE films can be observed in figures 5 (b) and (c), due to the presence of PVP, which has been reported to be a pore-forming agent [37]. The average pore size is in the range of ~ 1-2 μm, as seen in the magnified image given in figure 5(d). Porous nature of the films facilitates easier ion penetration, improving total ionic conduction. The presence of smoother and porous surfaces with enhanced amorphous nature, makes SPE films more flexible.

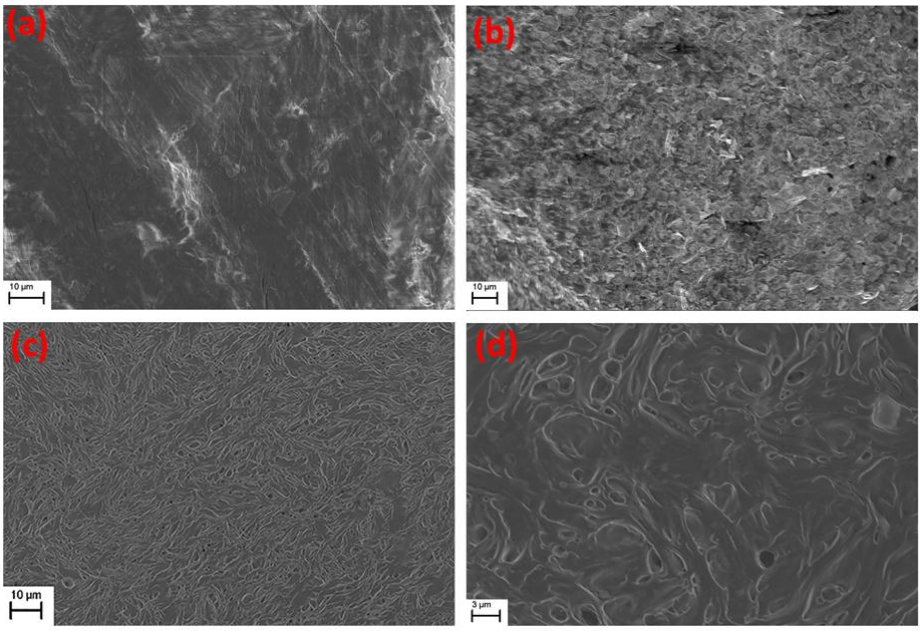

Figure 5: FE-SEM images of **(a)** PEO (b) PEO/PVP blend, **(c)** SPE film A3 (PEO/PVP/15weight % of $LiNO_3$) and **(d)** magnified image of SPE film A3.

3.3.4 Thermal characterization

3.3.4.1 Thermo-gravimetric analysis

Thermal analysis is crucial to investigate the thermal stability of the SPEs when put to practical applications. Under working conditions

of a cell, heat generated in the cell can degrade or melt the solid polymer electrolyte within the cell [34], which in turn may cause internal short circuit. Hence for safe and durable operation of the cell, thermal stability of SPEs is a significant parameter.

The thermo-grams of PEO, PEO/PVP blend and the SPE film A3 are shown in figure 6. There is no initial weight loss observed in the figure which indicates the absence of water absorbed on the surface of the material. It is observed that PEO, PEO/PVP blend and the SPE film A3 are thermally stable up to 340, 420 and 410 $^{\circ}$C respectively with no weight loss. It is also observed that PEO degrades at a comparatively lower temperature than the other two. On adding the lithium salt to the polymer blend, the weight loss curve slightly shifts towards the lower temperature region. The presence of the lithium salt contributes to a small decrease in the thermal stability of the polymer blend system [38]. However, this decrease is quite marginal and the SPE films can hence be considered to exhibit good thermal stability above 400 $^{\circ}$C.

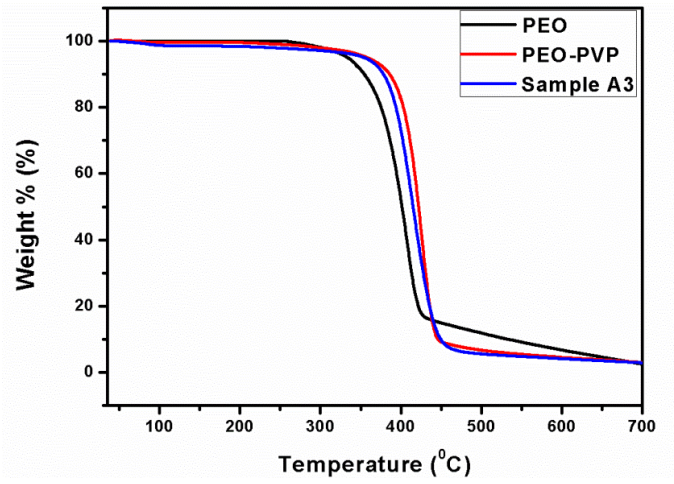

Figure 6: Thermo-grams of PEO, PEO/PVP blend and the SPE film A3.

3.3.4.2 Differential scanning calorimetric (DSC) studies

The DSC curves of PEO, PEO/PVP blend and SPE films are given in figure 7. The values of the glass transition temperature T_g, the melting temperature T_m and the percentage of crystallinity are given in Table 2. Glass transition temperature, T_g of a polymer is concerned with the mobility of the polymer chain and the lowering of T_g value indicates chain relaxation in the polymer system [31]. A shift in T_g value to lower temperatures is observed for the PEO/PVP polymer blend and the SPE film samples in comparison with PEO. For PEO, the T_g value is -65.22 °C which is in accordance with previous reports [15,31]. In the PEO/PVP blend, T_g shifts to -67.19 °C, and with the addition of $LiNO_3$, a continuous shift in the T_g value is observed with the lowest recorded value of -73.9 °C for the SPE film A3 (PEO/PVP/ 15 weight % of $LiNO_3$). Further addition of $LiNO_3$ results in the shift of T_g back to higher temperatures. A similar trend has been observed in the case of the crystallinity of the samples as well. Percentage of crystallinity decreases up to the SPE film A3. For $LiNO_3$ concentration higher than 15 weight %, the ion aggregation takes place resulting in a slight increase of crystallinity. The change in percentage of crystallinity is attributed to the interaction between the polymer backbone and $LiNO_3$. The Li^+ and NO_3^- ions interrupt the packing of polymer backbone and this in turn affects the relative crystallinity. This points out to an increased amorphous nature in the SPE films resulting in more flexible polymeric chains with enhancement in the segmental motion of the polymer electrolyte.

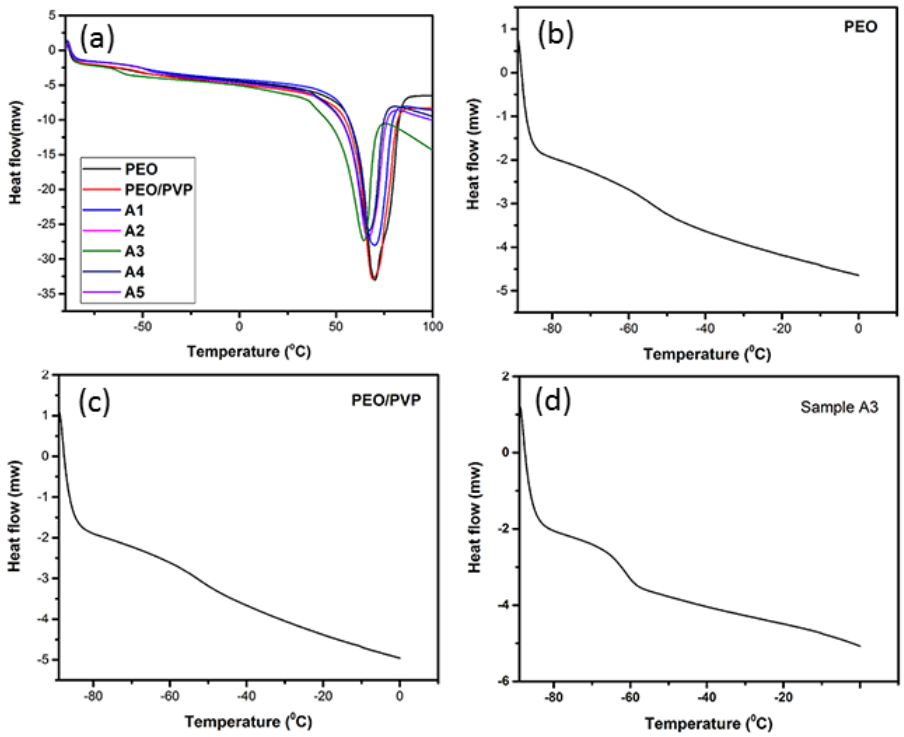

Figure 7: (a) DSC plots of PEO, PEO/PVP and the SPE films with different $LiNO_3$ concentrations; (b) and (c) are the DSC plots of PEO and PEO/PVP respectively indicating the onset of glass transition and (d) is the DSC plot of SPE film A3, showing the onset of glass transition.

An electrolyte with low T_g value always implies fast ion conduction. The decrease in T_g and crystallinity leads to an increased ion transport through the SPE films and this explains their improved ionic conductivity.

Table 2: Thermal properties of PEO, PEO/PVP blend and the SPE films

Sample	T_g (°C)	T_m (°C)	ΔH_m (J g^{-1})	χ_c (%)
PEO	-65.22	69.07	153.37	71.76
PEO/PVP	-67.19	68.13	127.75	59.89
A1	-68.21	66.23	102.32	48.08
A2	-70.01	64.12	92.89	43.46
A3	-73.09	58.35	74.75	34.04
A4	-71.23	63.24	84.82	40
A5	-69.15	66.41	99.12	44.80

3.3.5 A C Conductivity studies

3.3.5.1 Impedance analysis

The major challenge associated with solid polymer electrolytes is the low ionic conductivity at room temperature. The present investigation is hence directed towards identifying solid polymer electrolyte films with high ionic conductivity comparable to that of liquid electrolytes at room temperature. The impedance analysis of the SPE films was carried out using SS/SPE/SS configuration, where SS stands for stainless steel discs which act as blocking electrodes [12] for Li^+ ions under an applied electric field. The complex impedance plots for the SPE films at room temperature are shown in figure 8. The semi-circular portion in the high frequency region of the plots indicates that the conduction is mainly due to ions. In the low frequency region, the presence of the inclined line suggests the effect of the blocking electrodes. The ionic conductivity of the SPE film depends on the concentration of the conducting species and their mobility. High ionic conductivity around 1.13×10^{-3} S cm^{-1} is obtained for the SPE film A3 which contains 15 weight % of $LiNO_3$ in the PEO/PVP polymer blend. The film A3 has lower bulk resistance R_b compared to the other SPE films. It is evident that the low bulk resistance corresponds to high ionic conductivity

as seen in figure 8(a). The room temperature ionic conductivity values for the SPE films A1, A2, A3, A4, and A5 are tabulated in Table 3. The observed room temperature ionic conductivity around $1.13x10^{-3}$ S cm^{-1} for the SPE film A_3 is quite high compared to the previously reported ionic conductivity data for solid polymer electrolytes [3,16,17,24]. It is also observed from Table 3, that the ionic conductivity increases up to 15 weight % of $LiNO_3$ and further increase in $LiNO_3$ concentration results in the decrease of ionic conductivity. This decrease in ionic conductivity is due to the increased ion aggregation which lowers the mobility of ions [39,40]. An equivalent circuit is used to fit the impedance plot of the SPE film A_3 with maximum ionic conductivity as depicted in figure 8 (b). The double layer at the blocking electrodes causes an inclined line instead of a straight line parallel to the imaginary axis. The interfacial impedance for the configuration SS/SPE film/SS can be accounted for by the constant phase element (CPE). The equivalent circuit shown as the inset of figure 8 (b) consists of bulk resistance R_b [41, 42] in parallel with geometrical capacitance Cg and in series with CPE.

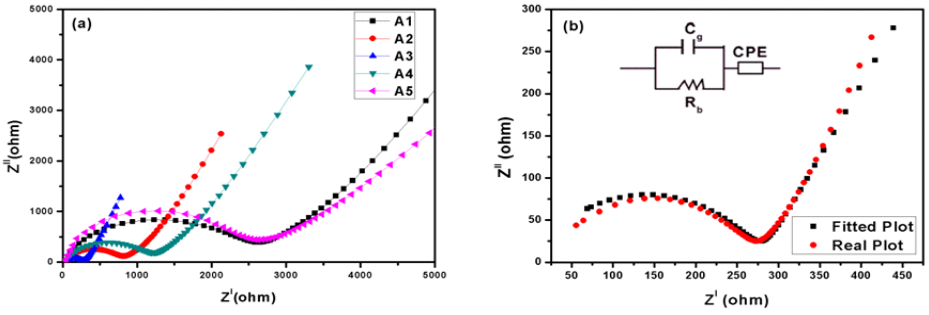

Figure 8: **(a)** Room temperature complex impedance plots. **(b)** The fitting of impedance data for the SPE film A3. Inset of (b) shows the equivalent circuit.

3.3.5.2 Temperature dependence of ionic conductivity

The ionic conductivity of the SPE films was measured in the temperature range of 288K to 328K. At room temperature, maximum ionic conductivity has been observed for the SPE film A3 compared to other compositions. The impedance plots of the SPE film A3 at different temperatures are presented in figure 9 (a). An enhancement in the magnitude of ionic conductivity is observed with increase in measurement temperature [43]. This enhancement is mainly due to increase in ionic mobility and the concentration of carrier ions. It is observed that the real impedance parameter Z^I (diameter of semi-circular arc or R_b value) decreases with increase of temperature which is characteristic of activation of charge carriers between the coordinating sites and the segmental motion of polymeric chains [42]. In order to construct the Arrhenius plot, the working temperature for the impedance measurement has been gradually increased to 328 K.

The dependence of ionic conductivity on the lithium salt concentration for the film A3 at different temperatures is depicted in figure 9 (b). It is observed that ionic conductivity increases with increase of the lithium nitrate concentration until an optimum concentration is reached and there after decreases with further addition of the salt. Beyond the optimum salt concentration, any further addition of the salt results in the formation of ion pairs and ion clusters, which cause constraints to ionic and polymeric segmental mobility [44,45]. The ionic conductivity reaches the maximum value at the optimum concentration of 15 weight % of $LiNO_3$. Higher concentrations might result in the aggregation of free

ions and the crystallization of $LiNO_3$ in PEO/PVP blend system, which results in the decreases of ionic conductivity of the SPE film. Moreover, higher ionic conductivity is observed with decreased crystallinity as seen in the case of the SPE film A3 shown in figure 3(f), with 15 weight % of $LiNO_3$, compared to other compositions. This result is in good agreement with the X-ray diffraction studies [46].

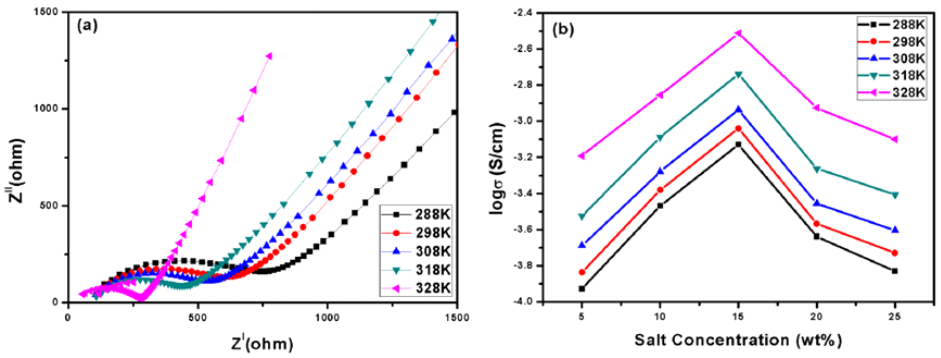

Figure 9: **(a)** Impedance plots of the SPE film A3 at different temperatures. **(b).** Effect of salt concentration on the ionic conductivity of the SPE film A3 at different temperatures.

3.3.5.3 Thermal activation energy measurement

The thermal activation energy is calculated from the slope of the linear portion of the Arrhenius plots shown in figure 10. The energy of defect formation and that of ion migration together is referred to as the activation energy [47,48]. The calculated activation energy E_a is the energy that facilitates the conditions suitable for the migration of ions. From the observed results, the SPE film A3 which has the highest ionic conductivity has the lowest activation energy compared to other samples. For the film A3, the softening and the melting of the crystalline phase of PEO lead to the decrease in activation energy and the increase

in ionic conductivity. The values of conductivity and activation energy for different SPE film samples are shown in Table 3. The activation energy of all the SPE films lies in the range 0.1 eV to 0.2 eV, which is the optimum thermal activation energy estimated for good electrolyte materials for Li ion cell applications.

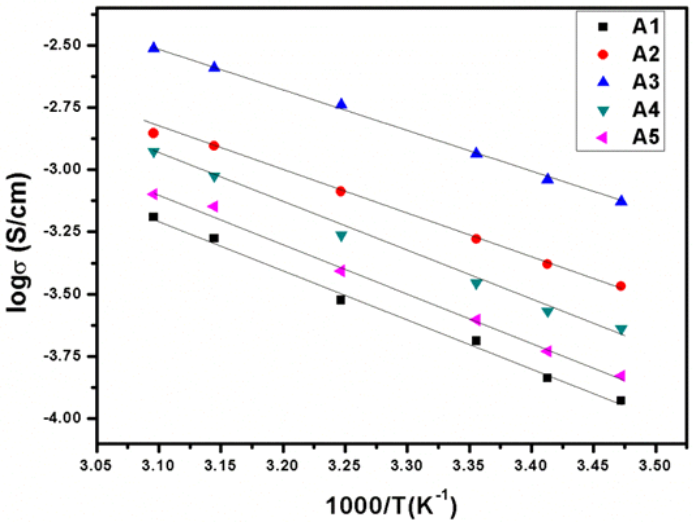

Figure 10: Arrhenius plots for SPE films

Table 3: Room temperature ionic conductivity and thermal activation energy of the SPE films

Sample code	Weight percentage of $LiNO_3$ (%)	Ionic conductivity at room temperature (S cm^{-1})	Activation energy, Ea (eV)
A1	5	$1.20x10^{-4}$	0.170
A2	10	$3.7x10^{-4}$	0.158
A3	15	$1.13x10^{-3}$	0.139
A4	20	$2.6x10^{-4}$	0.167
A5	25	$1.22x10^{-4}$	0.173

3.3.6 Ion transport number and transference number measurement

Wagner's DC polarization technique is one of the important methods to calculate the total ion transport number [23] and the experimental data is given in figure 11. Theoretical value of total ion transport number is unity. The value of the total ion transport number, t_{ion} for the highest ionic conducting, SPE film A3 is found to be 0.9997 using equation (4). This result indicates that the overall conductivity of the SPE films is predominantly ionic [49] and the ion transport number is quite comparable with the theoretical value.

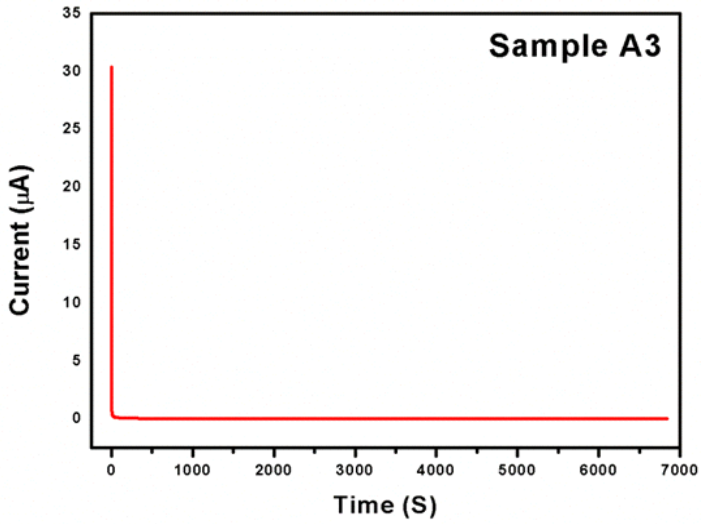

Figure 11: The variation of current with respect to time across the cell with configuration SS/SPE film A3/SS

Evans and Vincent method was used to find the lithium ion transference number. On applying a potential of 1V to the assembled cell with the configuration, Li/SPE film A3/Li, the initial current through the cell was found to decrease with time until a steady state value [50] was obtained as shown in figure 12 (a). The decrease in current is due to the

formation of a concentration gradient across the cell. The number of active charge carriers decreases and as a result current also decrease. The current carried by lithium ions is the same at the beginning of the experiment corresponding to t=0 and at steady state, t=infinity. They are the only charge carrying species in the steady state and contribute towards the steady state current. The Li ion transference number can calculated using the equation,

$$t_{Li}=i_{ss}/i_o \text{---------- (5)}$$

where i_o is the initial current and i_{ss} , the steady state current. The above equation representing ideal conditions has to be modified to account for the possibility of the formation of passivation layers [32] on the surface of the lithium electrodes. The reactions occurring on the electrode surfaces affect the steady state current. Hence some additional terms are included in equation (5), to calculate the lithium ion transference number and the modified equation is,

$$t_{Li}= \frac{i_{ss}(\Delta V - i_o R_o^I)}{i_o(\Delta V - i_{ss} R_{ss}^I)} \text{ ---------- (6)}$$

where ΔV is the applied voltage, also known as the polarizing voltage and i is the current. The subscripts o and ss denote the initial and the steady state values respectively. Sum of the charge transfer resistance R_{ct} and the passivation layer resistance R_{film} gives the value of R^I. R_o^I and R_{ss}^I can be obtained from the impedance plots given in figure 12(b), before the polarization and after the steady state has been reached.

The equivalent circuit for deconvolution of the electrochemical impedance plot is shown in the inset of figure 12(b), which consists of

pure resistive and pure capacitive elements in parallel. The pure capacitive elements are replaced by constant phase elements. From the impedance plot, the diameter of the semicircle is approximately equal to the sum of R_{ct} and R_{film}. The Li ion transference number calculated from equation (6) is 0.332. Theoretically predicted, lithium ion transference number is less than 0.5 [51]. Hence the present calculation of lithium ion transference number is in good agreement with the theoretical value.

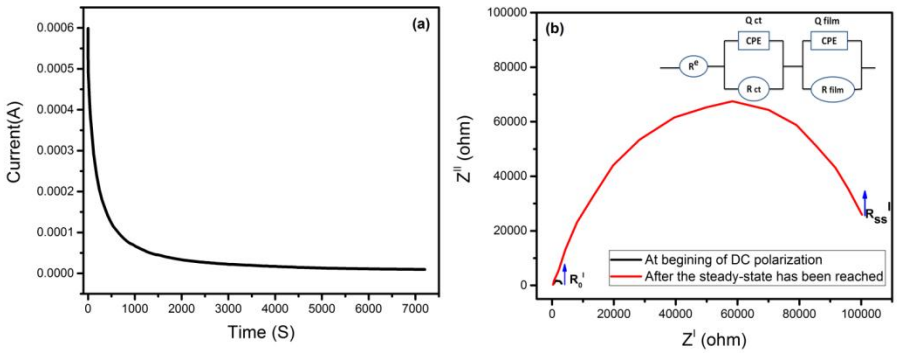

Figure 12: **(a)** Polarization curve of the cell. **(b)** Impedance plots of the cell before polarization and after the steady state has been reached. Inset of (b) represents the equivalent circuit for deconvolution of the electrochemical impedance plot.

3.3.7 Electrochemical stability studies

Electrolyte stability is an important parameter that determines the maximum potential limits possible for device applications [52]. Electrochemical stability defines a reliable potential window for the electrolyte. Linear sweep voltammetry is used to study the electrochemical stability window of the SPEs in the configuration of SS/SPE film/Li, using Swagelok type cell at room temperature [3]. Measurements were carried out within the potential window of 1 to 6V (versus Li/Li^+) at a scan rate of 5 mV s^{-1}. Due to the decomposition of the

electrolyte, a sudden increase of current is observed around 5V indicating the anodic break down of the electrolyte film. The PEO/PVP/$LiNO_3$ based solid electrolyte film is stable up to at least 4.8 V versus Li/Li^+, which is clear from figure 13 (a). Previous reports on PEO based polymer electrolytes show stability windows up to 4V (versus Li/Li^+) [3,4,53,54]. The synthesized SPE films of the present work, based on PEO/PVP/$LiNO_3$, are stable up to 4.8V, which highlights their prospective applications as potential candidates in the design of high voltage, solid state Li ion cells. The cyclic voltammetry (CV) study of the SPE film A3 was carried out for 5 cycles at a scan rate of 0.5 mV s^{-1}, in which the SPE film was placed between two stainless steel electrodes [55,56]. The CV curves shown in figure 13 (b), establish the repeatability and the electrochemical stability of the SPE film in the voltage range up to 5V. The absence of oxidation-reduction peaks in the CV curves indicates good electrochemical stability of the film.

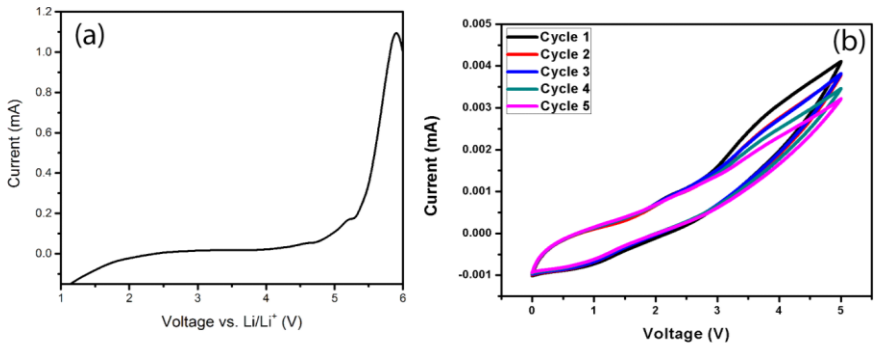

Figure 13: **(a)** Linear sweep voltammetry curve of Li/SPE film A3/SS. **(b)** Cyclic voltammetry curves of the system, SS/SPE film A3/SS

3.4 Conclusions

The present study introduces a novel type of solid polymer electrolyte (SPE), based on lithium enriched PEO/PVP polymer blend. These SPE films are obtained as free standing and flexible films using the simple technique of solution casting. Reduced crystallinity of the PEO/PVP/$LiNO_3$ based SPE films and the complex formation between the polymer blend and the lithium salt are confirmed from XRD and FTIR spectroscopic studies. The smooth surface morphology and the porous nature of the SPE films are established from the FE-SEM analysis. These SPE films are found to exhibit excellent thermal stability above 400 $^{\circ}$C. The maximum room temperature ionic conductivity observed for these films is 1.13×10^{-3} S cm^{-1}, which is quite close to that of liquid electrolytes. They are electrochemical stable up to 4.8V. The highlight of the work presented in this chapter is the identification of this unique type of solid polymer electrolyte films with quite impressive electrochemical characteristics. They are highly flexible and can be obtained as free standing films. They offer excellent application prospects in the development of all solid state Li ion cells, capable of giving stable and safe operation at room temperature and at much higher temperatures as well.

3.5 References

[1] J. M. Tarascon,M. Armand, Issues and challenges facing rechargeable lithium batteries, Nature, 414 (2001) 359–367.

[2] Y. Zhao, C. Wu, G. Peng, X. Chen, X. Yao, Y. Bai, et al., A new solid polymer electrolyte incorporating Li 10 GeP 2 S 12 into a polyethylene oxide matrix for all-solid-state lithium batteries, J. Power Sources. 301 (2016) 47–53.

[3] B. Liang, S. Tang, Q. Jiang, C. Chen, X. Chen, S. Li, et al., Preparation and characterization of PEO-PMMA polymer composite electrolytes doped with nano-Al_2O_3, Electrochim. Acta. 169 (2015) 334–341.

[4] M. Ueno, N. Imanishi, K. Hanai, T. Kobayashi, A. Hirano, O. Yamamoto, et al., Electrochemical properties of cross-linked polymer electrolyte by electron beam irradiation and application to lithium ion batteries, J. Power Sources. 196 (2011) 4756–4761.

[5] Y. Sun, J. Zhang, T. Huang, Z. Liu, A. Yu, Fe 2 O 3 / CNTs Composites as Anode Materials for Lithium-Ion Batteries,Int. J. Electrochem. Sci., 8 (2013) 2918–2931.

[6] M Armand, Extended Abstracts Second International Conference on Solid Electrolytes JM Chabagno, M Duclot -St Andrews, Scotland, (1978).

[7] A.B. Puthirath, B. John, C. Gouri, S. Jayalekshmi, Lithium-doped PEO—a prospective solid electrolyte with high ionic conductivity, developed using n-Butyllithium in hexane as dopant, Ionics (Kiel). 21 (2015) 2185–2191.

[8] J.W. Fergus, Ceramic and polymeric solid electrolytes for lithium-ion batteries, J. Power Sources. 195 (2010) 4554–4569.

[9] R.C. Agrawal, G.P. Pandey, Solid polymer electrolytes: materials designing and all-solid-state battery applications: an overview, J. Phys. D. Appl. Phys. 41 (2008) 223001.

[10] F. M. Gray, Solid polymer electrolytes: Fundamentals and technological applications, VCH, New York, (1991).

[11] B. Scrosati (Ed.) Application of Electroactive Polymers, Chapman & Hall, London, (1993).

[12] W. Liu, N. Liu, J. Sun, P.C. Hsu, Y. Li, H.W. Lee, et al., Ionic Conductivity Enhancement of Polymer Electrolytes with Ceramic Nanowire Fillers, Nano Lett. 15 (2015) 2740–2745.

[13] H. Zhang, Preparation and characterization of composite electrolytes based on PEO(375)-grafted fumed silica, Solid State Ionics. 178 (2008) 1975–1983.

[14] C.H. Manoratne, R.M.G. Rajapakse, M. a K.L. Dissanayake, Ionic Conductivity of Poly (ethylene oxide) (PEO) - Montmorillonite (MMT) Nanocomposites Prepared by Intercalation from Aqueous Medium, Int. J. Electrochem. Sci. 1 (2006) 32–46.

[15] M.R. Johan, L.M. Ting, Structural, Thermal and Electrical Properties of Nano Manganese-Composite Polymer Electrolytes, Int. J. Electrochem. Sci. 6 (2011) 4737–4748.

[16] K. Kesavan, C.M. Mathew, S. Rajendran, M. Ulaganathan, Preparation and characterization of novel solid polymer blend electrolytes based on poly (vinyl pyrrolidone) with various concentrations of lithium perchlorate, Mater. Sci. Eng. B. 184 (2014) 26–33.

[17] K. Kesavan, C.M. Mathew, S. Rajendran, Lithium ion conduction and ion-polymer interaction in poly(vinyl pyrrolidone) based electrolytes blended with different plasticizers, Chinese Chem. Lett. 25 (2014) 1428–1434.

[18] G.B. Appetecchi, M. Montanino, A. Balducci, S.F. Lux, M. Winter, S. Passerini, Erratum: Lithium insertion in graphite from ternary ionic liquid-lithium salt electrolytes I. Electrochemical characterization of the electrolytes (Journal of Power Sources (2009) 192 (599-605)), J. Power Sources. 219 (2012) 371.

[19] B. Scrosati, C. a. Vincent, Polymer Electrolytes: The Key to Lithium Polymer Batteries, MRS Bull. 25 (2000) 28.

[20] R. Prasanth, N. Shubha, H.H. Hng, M. Srinivasan, Effect of poly(ethylene oxide) on ionic conductivity and electrochemical properties of poly(vinylidenefluoride) based polymer gel electrolytes prepared by electrospinning for lithium ion batteries, J. Power Sources. 245 (2014) 283–291.

[21] X. Zhang, K. Takegoshi, K. Hikichi, High-resolution solid-state 13C nuclear magnetic resonance study on poly(vinyl alcohol)/poly(vinylpyrrolidone) blends, Polymer (Guildf). 33 (1992) 712–717.

[22] H. Feng, Z. Feng, L. Shen, A high resolution solid - state n .m .r .and d . s .c .study of miscibility and crystallization behaviour of poly (vinyl alcohol) poly (N - vinyl - 2 - pyrrolidone) blends, Polymer. 34 (1993) 2516–2519.

[23] A.R. Polu, R. Kumar, H.W. Rhee, Magnesium ion conducting solid polymer blend electrolyte based on biodegradable polymers and application in solid-state batteries, Ionics (Kiel). (2014) 125–132.

[24] K.K. Kumar, M. Ravi, Y. Pavani, S. Bhavani, A.K. Sharma, V.V.R.N. Rao, Investigations on the effect of complexation of NaF salt with polymer blend (PEO/PVP) electrolytes on ionic conductivity and optical energy band gaps, Phys. B Phys. Condens. Matter. 406 (2011) 1706–1712.

[25] S. Ibrahim, M.M. Yassin, R. Ahmad, M.R. Johan, Effects of various LiPF 6 salt concentrations on PEO-based solid polymer electrolytes, Ionics 17 (2011) 399–405.

[26] C.V.S. Reddy, W. Chen, S. Mho, Mesoporous silica (MCM-41) effect on (PEO + LiAsF 6) solid polymer electrolyte, Current Applied Physics, 7 (2007) 655–661.

[27] Z. Xue, D. He, X. Xie, Poly(ethylene oxide)-based electrolytes for lithium-ion batteries, J. Mater. Chem. A. 3 (2015) 19218–19253.

[28] Y. Ma, L.B. Li, G.X. Gao, X.Y. Yang, Y. You, ElectrochimicaActa Effect of montmorillonite on the ionic conductivity and electrochemical properties of a composite solid polymer electrolyte based on polyvinylidenedifluoride / polyvinyl alcohol matrix for lithium ion batteries, ElectrochimicaActa, 187 (2016) 535–542.

[29] K.N. Kumar, M. Kang, K. Sivaiah, M. Ravi, Y.C. Ratnakaram, Enhanced electrical properties of polyethylene oxide (PEO) + polyvinylpyrrolidone (PVP): Li + blended polymer electrolyte films with addition of Ag nanofiller, Ionics (Kiel). 22 (2016) 815–825.

[30] S. Chapi, S. Raghu, H. Devendrappa, Enhanced electrochemical, structural, optical , thermal stability and ionic conductivity of (PEO / PVP) polymer blend electrolyte for electrochemical applications, Ionics. 22 (2016) 803-814.

[31] S. Ibrahim, M. R. Johan, Thermolysis and Conductivity Studies of Poly(Ethylene Oxide) (PEO) Based Polymer Electrolytes Doped with Carbon Nanotube, Int. J. Electrochem. Sci., 7 (2012) 2596 – 2615.

[32] J. Zhao, L. Wang, X. He, C. Wan, C. Jiang, Determination of Lithium-Ion Transference Numbers in LiPF 6 – PC Solutions Based on Electrochemical Polarization and NMR Measurements, J. Electrochem. Soc. 155 (2008) 292–296.

[33] M. Sulaiman, A.A. Rahman, N.S. Mohamed, Effect of water-based sol gel method on structural, thermal and conductivity properties of LiNO3-Al2O3 composite solid electrolytes, Arab. J. Chem. (2015).

[34] K.K. Kumar, M. Ravi, Y. Pavani, S. Bhavani, A.K. Sharma, V.V.R.N. Rao, Investigations on PEO/PVP/NaBr complexed polymer blend electrolytes for electrochemical cell applications, J. Memb. Sci. 454 (2014) 200–211.

[35] P.P. Chu, M.J. Reddy, H.M. Kao, Novel composite polymer electrolyte comprising mesoporous structured SiO 2 and PEO / Li, Solid State Ionics. 156 (2003) 141–153.

[36] Y.L. Yap, A.H. You, L.L. Teo, H. Hanapei, Inorganic Filler Sizes Effect on Ionic Conductivity in Polyethylene Oxide (PEO) Composite Polymer Electrolyte, Int. J. Electrochem. Sci. 8 (2013) 2154–2163.

[37] J. Qiao, J. Fu, R. Lin, J. Ma, J. Liu, Alkaline solid polymer electrolyte membranes based on structurally modi fi ed PVA / PVP with improved alkali stability, Polymer (Guildf). 51 (2010) 4850–4859.

[38] A.F. Nogueira, M.A.S. Spinace, W.A. Gazotti, E.M. Girotto, M. De Paoli, Poly ž ethylene oxide- co -epichlorohydrin / r NaI : a promising polymer electrolyte for photoelectrochemical cells, Solid State Ionics. 140 (2001) 327–335.

[39] S.A. Suthanthiraraj, D.J. Sheeba, Structural investigation on PEO-based polymer electrolytes dispersed with Al 2 O 3 nanoparticles,Ionics, 13 (2007) 447–450.

[40] B. Scrosati, F. Croce, L. Persi, Impedance Spectroscopy Study of PEO-Based Nanocomposite Polymer Electrolytes, Journal of The Electrochemical Society, 147 (2000) 1718–1721.

[41] R.J. Sengwa, P. Dhatarwal, S. Choudhary, Role of preparation methods on the structural and dielectric properties of plasticized polymer blend electrolytes: Correlation between ionic conductivity and dielectric parameters, Electrochim. Acta. 142 (2014) 359–370.

[42] N. Chilaka, S. Ghosh, Dielectric studies of poly (Ethylene glycol)-polyurethane/poly (Methylmethacrylate)/ montmorillonite composite, Electrochim. Acta. 134 (2014) 232–241.

[43] W. Zhai, H.J. Zhu, L. Wang, X.M. Liu, H. Yang, Study of PVDF-HFP/PMMA blended micro-porous gel polymer electrolyte incorporating ionic liquid [BMIM]BF4 for Lithium ion batteries, Electrochim. Acta. 133 (2014) 623–630.

[44] S. Rajendran, M. Sivakumar, R. Subadevi, Effect of salt concentration in poly(vinyl alcohol)-based solid polymer electrolytes, J. Power Sources. 124 (2003) 225–230.

[45] X.H. Flora, M. Ulaganathan, S. Rajendran, Influence of lithium salt concentration on PAN-PMMA blend polymer electrolytes, Int. J. Electrochem. Sci. 7 (2012) 7451–7462.

[46] M. Ulaganathan, S.S. Pethaiah, S. Rajendran, Li-ion conduction in PVAc based polymer blend electrolytes for lithium battery applications, Mater. Chem. Phys. 129 (2011) 471–476.

[47] F. Latif, M. Aziz, N. Katun, A.M.M. Ali, M.Z. Yahya, The role and impact of rubber in poly(methyl methacrylate)/ lithium triflate electrolyte, J. Power Sources. 159 (2006) 1401–1404.

[48] A.A. Mohamad, N.S. Mohamed, M.Z.A. Yahya, R. Othman, S. Ramesh, Y. Alias, et al., Ionic conductivity studies of poly(vinyl alcohol) alkaline solid polymer electrolyte and its use in nickel-zinc cells, Solid State Ionics. 156 (2003) 171–177.

[49] S.K. Deraman, N.S. Mohamed, R.H.Y. Subban, Conductivity and electrochemical studies on polymer electrolytes based on poly vinyl (chloride) - ammonium triflate-ionic liquid for proton battery, Int. J. Electrochem. Sci. 8 (2013) 1459–1468.

[50] S. Zugmann, M. Fleischmann, M. Amereller, R.M. Gschwind, H.D. Wiemhöfer, H.J. Gores, ElectrochimicaActa Measurement of transference numbers for lithium ion electrolytes via four different methods , a comparative study, Electrochim. Acta. 56 (2011) 3926–3933.

[51] M. Doyle, T. F. Fuller, J. Newman, The importance of the lithium ion transference number in lithium/polymer cells, Electrochim.Acta. 39 (1994) 2073-2081.

[52] D. Chen, J. Cheng, Y. Wen, G. Cao, Y. Yang, H. Liu, Impedance Study of Electrochemical Stability Limits for Electrolytes, Int. J. Electrochem. Sci. 7 (2012) 12383–12390.

[53] X. Zhang, C. Wang, A.J. Appleby, F.E. Little, Characteristics of lithium-ion-conducting composite polymer-glass secondary cell electrolytes, Journal of Power Sources, 112 (2002) 209–215.

[54] Y. Kim, E.S. Smotkin, The effect of plasticizers on transport and electrochemical properties of PEO-based electrolytes for lithium rechargeable batteries, Solid State Ionics, 149 (2002) 29–37.

[55] N. Vassal, E. Salmon, J.F. Fauvarque, Electrochemical properties of an alkaline solid polymer electrolyte based on P(ECH-co-EO), Electrochim. Acta. 45 (2000) 1527–1532.

[56] S. Rajendran, M. Sivakumar, R. Subadevi, Investigations on the effect of various plasticizers in PVA-PMMA solid polymer blend electrolytes, Mater. Lett. 58 (2004) 641–649.

Chapter 4

Realizing all solid state Li ion cells using solid polymer electrolyte films

The work presented in this chapter deals with the attempts carried out to practically accomplish the assembling of two different types of all solid state Li ion half cells for 3.2V and 5V, using the eco-friendly materials $LiFePO_4$ and $LiNiMnO_4$ as the cathode active materials respectively and lithium foil as the anode. The solid polymer electrolyte films based on PEO/PVP/$LiNO_3$, possessing the maximum Li ion conductivity at room temperature are used to serve as the solid electrolyte as well as the separator. The structural and electrochemical studies of the synthesized cathode materials are carried out. The performance of the assembled Li ion cells is assessed based on detailed electrochemical evaluation.

4.1 Introduction

The high gravimetric energy density and charge storage capacity of the Li ion cells make them quite attractive for applications as the power sources for lap-top computer and cellular telephone. However, cost, safety, stored energy density, charge/discharge rates, and service life are issues that continue to hinder their development for the potential mass market of electric vehicles to alleviate distributed CO_2 emissions and noise pollution. The choice of active materials in the individual cells

of a secondary battery, which consist of the cathode (positive electrode), the anode (negative electrode), and the electrolyte between the electrodes is crucial in the design of cells with desired performance efficiency [1]. One of the key challenges for adopting the lithium ion cell technology for powering the electric vehicles (EV), hybrid electric vehicles (HEV) and plug-in hybrid electric vehicles (PHEV) is the development of suitable high energy density cathode materials [2,3].

High energy density can be achieved for the Li ion cells by having either high voltage or high capacity. Many studies are going on the development of future generation cathode materials because the materials with promising theoretical properties have high potentials to serve the purpose. [4]. For cathode materials like lithium iron phosphate $LiFePO_4$, significant property improvements have been achieved during the past decade with the assistance of newly developed technologies. This material can be reversibly charged and discharged at a stable voltage of 3.2 V vs Li^+/Li [5]. The most promising candidate among the 5 V cathode materials for Li cells is the high-voltage, lithium nickel manganese oxide, $LiNiMnO_4$ [6]. Attempts are carried out, in the present work to realize all solid state Li ion cells using $LiFePO_4$ (3.2V) and $LiNiMnO_4$ (5V) as the cathode active materials, lithium as the anode and solid polymer electrolyte films as the electrolyte cum separator.

The material, $LiFePO_4$ has drawn attention as a potential cathode material for lithium ion cells, since the pioneering work by Goodenough and his co-workers due to its advantages of low cost, the relatively high theoretical specific capacity around 170 mAh g^{-1}, good cycling stability and nontoxicity [7, 8]. It is quite environmentally friendly compared to the

already commercialized cathode material, $LiCoO_2$ which is highly toxic. The other prospective cathode material $LiMn_2O_4$ although less toxic and much cheaper, suffers from Jahn-Teller distortion near room temperature, which significantly reduces the specific capacity of the cell. $LiFePO_4$ is free from such inherent defects, is highly cost effective and environment friendly [9]. Many synthesis methods have been reported to obtain $LiFePO_4$ with fine particle size, including sol-gel technique, hydrothermal method [7,10,11] and co-precipitation technique. In the present work, the easy, fast, and cost-effective, sol-gel method [12] is used to synthesize $LiFePO_4$.

High-voltage lithium-ion cells offer new possibilities for the next generation rechargeable batteries with high energy density. The high thermodynamic stability, moderate theoretical discharge capacity and stable discharge platform are some of the advantages of the $LiNiMnO_4$ cathode [13,14]. With the spinel structure, it is considered as one of the most promising cathode materials, due to the easier availability of the raw materials for its synthesis, superior rate capability due to the rapid three-dimensional lithium ion conduction, and most importantly its high energy density because of the high discharge plateau of about 4.7 V vs Li^+/ Li [15, 16] and large specific capacity around 146.6 mAh g^{-1} [6]. The progress in the development of high-voltage cathode materials and the corresponding matched electrolytes is summarized by Hu and co-workers in 2013 [17]. In 2017, XiaoLong Xu's group has investigated strategies for improving the cycling stability of high- voltage $LiNi_{0.5}Mn_{1.5}O_4$ cathode in lithium-ion cells [6].

For assembling all solid state Li-ion cells, solid polymer electrolytes (SPE) are quite attractive to serve as the electrolyte and the separator.

Polymer electrolytes offer pronounced advantages over conventional liquid electrolytes. These include the flexibility in the shape design, high mechanical strength and stable contact between the electrode and the electrolyte interfaces. Solid electrolytes are much safer than liquid electrolytes as the former do not have leakage problems and are non-toxic and non-flammable [18-20]. Our group has developed a novel type of solid polymer electrolyte for solid state lithium battery applications based on lithium enriched poly (ethylene oxide) (PEO)/poly (vinyl pyrrolidone) (PVP) blend polymer [9], the details of which are given in chapter 3. These SPE films based on PEO-PVP-$LiNO_3$ have quite high room temperature ionic conductivity around 1.13×10^{-3} S cm^{-1}, comparable to that of liquid electrolytes and are suitable for applications in all solid state Li ion cells. The all solid state Li ion cells for two voltages are assembled in the argon filled glove box to avoid moisture exposure

The structural characterizations of the synthesized cathode materials are done using XRD, FTIR spectroscopy and FE-SEM techniques and the electrochemical characterization of the assembled cells, using cyclic voltammetry and galvanostatic charge discharge testing.

4.2 Experimental details

4.2.1 Materials and methods

4.2.2 Synthesis of $LiFePO_4$ cathode material

The chemicals, ferrous oxalate dihydrate, lithium nitrate, ammonium dihydrogen phosphate, citric acid and nitric acid, all of AR grade, were purchased from Alpha Chemicals, India. Stoichiometric amounts of lithium nitrate and ferrous oxalate dihydrate were dissolved in

1 M nitric acid solution into which 20 ml citric acid solution was added drop wise with continuous stirring. A saturated solution of ammonium dihydrogen phosphate was added to the above solution. To remove the excess water, the mixture was heated gently at 50 °C with continuous stirring for 4 hours. The resulting gel precursor was dried in a circulation oven for a week at 80 °C and then fired at 700 °C in a tubular furnace under 99.99 % flowing argon for 2 hours to get $LiFePO_4$ powder, titled as LFP. In the above experiment, which is schematically shown in figure 1, the molarity of the citric acid solution was fixed at 1 M [5].

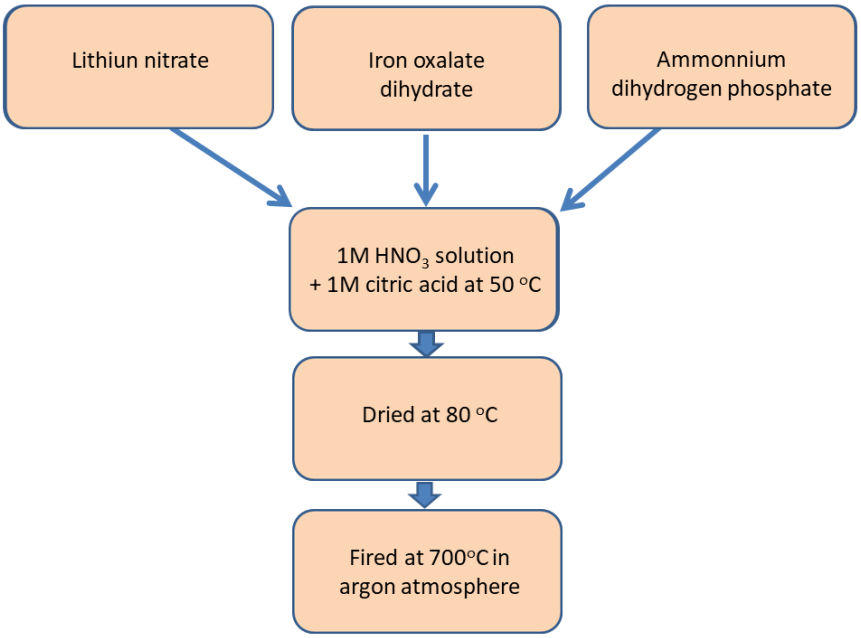

Figure 1: The schematic representation of the synthesis of LFP cathode material

4.2.3 Synthesis of $LiNi_{0.5}Mn_{1.5}O_4$ cathode material

The chemicals, $LiNO_3$, $Ni(NO_3)_2{\cdot}6H_2O$, and $Mn(CH_2COO)_2{\cdot}4H_2O$ in the molar ratio 1:0.05:1.5 were dissolved in water and then 5ml

hydrazine hydrate was added and heated. The resulting gel was dried at 100 °C using vacuum oven. This precursor was powdered using an agate mortar and calcinated at 450 °C for 3 hours and then fired at 600 °C for 8 hours in air to obtain the final product, $LiNi_{0.5}Mn_{1.5}O_4$. The synthesized $LiNi_{0.5}Mn_{1.5}O_4$ is titled as LNM. The synthesis route is schematically shown in figure 2.

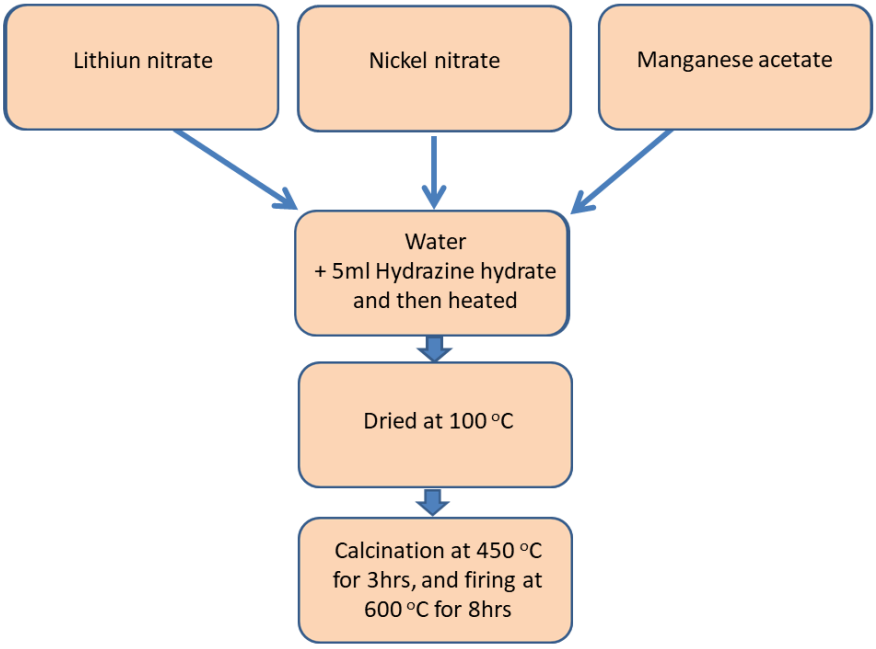

Figure 2: The schematic representation of the synthesis of LNM cathode material

4.2.4 Electrode making

The LFP and LNM based cathodes were prepared by mixing 90 weight % of the active materials LFP and LNM, 10 weight % of conducting carbon and 10 weight % of poly(vinylidene difluoride) (PVdF), in the presence of N-methyl pyrrolidinone (NMP), to make a

slurry. It was coated on aluminum sheet and heated at 120 °C under vacuum overnight.

The electrochemical behaviour of the LFP and LNM was investigated by assembling prototype lithium half cells using lithium metal as the counter electrode and the above materials as the working electrodes. The PEO-PVP-$LiNO_3$ based solid polymer electrolyte films were used to serve as the electrolyte and the separator. The cells were assembled inside the argon filled glove box, in which, the oxygen and the moisture levels were controlled to be < 1 ppm. The picture of the glove box used is shown in figure 3.

Figure 3: The Glove box (MTI Corporation)

4.2.5 Characterization

The structural and morphological aspects of the synthesized cathode materials were investigated using XRD and FE-SEM techniques. The XRD patterns were recorded using PANAlytical X'Pert PRO machine with Cu-Kα radiation of wavelength 1.54 Å. The FE-SEM

images were collected using Carl-Zeiss Sigma electron microscope. The assembled cells were subjected to cyclic voltammetry and charge-discharge testing using the Bio-Logic SP300 Unit.

4.3 Results and Discussion

4.3.1 XRD Analysis

The XRD pattern of the LFP sample is shown in figure 4. The peaks can be perfectly indexed to the ordered orthorhombic olivine crystal structure (JCPDS 40-1499, space group Pnma) [21]. The pattern shows all the characteristic peaks of $LiFePO_4$. Absence of any extra peaks confirms the phase purity of the synthesized $LiFePO_4$, obtained by the sol-gel synthesis route.

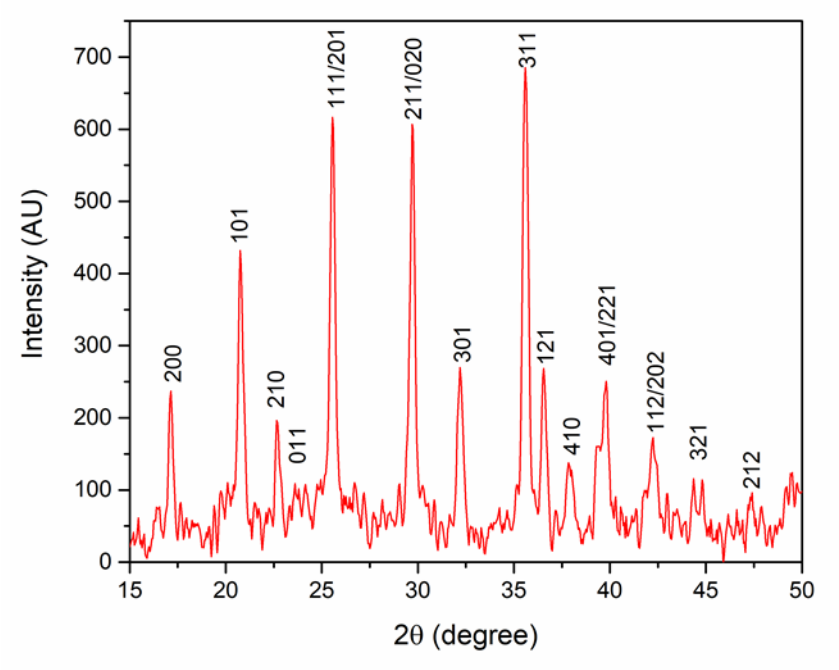

Figure 4: XRD pattern of $LiFePO_4$

The XRD pattern shown in figure 5 can be indexed to the cubic spinel $LiNi_{0.5}Mn_{1.5}O_4$ (JCPDS Card No.: 80-2162, space group: Fd3 m) [22]. The diffraction peaks are sharp and strong, indicating good crystallinity of the sample. The pattern shows all the characteristic peaks of $LiNiMnO_4$.

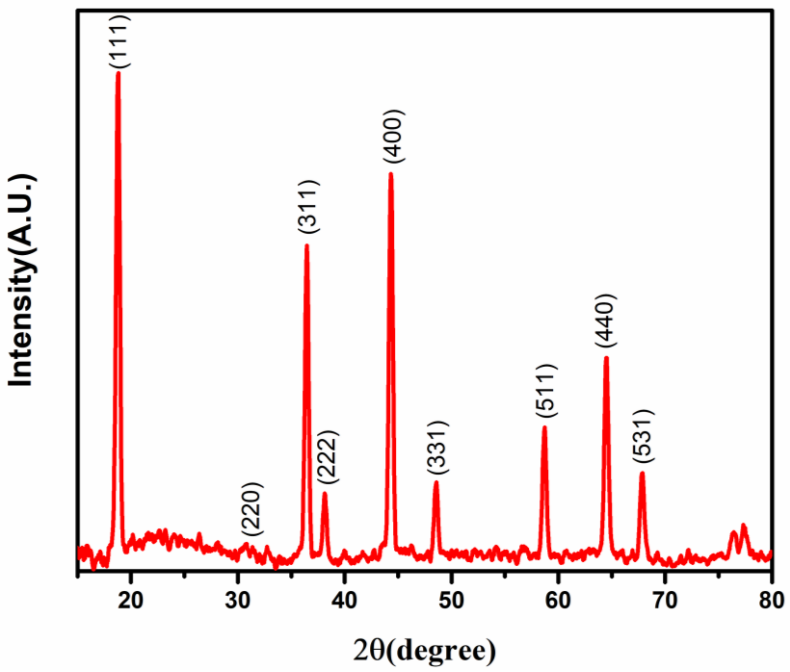

Figure 5: XRD pattern of $LiNi_{0.5}Mn_{1.5}O_4$

4.3.2 The FE-SEM analysis

The FE-SEM image of pure $LiFePO_4$ cathode material is shown in figure 6. The $LiFePO_4$ particles seem to be bulky, and the particle size distribution is quite wide [23] as observed from the figure. The particle size is around 200 nm.

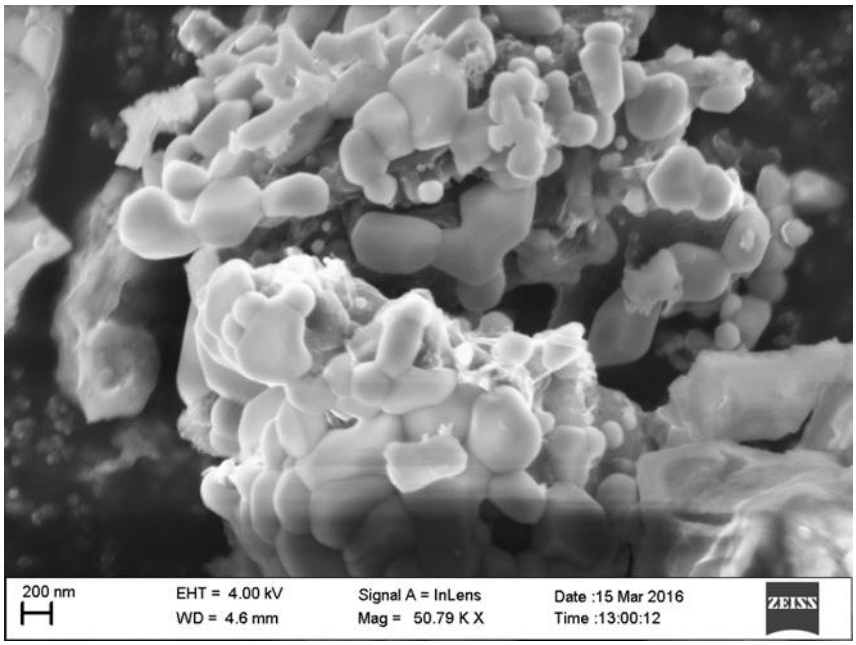

Figure 6: FE-SEM pattern of $LiFePO_4$

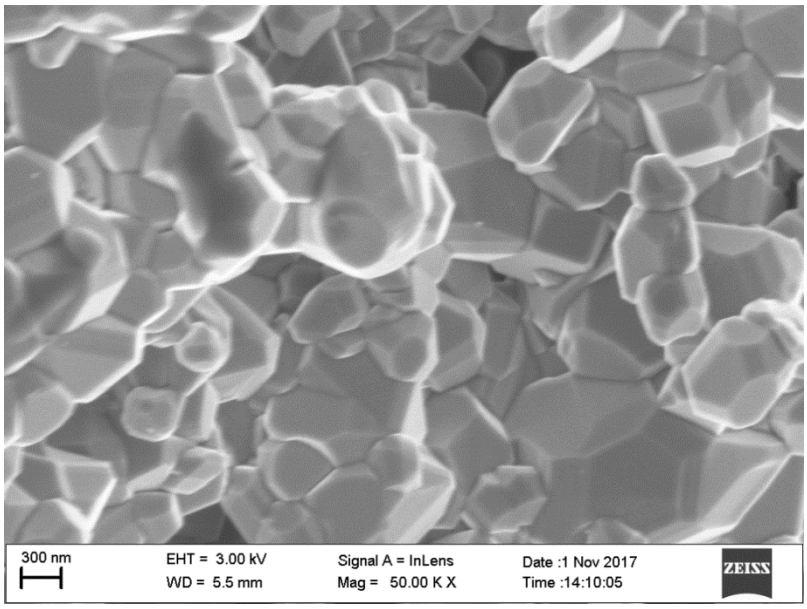

Figure 7: FE-SEM pattern of $LiNi_{0.5}Mn_{1.5}O_4$

The FE-SEM pattern of $LiNi_{0.5}Mn_{1.5}O_4$ is shown in figure 7. The image is composed of 30~300 nm sized primary particles with smooth surfaces and irregular shapes [22].

4.3.3 Cyclic voltammetry studies

Prototype coin cells were assembled in the argon filled glove box using $LiFePO_4$ as the cathode active material, Li metal as the anode and the synthesised PEO-PVP-$LiNO_3$ based solid polymer electrolyte film as the electrolyte and the separator. These cells show open circuit voltage around 3.26 V as shown in figure 8 (a). The closed loop nature of the cyclic voltammetry curves indicates good electrochemical performance possibility of the assembled cells at the scan rate of 0.5 mV s^{-1} between 2.5 to 4.2 V and the CV curves for 5 cycles are depicted in figure 8 (b). The lithium ions are extracted from the $LiFePO_4$ structure during anodic sweep. The oxidation peak is located at ~ 3.9V versus Li/Li^+. In the reverse scan from 4.2 V to 2.5V, the reduction peak is observed at ~3.1V, corresponding to lithium insertion, back into the $LiFePO_4$ structure. The high electrochemical reactivity of the LFP contributes towards the well-defined peaks, the high Li-ion diffusion rate and the low inner resistance. The lithium ion intercalation/deintercalation reactions, accompanied by electron removal, essentially depend on the electronic conducting nature of the electrode material. During the extraction and the insertion of the lithium ions, the diffusion length of the ions in $LiFePO_4$ gets considerably reduced which helps to facilitate reversible electrochemical reactions [5]. The voltage difference corresponding to oxidation and reduction [24] peaks is 0.7 V. The CV curves of the Li-ion cells for different cycles show

more symmetry of oxidation and reduction peaks, which confirms better electrochemical activity [25].

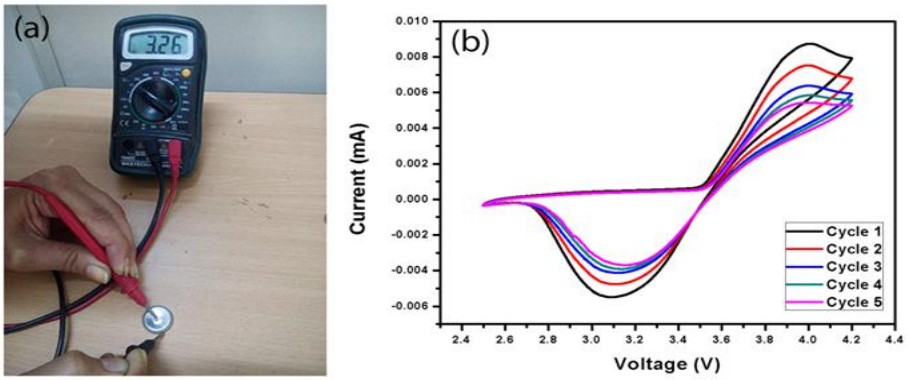

Figure 8: **(a)** Open Circuit Voltage of the assembled Li ion cell with $LiFePO_4$ as the cathode **(b)** Cyclic Voltammetry curves of the assembled cell

The CV curves of the assembled Li ion cells with LNM as the cathode are shown in figure 9. Since solid polymer electrolyte films are used, the oxidation and the reduction peaks obtained in the CV curves are of low intensity. However, the peak positions are almost the same as those of liquid electrolyte used cells. The anodic scans of Ni spinels generally exhibit two regions of electrochemical activity over the voltage ranges 3.9 V–4.4 V and 4.5 V–5.0 V [26]. The former is related to the Mn^{3+}/Mn^{4+} redox couple. The electrochemical response of the Ni spinels in the 3.9 V–4.3 V region is barely detected in the present case, consistent with a higher oxidation state of Mn in the spinel and consequently the presence of a small fraction of Mn^{3+} .The main electrochemical activity occurs in the 4.6 V–5.0 V region where a double peak associated with the $Ni^{2+} \rightarrow Ni^{4+}$ process [27] is observed. During the reversible process, the strong, reduction peak is observed around 4.49 V.

The CV curves exhibit large difference between the area of the anodic and the cathodic scans. This is because the amount of lithium apparently being extracted in the anodic scan substantially exceeds that being inserted in the cathodic scan [26].

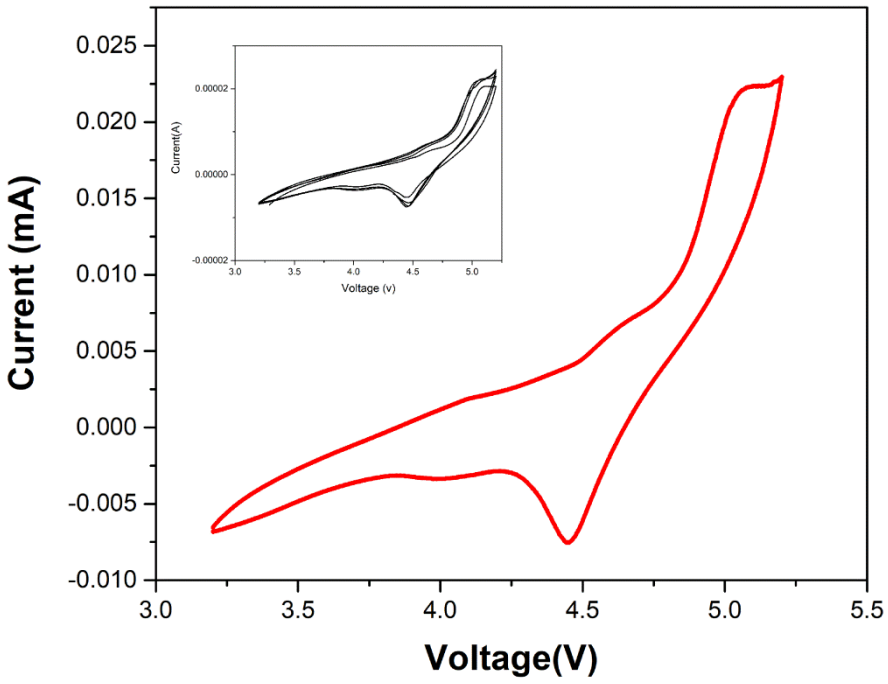

Figure 9: Cyclic Voltammetry curve of the assembled Li ion cell with LNM as the cathode. Insect shows the CV curves for 5 cycles.

4.3.4 Galvanostatic charge discharge studies

The galvanostatic charge discharge (GCD) curves of the LFP based half-cells, at different cycles at a current rate of C/2 are shown in figure 10. The voltage plateaus in the range of 3.3V-3.5 V which correspond to the Fe^{3+}/Fe^{2+} redox couple, indicate the lithium extraction reactions of LFP. Higher electrochemical reactivity and excellent

kinetics are responsible for the flattened voltage plateau seen in the CD curve. This material exhibits higher capacities of 149 mAh g^{-1}, 145 mAh g^{-1} and 125 mAh g^{-1} at current rates of C/2, in the 1st, 2nd and 3rd cycles respectively. The fast reaction and ionic diffusion kinetics of the small sized particles and good electronic contact are responsible for the high, initial discharge capacity of the material.

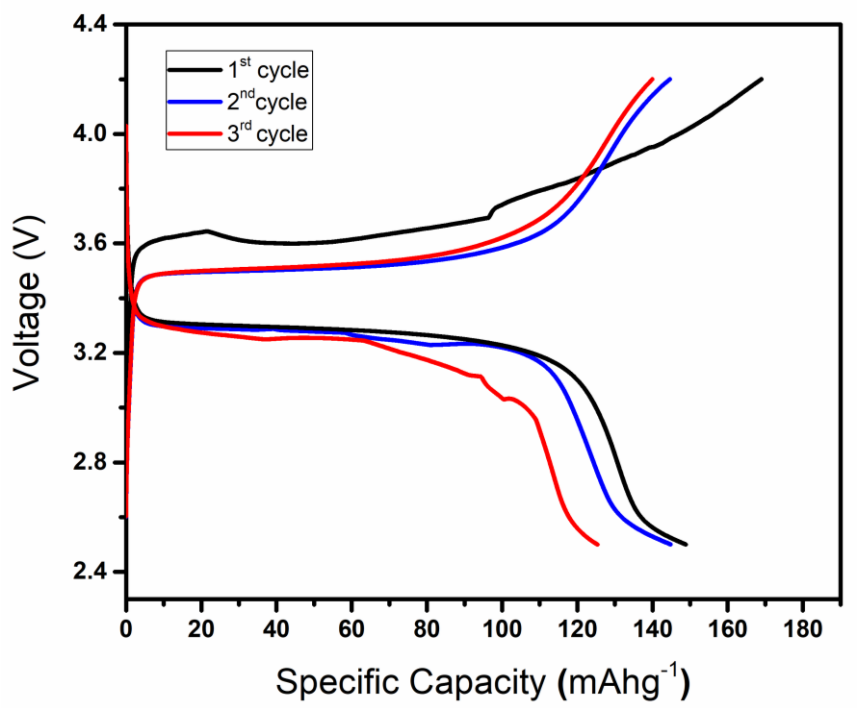

Figure 10: The GCD curves of the LFP based half cells at different cycles at the current rate of C/2

The charge-discharge profile of the LNM based half cells at the current rate of C/2 is depicted in figure 11. The working potential window used to investigate the electrochemical performance of the synthetized LNM samples is set as 3.2 V–5V. In the present case, the Li extraction and insertion occur at potential plateaus, which confirms that

all of the Li ions in the structure are electrochemically active. The first one is the high-voltage plateau at 4.7 V related to the Ni^{2+}/Ni^{4+} redox reaction [28], which provides theoretically a capacity of 143 $mAhg^{-1}$ for the cell. The discharge capacities of LNM are 103 and 86 $mAhg^{-1}$, at the 1st and the 10th cycles respectively. It is observed that the discharge capacity of LNM decreases with increase in the number of cycles. This may be due to the decomposition of the solid electrolyte at higher voltages, which results in faster capacity loss with the increase in the number of cycles [22].

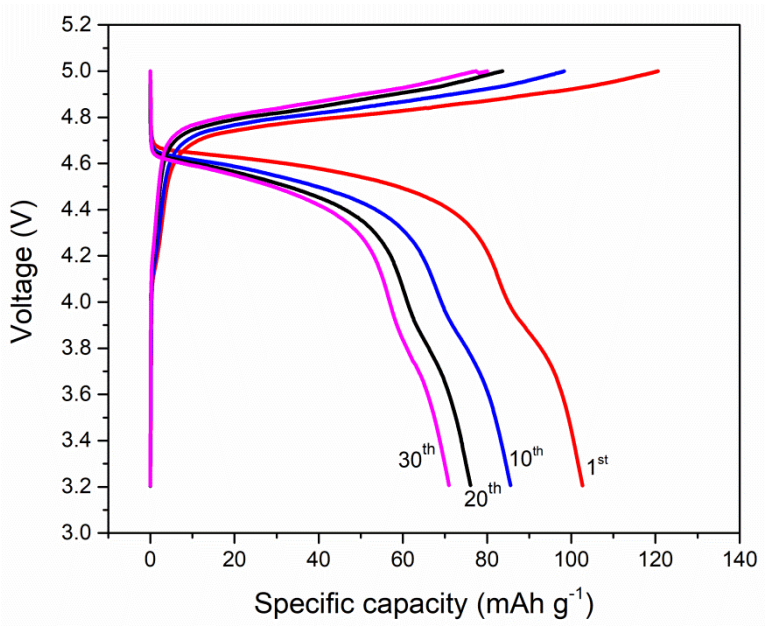

Figure 11: The GCD curves of the LNM based half cells at different cycles at the scan rate of C/2

4.4 Conclusions

The present work illustrates the first attempts carried out to assemble all solid state Li ion cells for 3.2 V and 5 V using the LFP and the LNM cathodes respectively. The performance of the half cells is promising as far as the initial discharge capacity values and the behaviour of the CV curves are concerned. However there are many challenges to be addressed to achieve good capacity retention over larger number of cycles. The synthesis conditions of the cathode materials have to be optimized to get particle size in the 10-20 nm range and a more uniform particle size distribution. As an initial attempt, the present work offers ample scope for developing high voltage, all solid state Li ion cells based on the cost effective and eco-friendly cathode materials, LFP and LNM.

4.5 References

[1] John B. Goodenough, Youngsik Kim, Challenges for Rechargeable Li Batteries, Chem. Mater. 2010, 22, 587–603 587, DOI:10.1021/cm901452z.

[2] Li Wang, Dan Chen, JiangfengWang, Guijuan Liu, Wei Wu, Guangchuan Liang, Synthesis of LiNi0.5Mn1.5O4 cathode material with improved electrochemical performances through a modified solid-state method, Powder Technology 292 (2016) 203–209.

[3] R. Ruffo, R.A. Huggins, C.M. Mari, M. Piana, W. Weppner, Phosphate materials for cathodes in lithium ion secondary batteries, Ionics 11 (2005) 213–219.

[4] Bo Xu, Danna Qian, Ziying Wang, Ying Shirley Meng, Recent progress in cathode materials research for advanced lithium ion batteries, Materials Science and Engineering R 73 (2012) 51–65.

[5] Anilettan thesis

[6] XiaoLong Xu, SiXu Deng, Hao Wang, JingBing Liu, Hui Yan, Research Progress in Improving the Cycling Stability of High- Voltage LiNi0.5Mn1.5O4 Cathode in Lithium-Ion Battery, Nano-Micro Lett. (2017) 9:22, DOI 10.1007/s40820-016-0123-3.

[7] Wei Quan, Zilong Tang, Junying Zhang, Zhongtai Zhang, Enhanced properties of LiFePO4/C cathode materials modified by CePO4 nanoparticles, Materials Chemistry and Physics 147 (2014) 333-338.

[8] A.K. Padhi, K.S. Nanjundaswamy, J.B. Goodenough, Phospho-olivines as positive-electrode materials for rechargeable lithium batteries, J. Electrochem. Soc. 144 (1997) 1188-1194.

[9] Jinisha B, Anilkumar KM, Manoj M, Pradeep V.S, Jayalekshmi S, Development of a novel type of solid polymer electrolyte for solid state lithium battery applications based on lithium enriched poly (ethylene oxide) (PEO)/poly (vinyl pyrrolidone) (PVP) blend polymer, Electrochimica Acta 235 (2017) 210–222.

[10] G. Meligrana, C. Gerbaldi, A. Tuel, S. Bodoardo, N. Penazzi, Hydrothermal synthesis of high surface LiFePO4 powders as cathode for Li-ion cells, J. Power Sources 160 (2006) 516-522.

[11] H. Nakano, K. Dokko, S. Koizumi, H. Tannai, K. Kanamura, Hydrothermal synthesis of carbon-coated LiFePO4 and its application of lithium polymer battery, J. Electrochem. Soc. 155 (2008) A909-A914.

[12] K.F. Hsu, S.Y. Tsay, B.J. Hwang, Synthesis and characterization of nano-sized LiFePO4 cathode materials prepared by a citric acid-based solegel route, J. Mater. Chem. 14 (2004) 2690-2695.

[13] J. Wang, S.Z. Yao, W.Q. Lin, B.H. Wu, X.Y. He, J.Y. Li, J.B. Zhao, Improving the electrochemical properties of high-voltage lithium nickel manganese oxide by surface coating with vanadium oxides for lithium ion batteries. J. Power Sources 280 (2015), 114–124. doi:10.1016/j.jpowsour. 2015.01.087.

[14] D. Zhao, Y. Wang, Y. Zhang, High-Performance Li-ion Batteries and Supercapacitors Based on Prospective 1-D Nanomaterials. Nano-Micro Lett. 3(1), 62–71 (2011). doi:10.3786/nml.v3i1. p62-71.

[15] Haidong Liu, Jun Wang, Xiaofei Zhang, Dong Zhou, Xin Qi, Bao Qiu, Jianhui Fang, Richard Kloepsch, Gerhard Schumacher, Zhaoping Liu, Jie Li, Morphological Evolution of High-Voltage Spinel LiNi0.5Mn1.5O4 Cathode Materials for Lithium-Ion Batteries: The Critical Effects of Surface Orientations and Particle Size, ACS Appl. Mater. Interfaces 2016, 8, 4661−4675. DOI: 10.1021/acsami.5b11389.

[16] Qiming Zhong, Arman Bonakdarpour, Meijie Zhang, Yuan Gao, J. R. Dahn, Synthesis and Electrochemistry of LiNixMn2 ‑xO4. J. Electrochem. Soc. 1997, 144 (1), 205−213.

[17] M. Hu, X.L. Pang, Z. Zhou, Recent progress in high-voltage lithium ion batteries. J. Power Sources 237, 229–242 (2013). doi:10.1016/j.jpowsour.2013.03.024.

[18] D. Golodnitsky, E. Strauss, E. Peled, S. Greenbaum, Review—On Order and Disorder in Polymer Electrolytes, Journal of The Electrochemical Society, 162 (14) A2551-A2566 (2015).

[19] S. M. Said, A. Z. S. Zulkifli, M. A. Kamarudin, A. Mainal, B. Subramanian, and N. S. Mohamed, Polymer electrolyte liquid crystal system for improved optical and electrical properties, Eur. Polym. J., 66, (2015), 266-272.

[20] M. Marcinek, J. Syzdek, M. Marczewski, M. Piszcz, L. Niedzicki, M. Kalita, A. Plewa-Marczewska, A. Bitner, P.Wieczorek, T. Trzeciak,M. Kasprzyk, P. Ł e˙zak, Z. Zukowska, A. Zalewska, and W. Wieczorek, Electrolytes for Li-ion transport – Review, Solid State Ionics, 276, (2015) 107-126.

[21] F. Fathollahi, M. Javanbakht, H. Omidvar, M. Ghaemi, Improved electrochemical properties of LiFePO4/graphene cathode nanocomposite prepared by one-step hydrothermal method, J. Alloys Compd. 627 (2015) 146–152. doi:10.1016/j.jallcom.2014.12.025.

[22] Qingtang Zhang, Juntao Mei, Xiaomei Wang, Fuling Tang, Weifeng Fan, Wenjiang Lu, High performance spinel LiNi0.5Mn1.5O4cathode material by lithiumpolyacrylate coating for lithium ion battery, Electrochimica Acta 143 (2014) 265–271.

[23] Guohui Qin, Qianqian Ma, Chengyang Wang, A new route for synthesizing C/LiFePO4/multi-walled carbon nanotube secondary particles for lithium ion batteries, Solid State Ionics 257 (2014) 60–66.

[24] D.Y.W. Yu, C. Fietzek, W. Weydanz, K. Donoue, T. Inoue, H. Kurokawa, S. Fujitani, Study of LiFePO 4 by Cyclic Voltammetry, J. Electrochem. Soc. 154 (2007) 253– 257.

[25] W.L. Wang, E.M. Jin, H. Gu, Electrochemical Performance of Lithium Iron Phosphate by Adding Graphite Nanofiber for Lithium Ion Batteries, Trans. Electr. Electron. Mater. 13 (2012) 121–124.

[26] By José C. Arrebola, Alvaro Caballero, Manuel Cruz, Lourdes Hernán, Julián Morales, Enrique Rodríguez Castellón, Crystallinity Control of a Nanostructured LiNi0.5Mn1.5O4 Spinel via Polymer-Assisted Synthesis: A Method for Improving Its Rate Capability and Performance in 5 V Lithium Batteries, Adv. Funct. Mater. 2006, 16, 1904–1912.

[27] K. Ariyoshi, Y. Iwakoshi, N. Nakayama, T. Ohzuku, Topotactic Two-Phase Reactions of Li†Ni1Õ2Mn3Õ2‡O4 „$P4_332$… in Nonaqueous Lithium Cells J. Electrochem. Soc. 2004, 151, 296-303.

[28] Marilena Mancini,[a] Peter Axmann,*[a] Giulio Gabrielli,[a] Michael Kinyanjui,[b, c] Ute Kaiser,[b] and Margret Wohlfahrt-Mehrens, A High-Voltage and High-Capacity Li1+xNi0.5Mn1.5O4 Cathode Material: From Synthesis to Full Lithium-Ion Cells, ChemSusChem 2016, 9, 1843 – 1849.

Chapter 5

Poly (ethylene oxide) based, solid polymer electrolyte films for applications in sodium ion cells

The studies on the solid polymer electrolyte (SPE) films with high ionic conductivity suitable for the realization of all solid state sodium ion cells, form the focal theme of the work presented in this chapter. The SPE films are obtained by the solution casting technique using the blend solution of poly (ethylene oxide) (PEO) with ethylene carbonate (EC) and propylene carbonate (PC) and treated with sodium nitrate. The ionic conductivity of the SPE films is determined from the electrochemical impedance spectroscopy studies. Addition of nanostructured Al_2O_3, as the filler material is found to enhance the ionic conductivity of the SPE films significantly.

5.1 Introduction

Lithium ion cells with high energy density are being extensively used as power sources in portable electronic gadgets, electric vehicles and stand alone power supplies [1]. The availability of lithium from natural sources is a matter of concern, for their extensive applications as the power sources. The limited availability and the increasing cost of lithium with worldwide commercialization are posing challenges for the wide spread use of the Li based electrochemical cells [2]. Search for other appropriate and competent materials is in full swing for identifying

alternative energy storage solutions, apart from the lithium based one. It is a difficult task to identify new approaches as alternatives for the well established Li ion technology. Recently, the prospects of developing sodium as a substitute to lithium for future energy storage applications are being pursued, considering its high electrochemical reduction potential (E° (Na^{+}/Na) = −2.71 V), the possibility of intercalation in both the cathode and the anode materials, its earth abundance, low cost and most importantly, its non-toxic nature [3,4]. Working of Li-ion cells and Na-ion cells shares the same principle for energy storage applications. Many materials are presently under investigation as the active cathodes and anodes for reversible Na-ion storage applications.

In the development of safe and durable electrochemical cells based on Na ion, electrolytes play a crucial role. At present, liquid electrolytes are being used in Na ion cells and the safety issues related to the possible leakage of the electrolyte pose many limitations for the system design. Replacing the conventional liquid electrolytes with solid ones is advantageous in many respects. The robust sealing of the cells which is mandatory with liquid electrolytes, can be completely eliminated and the cell design can be made more compact and easier to handle, as explained earlier. The need for the separator material can also be avoided, since the solid electrolyte can function both as the electrolyte and the separator material. Studies have been intensified in recent times to identify solid polymer electrolyte (SPE) films, suitable for developing all solid state Na ion cells, which are flexible and stable up to high potential windows, so that it might be possible to use high voltage cathode materials.

Solid polymer electrolyte films based on suitable polymer blends as hosts and treated with appropriate types of sodium salts have been widely investigated for developing all solid-state Na ion cells due to their advantages in terms of flexibility, high ambient ionic conductivity, effective electrode- electrolyte contacts, good chemical compatibility, enhanced mechanical properties and ease of device fabrication [5]. The mostly used host polymers for generating sodium ion conducting SPE films include, poly (ethylene oxide) (PEO), poly (methyl metha acrylate) (PMMA), poly (vinylidene fluoride) (PVdF) and poly (vinyl alcohol) (PVA),which can be solvated with different sodium salts like $NaClO_4$, $NaPF_6$, $NaBF_4$, NaTFSI , Na_2SO_4, NaFSI, $NaYF_4$, NaI and $NaCF_3SO_3$ to synthesize the [6-17] SPEs. Different research groups have conducted studies on the SPEs based on PEO complexes with $NaNO_3$ salt and have obtained maximum ionic conductivity around 3.5 $x10^{-6}$ S cm^{-1} [5,6]. The extensively studied polymer host for solid polymer electrolyte applications is PEO, which is a semi-crystalline polymer, having high dielectric constant and the ion transportation in this material is due to the support of the amorphous phase with activated chain segments. Various approaches are used to enhance the ionic conductivity of PEO based electrolytes by blending of polymer and the addition of plasticizers and ceramic fillers. The crystalline nature of PEO has to be suppressed to some extent to enhance the amorphous phase to facilitate better ion transport which leads to good ionic conductivity [18]. Synthesis of polymer electrolytes by blending or compositing methods leads to improved ionic conductivity for the resulting electrolyte materials by enhancement in the amorphous nature [19]. Introducing plasticizers to the PEO based SPEs further enhances the room temperature ionic

conductivity [20].Organic solvents like ethylene carbonate (EC), propylene carbonate (PC), dimethyl carbonate (DMC),[21,22] ethyl methyl carbonate (EMC), and diethyl carbonate (DEC) and plastic crystals are mainly used as plasticizers for the synthesis of the SPEs [11,18]. Dispersion of inert, ceramic oxide nano-fillers like TiO_2, Al_2O_3, SiO_2, ZrO_2, $BaTiO_3$, Sb_2O_3, Na_2SiO_3 and SnO_2 [23-27] is an interesting approach to further improve the electrochemical properties of the SPE films. Addition of the nano-fillers is expected to modify the crystalline nature and tailor the local structure, morphology and the flexibility of the polymer backbone and the ion mobility through the SPE films [28]. This improves the amorphous nature of the host polymer by reducing the recrystallization rate and enhances the interfacial stability and the ionic conductivity [7].

In the present work, good quality SPE films are grown by optimizing the concentration of the sodium salt, $NaNO_3$ in the polymer blend of PEO with EC and PC. To achieve high ionic conductivity, nanostructured Al_2O_3 is added as the filler material to the PEO-EC-PC blend, solvated with the sodium salt, $NaNO_3$. Among the various organic carbonates, in the present work, the plasticizers EC and PC are chosen to make the polymer blend with PEO. Addition of high dielectric constant, low molecular weight plasticizers to the polymer PEO, modifies the heterogeneous polymer composite structure by improving the amorphous nature. Addition of Al_2O_3 to the polymer blend as an active filler material leads to surface functionalization with the formation of O-OH groups at the grain surfaces, which in turn results in hydrogen bonding with the migrating ionic species and contributes to the enhanced final ionic conductivity of the SPE films. The SPE film samples are

characterized in detail using different experimental techniques such as XRD, FTIR spectroscopy, FESEM, TGA, AC impedance analysis, transport number studies and cyclic voltammetry studies.

5.2 Experimental

5.2.1 Materials

The materials, PEO (Average Molecular weight (Mw)=200,000, bought from Aldrich), the plasticizers EC (Mw=88.06, bought from Spectrochem), PC (Mw=102.09, bought from Sigma-Aldrich), $NaNO_3$ (Mw= 84.99, obtained fom Sigma-Aldrich), Al_2O_3 (Mw=101.96, obtained from Sigma-Aldrich) and methanol (bought from Spectrochem) are used for the synthesis of the SPE. Flexible and free standing SPE films are obtained by solution casting.

5.2.2 Synthesis details

In a typical experiment, 0.4g of PEO was dissolved in methanol and stirred for 2 hours. After that, 0.1g of the plasticizers, EC and PC in 1:1 ratio was added to the above solution and stirred. To the polymer-plasticizer blend solution, 4 weight % $NaNO_3$ was added and stirred for 6 hours. The resulted solution was poured onto a Teflon petri-dish and allowed to evaporate slowly at 40 °C for 12 hours. The flexible, transparent and free standing SPE films were peeled off from the petri-dish and used for further studies. The experiment was repeated for 6 weight %, 8 weight % and 12 weight % of $NaNO_3$. The structure of the SPE films based on the PEO-plasticizer blend- $NaNO_3$ salt, was modified by adding 4weight %, 8weight % and 12weight % of the Al_2O_3

nano-filler and the same procedure was repeated. The photographs of the solution cast SPE films are shown in figure 1.

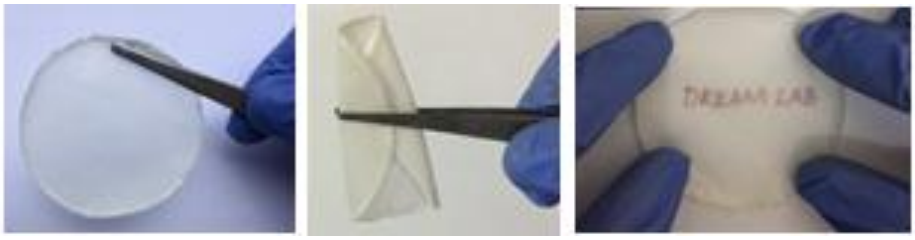

Figure 1: Freestanding, flexible and transparent SPE films

5.2.3 Characterization

The structural characterization of the SPE films was carried out using Rigaku Max C, X-ray diffractometer with Ni filtered Cu Kα radiation of 1.54 Å. The FTIR spectrophotometer (SHIMADSU) in the range of 400–4000 cm^{-1} was used to analyse the structural aspects of the SPE films based on FTIR spectroscopy. The surface morphology of the films was studied using the Carl Zeiss Sigma FESEM instrument. Thermo-gravimetric analysis using the Perkin Elmer STA 6000 was used to assess the thermal stability of the films in the temperature range from room temperature to 700°C. Different electrochemical analysis techniques were used to understand the ionic transport properties of these SPE films. The ac impedance analyser HP4192A (5Hz-13MHz) was used for measuring the ionic conductivity. The temperature dependence of the ionic conductivity of the SPE films was studied using the Arrhenius plot, and the thermal activation energy was also determined. The total ionic transport number was calculated using Wagner's DC polarization method. Cyclic voltammetry studies were carried out using the Bio-Logic SP-300 potentiostat.

5.3 Results and Discussions

5.3.1 XRD Analysis

The XRD patterns of pure PEO, the PEO-EC-PC (polymer-plasticizer) blend, the PEO-EC-PC blend solvated with $NaNO_3$ salt of different concentrations (4, 8, 12 and 16 weight %), Al_2O_3 filler material and Al_2O_3 (4, 8 and 12 weight %) dispersed in PEO-EC-PC with 16 weight % $NaNO_3$ are depicted in figure 2 (a-j). The plot of pure PEO, shown in figure 2(a), displays the characteristic semi-crystalline peaks of PEO at $2\theta = 19°$ and $2\theta = 23.2°$ which are represented as + and * [29, 30]. For the PEO-EC-PC, polymer-plasticizer blend, the XRD pattern shown in figure 2(b) also shows the characteristic semi-crystalline peaks of PEO. The addition of $NaNO_3$ salt to the PEO-EC-PC blend, decreases the intensity of the crystalline peaks of PEO as observed in figure 2 (c-f). The plasticizers EC and PC reduce the columbic interactions between the ions [12]. The SPE film, based on the PEO-EC-PC blend, treated with 16 weight % of $NaNO_3$ is observed to have lower crystallinity, compared to the other SPE films. Semi-crystallinity in the polymer PEO, originates from the ordering of the polyether side chains. With the addition of the sodium salt to the polymer, complexes are formed between the Na^+ ions and the oxygen atoms in the side chains. This disrupts the previous ordering and results in the reduction of the crystalline nature of the polymer [5]. Further decrease in crystallinity is observed on adding the filler Al_2O_3 to the PEO-EC-PC with 16 weight % of $NaNO_3$ based SPE sample, as seen from figure 2(h-j). For optimising the filler content, different concentrations of the filler material are tried,

by varying the filler content in the 4 to 12 weight % range. It has been observed that the SPE sample with 8 weight % Al_2O_3 added is having the lowest extent of crystalline nature, compared to the other samples. The addition of more than 8 weight % of the Al_2O_3 filler is found to affect the quality of the resulting SPE films. The XRD analysis establishes the additional increase in the amorphous phase of the sodium salt complexed, PEO-EC-PC based SPEs by the addition of the Al_2O_3 filler, which facilitates the enhancement of the mobility of the sodium ions in the films and leads to significant increase in the ionic conductivity [30,31].

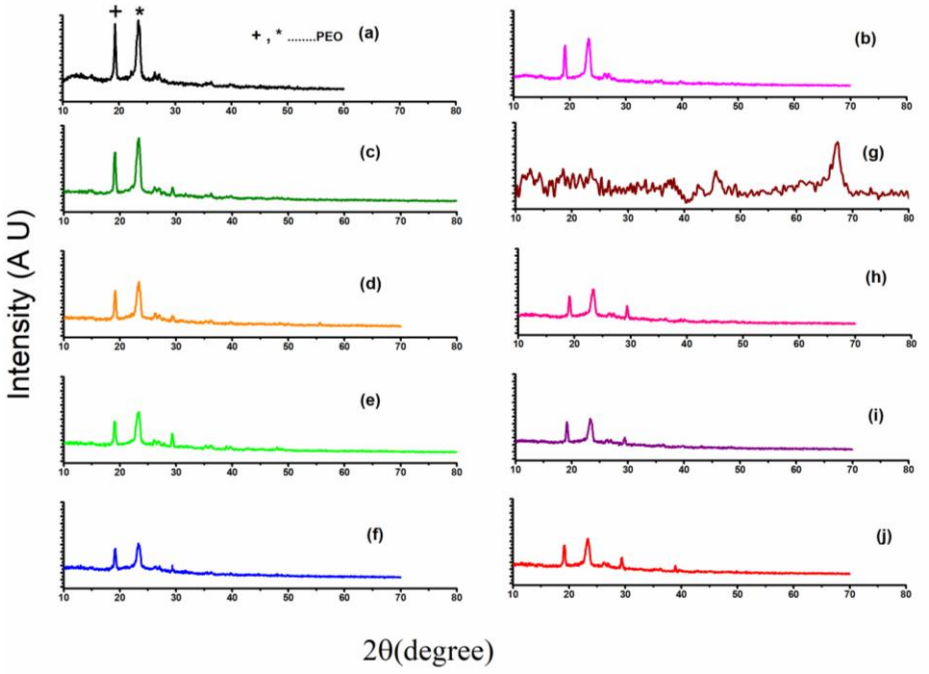

Figure 2: The XRD patterns of (a) PEO; (b)PEO-EC-PC blend; (c-f) PEO-EC-PC with 4, 8 12 and16 weight % of $NaNO_3$ respectively; (g) pure Al_2O_3 filler; (h-j) PEO-EC-PC with 16 weight % of $NaNO_3$ and 4,8 and 12 weight % of Al_2O_3.

5.3.2 FTIR spectroscopy studies

The FTIR spectra of the $NaNO_3$ salt, the Al_2O_3 filler material, the PEO-EC-PC blend, the PEO-EC-PC blend with 16 weight % $NaNO_3$ and the PEO-EC-PC blend with 16 weight % $NaNO_3$ and 8 weight % Al_2O_3 are depicted in figure 3 (a-i), respectively. The FTIR spectroscopic data provides evidence for the complexation between the different constituents in the SPE system.

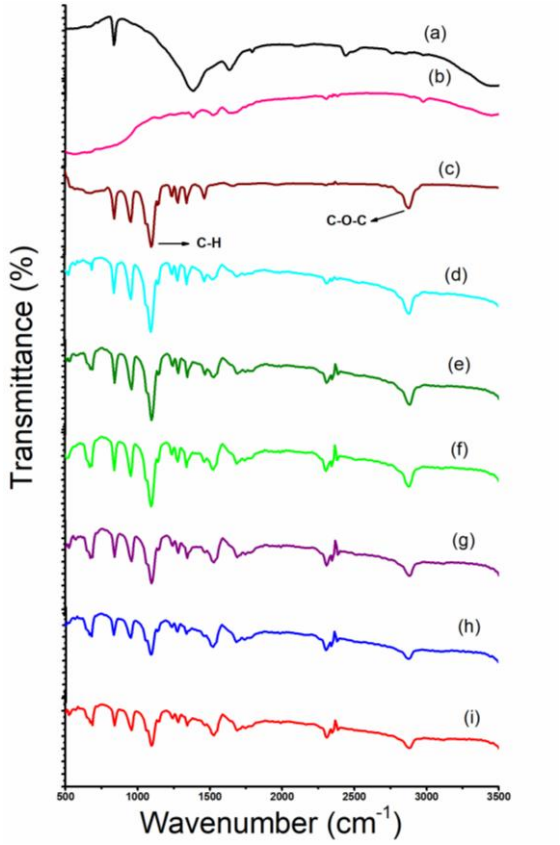

Figure 3: The FTIR spectra of (a) pure $NaNO_3$, (b) pure Al_2O_3 filler, (c) pure PEO, (d) PEO-EC-PC blend, (e-h) PEO-EC-PC blend with4,8,12 and 16weight % of $NaNO_3$, (i) PEO-EC-PC blend with 16 weight % of $NaNO_3$ and 8 weight % of Al_2O_3.

Significant complexation changes are observed only in the PEO-EC-PC with 16 weight % of $NaNO_3$ and PEO-EC-PC with 16 weight % of $NaNO_3$ and 8 weight % of Al_2O_3 and hence other compositions are excluded. The spectrum of PEO-EC-PC, polymer- plasticizer blend, depicted in figure 3(d), is almost similar to that of pure PEO. The FTIR spectral studies of pure PEO and the blend of PEO with different polymers and plasticizers have already been done by many research groups [5,29,32]. The strong absorption peak between 2810-2960 cm^{-1} corresponds to the (C-H) stretching vibrations of the CH_2 group of PEO as observed in the spectrum of the PEO-EC-PC blend shown in figure 3 (d). The intensity of this peak is reduced in figure 3 (e-i) due to the presence of the $NaNO_3$ salt [6]. In pure PEO, the peak at 1100 cm^{-1} is related to the C-O-C stretching mode. In figure 3 (e-i), the corresponding peak is broadened and its intensity is reduced. The co-ordination of the Na^+ ions of $NaNO_3$ with the ether oxygen of PEO is responsible for the observed reduction in the peak intensity [5] and this observation indicates the possible complexation of $NaNO_3$ with the PEO-EC-PC blend. The characteristic absorption peaks of PEO are retained in figure 3 (i) which shows that the addition of Al_2O_3 does not affect the structure of the PEO system [19, 33, 34].

5.3.3 FESEM analysis

The FESEM images of the PEO-EC-PC blend, the PEO-EC-PC blend with 16 weight% of $NaNO_3$ and the PEO-EC-PC blend with 16 weight % of $NaNO_3$ and 8 weight % of Al_2O_3 are shown in figure 4 (a-c) respectively. The microstructure of PEO-EC-PC blend shows rough

surface features with several micro cracks and crystalline domains [20, 29]. After the addition of the sodium salt and the Al_2O_3 filler, the surface morphology of the PEO-EC-PC polymer blend is found to be altered, significantly. The surface becomes more smooth and porous, as seen from figures 4(b) and 4 (c), compared to the morphology depicted in figure 4(a). On adding the filler Al_2O_3 to the PEO-EC-PC-$NaNO_3$ film, the porosity and the surface smoothness are found to increase significantly due to the filler particle aggregation. The Al_2O_3 dispersed SPE film also has more uniform distribution of pores. This property may help in reducing the interfacial resistance of the SPE film [19].

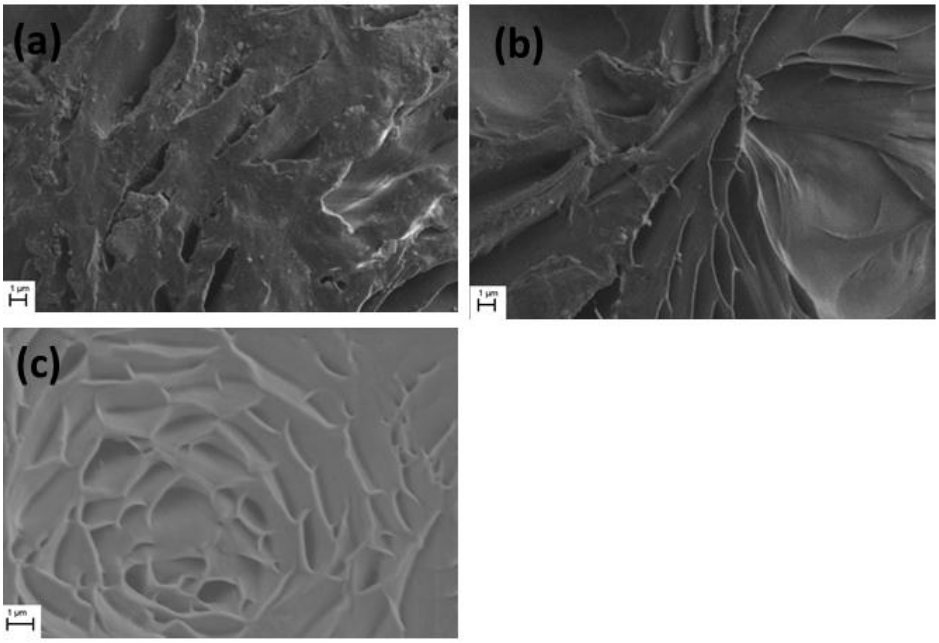

Figure 4: The FESEM images of (a) PEO-EC-PC blend (b) PEO-EC-PC with16 weight % of $NaNO_3$ without filler and (c) PEO-EC-PC with 16 weight % of $NaNO_3$ and 8 weight % of Al_2O_3 filler

5.3.4 Thermal characterization

5.3.4.1 Thermo-gravimetric (TG) analysis

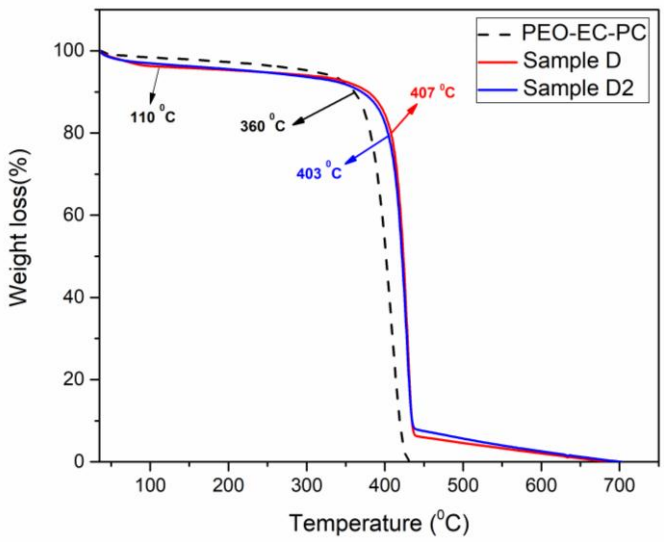

Figure 5: The TG curves of the PEO-EC-PC blend, the PEO-EC-PC with16 weight % of $NaNO_3$ without filler (Sample D) and the PEO-EC-PC with 16 weight % of $NaNO_3$ and 8 weight % of Al_2O_3 filler (Sample D2)

The TG curves of the PEO-EC-PC, the PEO-EC-PC with $NaNO_3$ (Sample D) and the PEO-EC-PC with $NaNO_3$ and the Al_2O_3 filler (Sample D2) are depicted in figure 5. There is an initial weight loss of 3.8% and 3% around 110 °C for the samples D and D2 due to the evaporation of small amounts of moisture or solvents in the SPE films [19,32]. A sharp weight loss region is observed around 360 °C with a weight loss of 10%, for the polymer-plasticizer blend (PEO-EC-PC) system. Compared to the blend system, there is significant enhancement in the thermal stability of the samples D and D2 due to the addition of

the sodium salt and the ceramic filler. With a weight loss around 20%, the decomposition temperatures of the samples D and D2 are observed at 407 °C and 403 °C respectively. Increase in thermal stability to higher temperatures has been observed for the samples D and D2. Homogeneous dispersion of the sodium salt and the ceramic filler within the polymer blend is reported to oppose the quick expansion of heat into the polymer blend matrix, thereby slowing down the thermal degradation of the SPE films [35]. The thermal stability of the filler incorporated SPE films of the present work is as high as 400 °C, which is suitable for designing sodium ion cells, capable of stable operation at temperatures much higher than room temperature [36].

5.3.5 A C Conductivity studies

5.3.5.1 Impedance analysis

Using Swagelock type cell, the SPE films were sandwiched between two stainless steel (SS) [29] electrodes. The impedance data was obtained in the frequency range 5 Hz to 13 MHz at room temperature. The ionic conductivity is calculated using the equation (1),

$$\sigma = \frac{t}{R_b A} \text{---------- (1)}$$

where, R_b is the bulk resistance, t, the thickness of the SPE film and A, the area of the SPE film. The impedance plots for the SPE films are shown in figure 6. The fitting of the impedance data and the corresponding equivalent circuit are shown in figure 6(c). The parameters represented in the equivalent circuit are, the SPE resistance R_b, the constant phase element Q and the coupling capacitance between the SPE film and the

electrode in the measuring circuit, C_{dl} [37,38]. The impedance plots for the PEO-EC-PC blend system, complexed with different weight percentages of $NaNO_3$ are shown in figure 6(a). The impedance plots show two regions. The inclined or linear region in the low frequency range is due to the presence of the stainless steel blocking electrodes and the semicircle in the high frequency range is due to the bulk effect of the SPE films. The ionic conductivity values of the SPE films are given in Table 1.The maximum ionic conductivity observed is 1.08×10^{-5} S cm^{-1} for the SPE film with 16 weight % of $NaNO_3$ in the PEO-EC-PC blend.

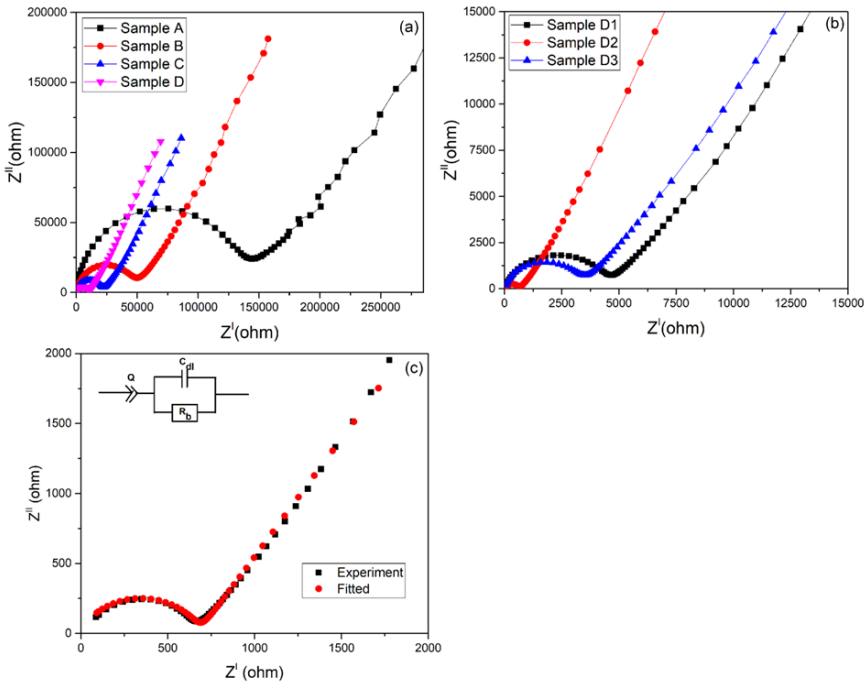

Figure 6: The room temperature complex impedance plots for (a) PEO-EC-PC with 4, 8, 12 and 16 weight % of $NaNO_3$ with sample code A to D; (b) PEO-EC-PC with 16 weight % of $NaNO_3$ and 4,8 and 12 weight % of Al_2O_3 with sample code D1 to D3; (c) The fitting of the impedance data. The inset of (c) shows the equivalent circuit

The plasticizers EC and PC reduce the coulombic interactions due to their high dielectric constant and prevent the crystal formation between the ions, as already mentioned in the XRD analysis. The action of EC and PC on the polymer host PEO is to make it more disordered and to create continuous conducting pathways for the ions. Adding sodium salt to the PEO-EC-PC blend results in increase in the charge carrier concentration and leads to the enhancement of the ionic conductivity. There is significant reduction in the bulk resistance, on adding different weight percentages of the sodium salt, which improves the ionic conductivity.

Table 1: Room temperature ionic conductivity values of the SPE films with different weight percentages of $NaNO_3$ added to the PEO-EC-PC, polymer-plasticizer blend.

Sample code	Polymer-plasticizer (PEO-EC-PC) with	Ionic conductivity S cm^{-1}
Sample A	4 weight % of $NaNO_3$	$8x10^{-7}$
Sample B	8 weight % of $NaNO_3$	$2.35x10^{-6}$
Sample C	12 weight % of $NaNO_3$	$5.28x10^{-6}$
Sample D	16 weight % of $NaNO_3$	$1.08x10^{-5}$

One of the striking outcomes of the present work is the superb effect of the filler Al_2O_3 on the structural and the electrochemical characteristics of the SPE films. Different weight percentages of the filler, Al_2O_3 are added to the PEO-EC-PC blend with 16 weight % of $NaNO_3$, which is the SPE film sample, coded as sample D, with the maximum ionic conductivity. The impedance plots of the Al_2O_3 incorporated SPE films, coded as the samples D1, D2 and D3 are shown in figure 6 (b) and the corresponding ionic conductivity values are given in Table 2. There is significant enhancement of ionic conductivity with

the addition of the filler Al_2O_3 and the maximum ionic conductivity observed for the SPE film sample D2 (PEO-EC-PC with 16 weight % of $NaNO_3$ and 8 weight % of Al_2O_3) is $1.86x10^{-4}$ S cm^{-1}. On adding different concentrations of Al_2O_3, the ionic conductivity increases initially to reach the maximum value for the SPE film with 8 weight % of Al_2O_3. Further addition of Al_2O_3, decreases the ionic conductivity, due to the blocking effect imposed by the more abundant alumina grains, which makes the polymer chains more immobilized and leads to lower conductivity [39]. The effects of Al_2O_3 filler, on enhancing the ionic conductivity are explained in many reports [40-43].

Table 2: Room temperature ionic conductivity values of the SPE films with different weight percentages of the filler Al_2O_3

Sample code	PEO-EC-PC blend with $NaNO_3$ and	Ionic conductivity (S cm^{-1})
Sample D1	4 weight % of Al_2O_3	$2.55x10^{-5}$
Sample D2	8 weight % of Al_2O_3	$1.86x10^{-4}$
Sample D3	12 weight % of Al_2O_3	$3.34x10^{-5}$

5.3.5.2 Thermal activation energy measurement

The ionic conductivity values at different temperatures ranging from 298 K to 358 K are measured for the sample D2, which has the maximum ionic conductivity as a consequence of the effect of the incorporation of the Al_2O_3 filler. When the temperature increases, the ionic conductivity also increases and the temperature dependence is shown as the Arrhenius plot in figure 7. The enhancement in conductivity is due to the increase in ionic mobility and the carrier ion concentration in the SPE film. The slope of the linear portion of the Arrhenius plot is used

to calculate the thermal activation energy of the SPE film, which is referred to as the energy required for defect formation and ion migration. The variation of the ionic conductivity with temperature can be tailored to the equation (2) which is given below [44],

$$\sigma = \sigma_0 \exp(-E_a/kT) \text{----------} \quad (2)$$

where σ_0 is the pre-exponential factor, Ea, the activation energy, k, the Boltzmann constant and T, the absolute temperature. The calculated thermal activation energy for the SPE film sample D2 is 0.1eV, which is suitable for the ion transport.

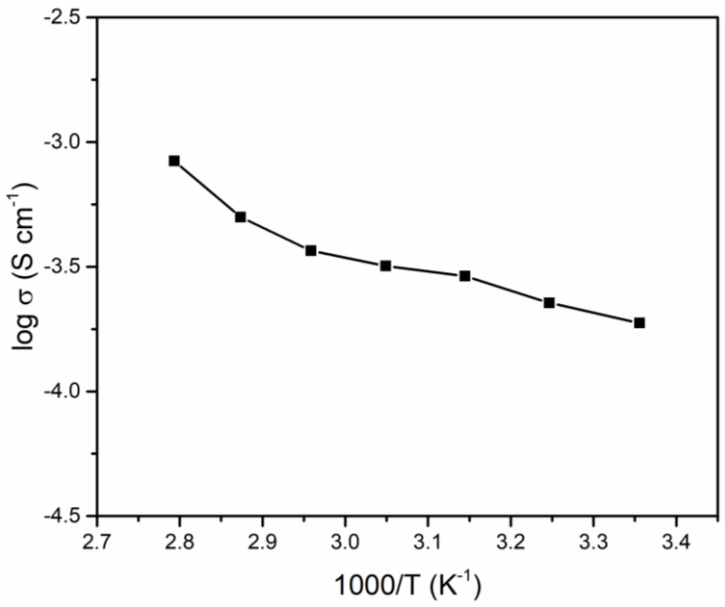

Figure 7: The Arrhenius plot for the SPE film sample D2.

5.3.6 Transport number measurement

The total ion transport number, t_{ion} of the SPE film D2 is determined by the Wagner's DC polarization method, using Swagelok

type cell with structure, SS/SPE/SS, where SS stands for stainless steel. On applying 0.5V across the cell, there is a dc current developed as a function of time, which is shown in figure 8. The t_{ion} can be calculated using the equation (3) is given below [12],

$$t_{ion}=(i_T-i_e)/i_T \quad \text{---------- (3)}$$

Here, i_T is the total current and i_e, the residual current. The total ion transport number obtained for the sample D2 is 0.989. The variation of current with respect to time across the cell with configuration SS/SPE film sample D2/SS is shown in figure 8. It indicates that the carrier transport is mainly due to ions and the electron contribution is quite negligible.

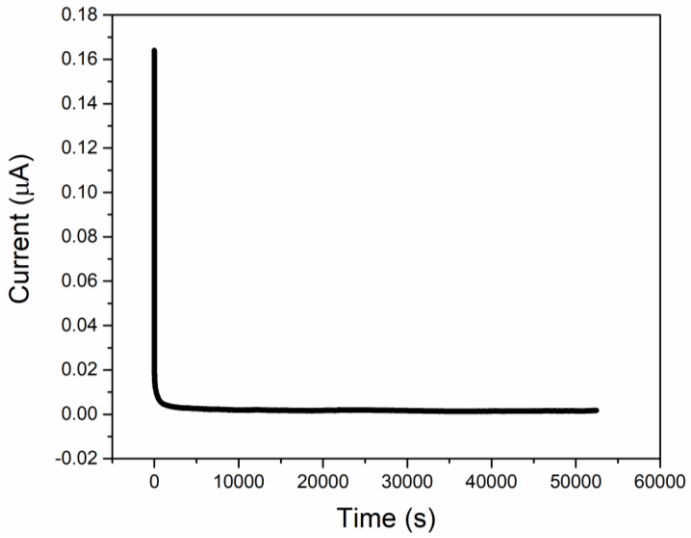

Figure 8: The variation of current with respect to time across the cell with configuration SS/SPE film sample D2/SS.

5.3.7 Electrochemical Stability

The cyclic voltammetry (CV) studies of the SPE film D2, which has the maximum ionic conductivity, are carried out for 3 cycles at a scan rate 5 mV s^{-1} in the configuration of SS/SPE film sample D2/SS. The CV curves are shown in figure 9. The electrochemical stability of the SPE film in the potential range up to 4V is clear from the CV curves. Good electrochemical stability window with repeatability [45] is observed from the CV curves.

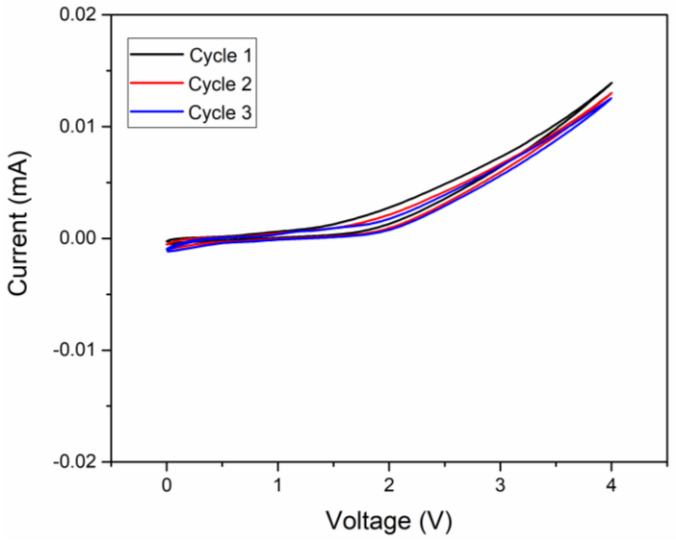

Figure 9: Cyclic voltammetry curves of the system, SS/SPE film sample D2/SS at a scan rate of 5mV s^{-1}

5.4 Conclusions

The present work highlights the realization of the solid polymer electrolyte (SPE) films, based on the polymer blend of PEO and the plasticizers EC and PC and complexed with $NaNO_3$ salt and modified

with the addition of the nano-filler material Al_2O_3. The SPE films are free standing, flexible and transparent and have good thermal stability upto 400° C as seen from the thermal studies. The XRD studies indicate the reduced crystalline nature of the SPE films, compared to the host polymer PEO, due to the complex formation with the sodium salt and the presence of the plasticizers and the filler material. The enhanced amorphous nature of the SPE films facilitates easier ion transport which in turn leads to high Na ion conductivity. The FTIR spectroscopy studies give evidence for the complex formation between the PEO based polymer blend and the $NaNO_3$. The FESEM analysis supports the smoother and porous surface morphology of the SPE films. The most striking result of the present work is concerned with the superb effect of the Al_2O_3 filler, in enhancing the ionic conductivity of the SPE films substantially and bringing it to around $1.86x10^{-4}$ S cm^{-1}. The high ionic conductivity and the electrochemical stability window upto 4V, as observed from the cyclic voltammetry studies, combined with the excellent thermal stability of these SPE films highlight their application prospects in the design of all solid state Na ion cells, capable of stable operation at temperatures much above room temperature.

5.5 References

[1] Kim S, Seo D, Ma X, et al (2012)Electrode Materials for Rechargeable Sodium-Ion Batteries: Potential Alternatives to Current Lithium-Ion Batteries.Adv. Energy Mater 2: 710–721.

[2] Guo S, Yu H, Liu P, Ren Y, Zhang T, et al (2014)High-performance symmetric sodium-ion batteriesusing a new bipolar material O3-type Na0.8Ni0.4Ti0.6O2Energy Environ.

Sci. 2014, 00, 1-3/1.

[3] Palomares V, Casas-Cabanas M, Castillo-Martinez E, et al (2013)Update on Na based battery materials. A growingresearch path. Energy Environ. Sci. 6: 2312–2337.

[4] Kundu D, Talaie E, Duffort V, Nazar LF (2015)The Emerging Chemistry of Sodium Ion Batteries for Electrochemical Energy Storage.Angew. Chem. Int 54: 3431–3448.

[5] Anantha PS, Hariharan K (2005)Physical and ionic transport studies on poly(ethylene oxide)–NaNO3polymer electrolyte system.Solid State Ionics 176: 155–162.

[6] Sreekanth T, Reddy MJ, Ramalingaiah S, Rao UVS (1999)Ion-conducting polymer electrolyte based on poly (ethylene oxide) complexed with NaNO3 salt-application as an electrochemical cell,J Power Sources 79: 105–110.

[7] Lailun Y, Cheng M, Hsiang J, et al (2015) Solid-state polymer nanocompositeelectrolyte of TiO2/PEO/NaClO4 forsodium ion batteries,J Power Sources 278:375–381.

[8] Stephan AM, Nahm KS (2006)Review on composite polymer electrolytes for lithium batteries,Polymer47:5952–5964.

[9] Mohapatra SR, Thakur AK, ChoudharyR. N. P (2008)Studies on PEO-based sodium ion conducting composite polymer films, Ionics 14:255–262.

[10] Patel M, Chandrappa KG, Bhattacharyya AJ (2010)Increasing ionic conductivity of polymer–sodium salt complex by addition of a non-ionic plastic crystal.Solid State Ionics 181:844–848.

[11] Boschin A, Johansson P (2016)Plasticization of NaX-PEO solid polymer electrolytes by Pyr13X ionic liquids.ElectrochimActa 211:1006–1015.

[12] [12] Xue Y, Quesnel DJ (2016) Synthesis and electrochemical study of sodium ion transport polymer gel electrolytes.RSC Adv 6:7504–7510.

[13] Rao SS,ReddyM J, NarsaiahE L, RaoUV S, (1995) Development of electrochemical cells based on (PEO + NaYF4) and (PEO + KYF4) polymer electrolytes. Materials Science and Engineering B 33: 173-177.

[14] Tripathi SK, Gupta A, Kumari M (2012)Studies on electrical conductivity and dielectric behaviour of PVdF–HFP–PMMA–NaI polymer blend electrolyte. Bull. Mater. Sci. 35:969–975.

[15] Kumar D, Hashmi SA (2010)Ion transport and ion–filler-polymer interaction in poly(methyl methacrylate)-based, sodium ion conducting, gel polymer electrolytes dispersed with silica nanoparticles.J Power Sources 195:5101–5108.

[16] Qi X, Ma Q, Liu L, Hu Y-S, Li H, Zhou Z, Huang X, Chen L, (2016) Sodium Bis(fluorosulfonyl)imide/Poly(ethylene oxide) Polymer Electrolytes for Sodium-Ion Batteries. ChemElectroChemdoi: 10.1002/celc.201600221.

[17] Che H, Chen S, Xie Y, et al (2017)Electrolyte design strategies and research progress for room-temperature sodium-ion batteries.Energy Environ Sci 10:1075–1101.

[18] Xue Z, He D,Xie X (2015)Poly(ethylene oxide)-based electrolytes for lithiumion batteries,J MaterChem A 3:19218–19253.

[19] Liang B, Tang S, Jiang Q, et al (2015)Preparation and characterization of PEO-PMMA polymer composite electrolytes doped with nano-Al_2O_3,ElectrochimActa169:334–341.

[20] Wang Y, Pan Y, Wang L, et al (2005)Conductivity studies of plasticized PEO-Lithium chlorate–FIC filler composite polymer electrolytes.Materials Letters59:3021–3026.

[21] Mohamad A A,Haliman H,Sulaiman M A,YahyaM Z A, Ali A MM,(2008)Conductivity studies of plasticized anhydrous PEO-KOH alkaline solid polymer electrolyte, Ionics 14:59–62.

[22] Pitawala H M J C,DissanayakeM A K L,Seneviratne V A,MellanderB.-E,AlbinsonI,(2008) Effect of plasticizers (EC or PC) on the ionic conductivity and thermal properties of the (PEO)9LiTf: Al2O3 nanocomposite polymer electrolyte system.J Solid State Electrochem 12:783–789.

[23] Tominaga Y, Endo M (2013)Ion-conductive properties of polyether-based composite electrolytesfilled with mesoporous silica, alumina and titania.Electrochim Acta113:361–365.

[24] Liu W, Lee SW, Lin D, et al (2017)Enhancing ionic conductivity in composite polymer electrolytes with well-aligned ceramic nanowires.Nature energy 2, 17035:1–7.

[25] Ravi M, Kumar K K, Mohan V M,Rao VVRN (2014)Effect of nano TiO2 filler on the structural and electrical properties of PVP based polymer electrolyte films.Polym Test 33:152–160.

[26] Suthanthiraraj SA, Paul BJ (2007) Investigation on structural characteristics of PVDF–AgCF3SO3–Al2O3 nanocomposite solid polymer electrolyte system.Ionics 13:365–368.

[27] Chew KW, Tan KW (2011)The Effects of Ceramic Fillers on PMMA-Based Polymer Electrolyte Salted With Lithium Triflate, LiCF3SO3.Int. J. Electrochem. Sci. 6:5792–5801.

[28] Pradhan DK, Samantaray BK, Choudhary RNP, Thakur AK (2005)Effect of plasticizer on structure—property relationship in composite polymer electrolytes.J Power Sources139:384–393.

[29] Jinisha B, Anilkumar KM, Manoj M, Pradeep VS, Jayalekshmi S (2017)Development of a novel type of solid polymer electrolyte for solid state lithium battery applications based on lithium enriched poly (ethylene oxide) (PEO)/poly (vinyl pyrrolidone) (PVP) blend polymer.ElectrochimActa 235:210–222.

[30] Koduru H K, Iliev M T, Kondamareddy K K, Karashanova D, Vlakhov T, et al (2016) Investigations on Poly (ethylene oxide) (PEO) – blend basedsolid polymer electrolytes for sodium ion batteries. Journal of Physics: Conference SeriesIOP Publishing 764 012006.

[31] Yang X, Zhang L, Zhang F, et al (2014)A high-performance all-solid-state supercapacitor with graphene-doped carbon material electrodes and a graphene oxide-doped ion gel electrolyte. Carbon 72:381–386.

[32] Anilkumar KM, Jinisha B, Manoj M, Jayalekshmi S (2017)Poly(ethylene oxide) (PEO) – Poly(vinyl pyrrolidone) (PVP) blend polymer based solid electrolyte membranes for developing solid state magnesium ion cells.EurPolym J 89:249–262.

[33] Gejji SP, Suresh CH, Babu K, Gadre SR (1999)Ab initio structure and vibrational frequencies of (CF3SO2)2N_Li+ ion pairs.J. Phys. Chem. A103, 7474-7480.

[34] Suthanthiraraj SA, Sheeba DJ (2007) Structural investigation on PEO-basedpolymer electrolytes dispersed with Al2O3 nanoparticles. Ionics 13:447–450.

[35] Awalendra K. T (2011) Mechanism for improvement in mechanical and thermal stability in dispersed phase polymer composites. Ionics 17:109–120.

[36] Kumar D, Hashmi SA (2010)Ionic liquid based sodium ion conducting gel polymer electrolytes.Solid State Ionics 181:416–423.

[37] Sengwa RJ, Dhatarwal P, Choudhary S (2014)Role of preparation methods on the structural and dielectric properties of plasticized polymer blend electrolytes: Correlation between ionic conductivity and dielectric parameters.ElectrochimActa 142:359–370.

[38] Zen J, Ilangovan G, Jou J (1999)Square-wave voltammetric determination and ac impedance study of dopamine on preanodizedperfluorosulfonatedionomercoated glassy carbon electrodes.Anal.Chem.71:2797–2805.

[39] Dissanayake MAKL, Jayathilaka PARD, Bokalawala RSP,et al (2003) Effect of concentration and grain size of alumina filler on the ionic conductivity enhancement of the (PEO)9LiCF3SO3:Al2O3 composite polymer electrolyte.J Power Sources 119-121:409–414.

[40] Golodnitsky D, Ardel G, Peled E (2002)Ion-transport phenomena in concentrated PEO-based composite polymer electrolytes.Solid State Ionics147:141–155.

[41] Jayathilaka PARD, Dissanayake MAKL, Albinsson I, Mellander B (2002)Effect of nano-porous Al2O3 on thermal, dielectric and transport properties of the (PEO)9LiTFSI polymer electrolyte system.ElectrochimActa 47:3257–3268.

[42] Ahn J, Wang GX, Liu HK, Dou SX (2003)Nanoparticle-dispersed PEO polymer electrolytes for Li batteries.J Power Sources 119-121:422–426.

[43] Pitawala HMJC, Dissanayake MAKL, Seneviratne VA (2007)Combined effect of Al2O3 nano-fillers and EC plasticizer on ionic conductivity enhancement in the solid polymer electrolyte (PEO)9LiTf.Solid State Ionics178:885–888.

[44] Yakuphanoglu F, Aydogdu Y, Schatzschneider U, Rentschler E, (2003)DC and AC conductivity and dielectric properties of the metal-radical compound: aqua[bis(2- dimethylaminomethyl-4-NIT-phenolato)]copper(II).Solid State Commun.128:63–67.

[45] Puthirath AB, John B, Gouri C, Jayalekshmi S (2015)Lithium-doped PEO—a prospective solid electrolyte with high ionic conductivity, developed using n- Butyllithium in hexane as dopant. Ionics 21:2185–2191.

Chapter 6

Solid-state supercapacitor with impressive performance characteristics, assembled using redox mediated gel polymer electrolyte

A solid-state supercapacitor is assembled using the redox mediated gel polymer as the electrolyte and separator and the coconut shell derived, steam activated carbon as the electrodes. The gel polymer electrolyte (GPE) is based on poly (vinyl alcohol) (PVA)- pottassium hydroxide (KOH)- hydroquinone (HQ), and is obtained using solution casting technique. Higher ionic conductivity around 53 mS cm^{-1} and superior flexibility serve as the main advantages of this redox mediated GPE. The electrode specific capacitance of the supercapacitor is found to be as high as 326.53 F g^{-1} with a capacity retention of 84.2% after being subjected 1000 charge-discharge cycles at a current density of 0.8 A g^{-1}. The assembled supercapacitors are found to offer quite high energy density and power density around 33.15 Wh kg^{-1} and 689.58 W kg^{-1}, respectively. These types of redox mediated, flexible, gel polymer electrolytes are desirable for designing high power solid state supercapacitors for energy storage applications.

6.1 Introduction

In recent years, great attention has been devoted for the development of supercapacitors (SCs) as potential energy-storage systems for high power applications in hybrid electric vehicles, pulse power supply for industrial applications and as backup sources for the next generation electronic devices [1,2,3]. They are endowed with high power capabilities (high specific power) and long cycle-life and offer opportunities to build more advanced, hybrid energy storage systems (ESSs), for both on-board and stationary applications [4]. Depending on the charge storage mechanism, SCs are mainly classified in to electric double layer capacitors (EDLCs), pseudocapacitors and hybrid-capacitors. In EDLCs, the capacitance is generated via a non -faradaic process due to the formation of an electrochemical double layer at the electrode-electrolyte interface [5]. Electrodes for EDLCs are usually based on highly porous carbon materials [6, 7, 8] which are ideal for the rapid storing and releasing of energy [9]. Wide availability, low cost, good electrical conductivity, and high surface area are the main advantages of porous carbon materials.

In pseudocapacitors, the capacitance is generated from a fast faradaic process due to the charge transfer reaction between the electrode and the electrolyte ions and this capacitance is called as the pseudocapacitance [5]. The electrodes based on conducting polymers, metal oxides and functionalized porous carbon materials are generally used for pseudocapacitive charge storage applications. These materials can hold much higher quantities of charge as compared to EDLCs, with

the charge storage mechanism relying on fast redox reactions occurring on the electrode surfaces [10]. In hybrid capacitors, both the electrical double-layer (EDL) formation and the faradaic mechanisms are responsible for energy storage process.

The SCs are emerging as the highly sought after energy storage devices in versatile fields, even with the limitation of having lower energy density, compared to rechargeable batteries. The initiatives for developing novel types of electrode and electrolyte materials are mandatory to improve the energy density of the next generation energy storage systems based on supercapacitors.. Electrolytes do play a key role in deciding the energy density and the safety level of supercapacitors. Currently, the aqueous, organic and ionic liquid electrolytes are being extensively used for charge storage processes in supercapacitors. There are however some serious issues related to the use of liquid electrolytes. Possibility of leakage of the liquid electrolytes, shorting of the electrodes and the corrosion issues of the liquid electrolytes are the main challenges to be considered when liquid electrolytes are used. Current research is hence focused on identifying suitable materials to serve as solid or quasi-solid electrolytes which can also take care of the safety issues of the supercapacitors [11]. Electrochemical energy devices based on solid electrolytes have high application prospects in portable electronics, micro-electronics, wearable electronics and specifically in flexible electronics. High ionic conductivity, wide potential window, wide operating temperature range, low cost, high chemical and electrochemical stability and environmental

safety are the mandatory properties expected, in ideal electrolytes. Each electrolyte type has its own advantages and limitations.

Solid polymer electrolytes (SPEs), gel polymer electrolytes (GPEs) and the polyelectrolytes constitute the three different types of polymer based solid electrolytes. The presence of liquid phase in GPEs, called as quasi-solid state electrolytes, leads to higher ionic conductivity, compared to conventional SPEs [14,15]. Currently, GPEs having high ionic conductivity and flexibility are gaining upper hand as the most suitable materials for the development of solid electrochemical supercapacitors of different shapes and bendable structures. Host polymers such as poly (vinyl alcohol) (PVA), poly (methylmethacrylate) (PMMA), poly (ethylene oxide) (PEO), poly (acrylic acid) (PAA), poly (vinylidene carbonate) and poly (vinylidene fluoride) have been widely explored for developing GPE films [16]. The GPEs based on PVA find applications in the development of various types of solid state super capacitors including, flexible and stretchable supercapacitors, printable micro supercapacitors and wearable, ultrathin and paper like supercapacitors [17,18,19,20,21,22]. Among the polymers, PVA is one of the most extensively studied polymers owing to its linear structure with high hydrophilicity, non-toxic characteristics, good film forming properties and low cost [23]. To prepare hydrogel electrolytes, PVA is mixed with various aqueous solutions of H_2SO_4, H_3PO_4, KOH, NaOH, KCl, NaCl and LiCl [23,24] to increase the capacitance of the assembled supercapacitors by prompting the pseudocapacitive contribution from the redox-active electrolytes. Redox additives (mediators) types of electrolytes offer a new direction in the field of

novel types of electrolytes to improve the performance of supercapacitors. [5,8]. The redox reaction of the electrolyte at the electrode-electrolyte interface will contribute towards an additional pseudocapacitance which will enhance the final capacitance of supercapacitors [12]. The redox mediators will provide quick reversible redox reaction, which will effectively enhance the ionic conductivity and contribute towards pseudocapacitance [13]. Many studies have been reported on the organic redox mediators as pseudocapacitive sources, including hydroquinone (HQ) [16], indigo carmine (IC) [25], methylene blue (MB) [26], p-phenylenediamine (PPD), [27] m-phenylenediamine (MPD) and sulfonated polyaniline (SPani) [28]. The specific capacitance value of the carbon based SCs are greatly influenced by the addition of these organic redox additives. Hydroquinone (HQ) is one of the electrochemically active organic compounds capable of having a two electron transfer redox reaction. Using HQ based redox-active electrolyte, it is possible to have a much faster self-discharge process [29]. A hydroquinone mediated PVA–H_2SO_4 gel electrolyte and activated carbon based supercapacitors are found to deliver a higher capacitance around 941 F g-1 at a current density of 1 mA cm^{-2} [16]. Guofu and his group have studied supercapacitors based on activated carbon with PVA-KOH-$K_3[Fe(CN)_6]$ based gel polymer electrolyte to obtain an electrode specific capacitance around 430.95 F g^{-1}[30]. At the electrode-hydrogel electrolyte interface, the choice of the electrode material and the hydrogel electrolyte is very critical in achieving high performance of the assembled supercapacitors. From many reports, it has been observed that advanced carbon structures [31,32,33,34] can

facilitate the infiltration of the hydrogel electrolyte into their porous structures, leading to significant improvement in the performance of the supercapacitors and extensive utilization of the active electrode materials [8]. Haijun and co-workers have obtained specific capacitance of 236.9 F g^{-1} for the devices assembled with PVA-KOH-KI based polymer gel electrolyte and activated carbon electrodes [11]. Present work introduces HQ redox material in the above PVA-KOH system, and the electrode specific capacitance of the assembled supercapacitor is around 326.53 F g^{-1} at a current density of 0.8 A g^{-1}, using coconut shell derived, activated carbon as the electrode material [35].

The work included in this chapter is focused on the development of a solid state supercapacitor using the redox mediated gel polymer as the electrolyte. The host polymer PVA along with KOH (strong base) and the redox mediator HQ constitute the gel polymer electrolyte (GPE). Structural properties of the GPE are analysed using X-Ray diffraction and FTIR spectroscopy studies. Thermal stability is estimated by thermo-gravimetric analysis. The ionic conductivity measurement of the GPE is carried out by impedance analysis and cyclic voltammetry is used to find the working voltage window of the GPE. Detailed electrochemical characterization of the assembled solid state supercapacitors is carried out using cyclic voltammetry and galvanostatic charge discharge test.

6.2 Experimental details

6.2.1 Materials

Poly (vinyl alcohol) (PVA, HIMEDIA, molecular weight: 140,000), KOH (SDFCL,), hydroquinone (Spectrochem), cocunut shell derived, steam activated carbon, purchased from local suppliers and purified by HF washing in our laboratory are the chemicals used in the present work.

6.2.2 Synthesis of the gel polymer electrolyte

The gel polymer electrolyte (GPE) films were grown using solution-casting method [11].In a typical synthesis, PVA and KOH (1 g each) were dissolved in deionized water and stirred at 80 $^{\circ}$C for 3 hours. The resulting solution was continuously stirred until it attained a homogeneous viscous appearance and was subsequently poured into a petri dish. The excess water was evaporated at 80 $^{\circ}$C by keeping in a vacuum oven overnight to obtain PVA–KOH gel electrolyte. To synthesize the PVA–KOH–HQ based electrolyte, PVA and KOH (1g each) were initially dissolved in deionized water by stirring at 80 °C for 3 hours and after complete dissolution, different amounts (0.1, 0.2, 0.3 and 0.4 g) of HQ were added . As before, the resulting solution was stirred continuously for attaining a homogeneous composition. This solution was poured into a petri-dish and kept in a vacuum oven at 80 °C for the evaporation of excess solvent. Both types of the GPE films, obtained as free standing and highly flexible ones, were stored in a desiccator. Schematic representation of the synthesis method is given in figure 1 (a).

6.2.3 Electrode making

The electrodes were made by mixing 80 weight % of the coconut shell derived, steam activated carbon, purified by HF washing and termed as CSAC, 10 weight % of the conducting carbon and 10 weight % of poly(vinylidene di fluoride) (PVdF), in the presence of N-methyl pyrrolidinone (NMP) as solvent to make a slurry. The slurry was then coated on aluminium foil by spray-coating and dried at 120 $^{\circ}$C under vacuum overnight. The mass of the working electrode was fixed as 2 mg.

6.2.4 Supercapacitor assembly

The solid state supercapacitor architecture consists the gel polymer electrolyte film, sandwiched between the two activated carbon electrodes as shown in figure 1 (b). The gel polymer electrolyte film serves as both the separator and the electrolyte.

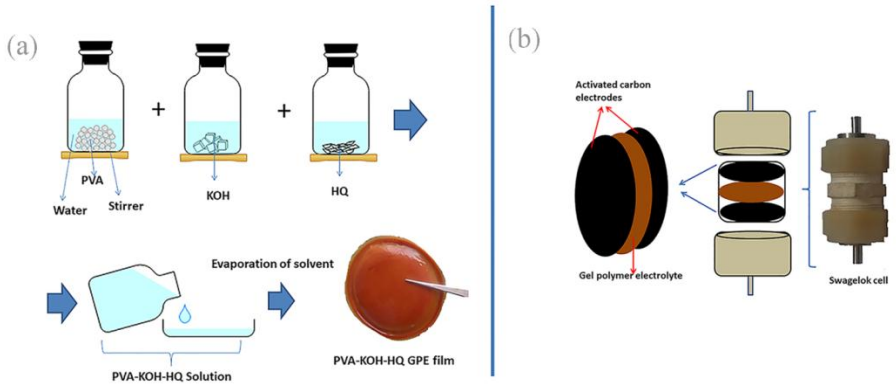

Figure 1: (a) Synthesis route of PVA-KOH-HQ based GPE and **(b)** Assembling of the solid supercapacitor

6.2.5 Characterization

6.2.5.1 Structural characterization

The structural aspects of the GPE films were investigated with the help of the Rigaku Max C, X-Ray diffractometer. The FTIR spectroscopic studies were done using the SHIMADSU machine in the range of 400–4000 cm^{-1}, to confirm the complex formation in the PVA-KOH and the PVA-KOH-HQ based GPEs. Thermo-gravimetric analysis using the Perkin Elmer STA 6000 instrument was used to study the thermal stability of the GPE films in the temperature range from room temperature to 750 °C under controlled nitrogen atmosphere.

6.2.5.2 Electrochemical Analysis

Ionic conductivity of the gel polymer electrolyte was determined from impedance spectroscopy studies conducted using HP 4192A impedance analyser and the value is calculated using the equation, [30,36]

$$\sigma = \frac{t}{R_b A} \text{ ---------- (1)}$$

where t is the thickness of the GPE film, R_b , the bulk resistance and A , the area of the film., as explained earlier.

All the electrochemical studies were carried out using the two electrode device under ambient conditions. Cyclic voltammetry (CV) and galvanostatic charge discharge (GCD) test were conducted using SP 300 potentiostat. The CV measurements were carried out at various scan rates from 5 mV s^{-1} to 100mV s^{-1} at the potential range from -1V to 1V

and the GCD measurements,from -1 to 1V at various current densities 0.4, 0.6 0.8, 1 and 2 A g^{-1}.

The specific capacitance C and the electrode specific capacitance C_s,of the supercapacitor can be obtained from the charge discharge curves using the equations, [30, 37, 38]

$$C = \frac{I \times \Delta t}{\Delta V \times m_{ac}} \text{ ---------- (2)}$$

$$C_s = 4 \times C \text{ ---------- (3)}$$

Energy density E and power density P of the supercapacitor are determined using the equations [7, 39]

$$E = \frac{1}{2 \times 3.6} C \times \Delta V^2 \text{ ---------- (4)}$$

$$P = \frac{E}{T} \times 3600 \text{ ---------- (5)}$$

where I is the discharge current, Δt the discharge time, m_{ac} the mass of the active material in the electrode and ΔV, the operating voltage window.

6.3 Results and discussions

6.3.1 XRD Analysis

The X-ray diffraction pattern of pure PVA, PVA-KOH and PVA-KOH-HQ based GPE films are shown in figure 2. In the pattern of PVA, a small intense peak at 2θ = 19.6 °, showing the semicrystalline nature of PVA [40] is observed. On adding KOH to PVA, this peak becomes very weak and the combined system is almost amorphous in nature. There is a larger domain of amorphous phase, when the PVA matrix is modified with the addition of KOH. Consequently, the ionic conductivity of the

polymer electrolyte gets significantly enhanced [41]. On adding HQ to the PVA-KOH system, a fully amorphous phase pattern is obtained. The PVA-KOH-HQ based GPE is more amorphous compared to the one without HQ, which is desirable for effective ion transfer to achieve still higher ionic conductivity. The segmental motion of the polymer chains is more pronounced in the amorphous state. The transport of cations and anions in the polymer matrix is responsible for the ionic conductivity of the gel polymer electrolyte [41]. The ionic conductivity is mainly confined to the amorphous phase and the ionic mobility is improved by the segmental motion of the polymer host, PVA.

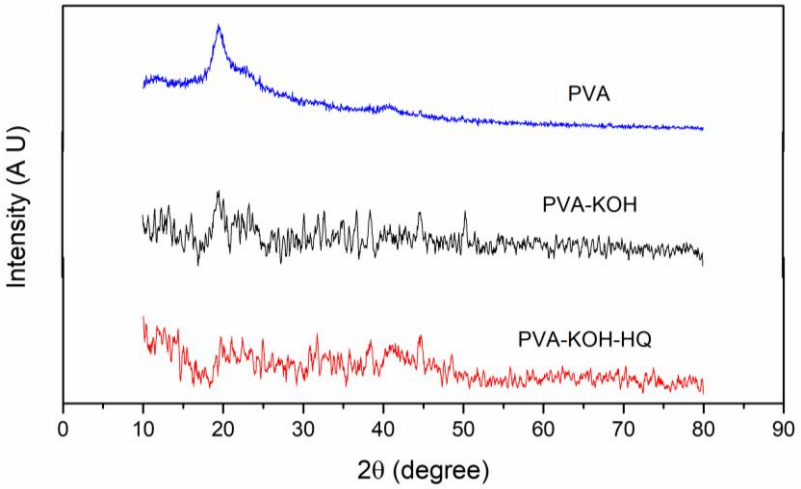

Figure 2: XRD patterns of PVA and the PVA-KOH and PVA-KOH-HQ based GPEs

6.3.2 FTIR spectroscopic studies

The FTIR spectra of PVA-KOH and PVA-KOH-HQ based GPE films are shown in figure 3. The spectrum of PVA-KOH based GPE shows peaks at 3329 and 1375 cm^{-1}, corresponding to the O–H

stretching and bending vibrations of PVA [42]. The asymmetric and symmetric stretching vibrations of the -CH_2 group have characteristic absorption peaks at 2917 and 2846 cm^{-1} respectively. The peak at 1103 cm^{-1} corresponds to the stretching vibration of C−O [40]. On adding HQ to the PVA-KOH system, the peak corresponding to C-O stretching vibration is widened. The peak related to OH bending vibration at 1375 cm^{-1} gets slightly shifted and the band intensity decreases. Changes in peak intensity and shifting of peak positions are observed as a consequence of the addition of HQ. The peak intensities get reduced, possibly due to the restricted motion of PVA chains [42] in the presence of HQ. The changes in peak positions and intensities establish the interaction between the PVA-KOH matrix and HQ.

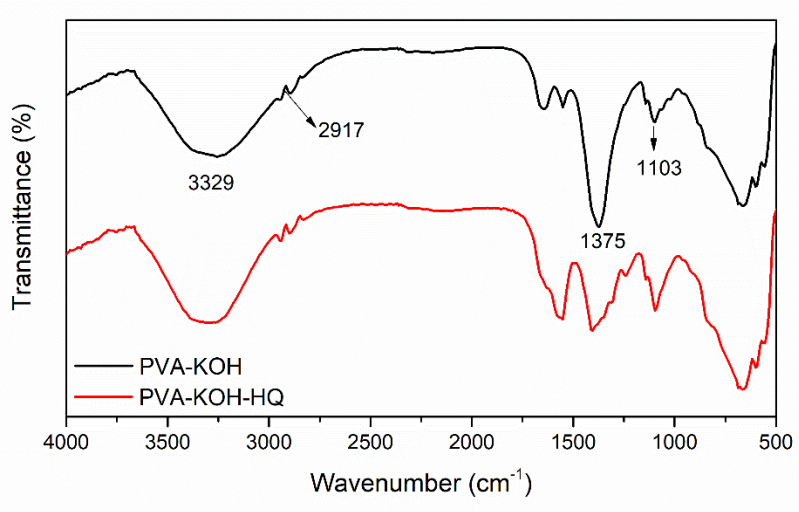

Figure 3: FTIR spectra of PVA-KOH and PVA-KOH-HQ based GPE films

6.3.3 Thermal characterization

6.3.3.1 Thermo-gravimetric analysis (TGA)

There is an initial weight loss of 2% for PVA at 82 °C due to the presence of the solvent, water, on the sample surface as seen in the thermo-grams, depicted in figure 4. At 230 °C, second decomposition of PVA takes place and this corresponds to 7 % weight loss. Around 98 % weight loss happens at 730 °C indicating that PVA can be almost completely thermo-decomposed [40] at this temperature. The initial weight loss is very fast in PVA-KOH and PVA-KOH- HQ based GPE films due to the water content present on the gel surface. The second decomposition of the former GPE film is at 185 °C and the latter one at 230 °C. The weight loss curve of PVA-KOH based GPE film is at lower temperature region than that of PVA-KOH-HQ based one. The HQ content increases the thermal stability of PVA-KOH-HQ based GPE film, compared to PVA-KOH based one. Around 70 % decomposition of PVA-KOH and PVA-KOH-HQ based GPE films occurs at 730 °C as shown in figure 4. It is evident that at 730 °C, PVA is completely decomposed, but 30% of the GPE films still remains at that temperature.

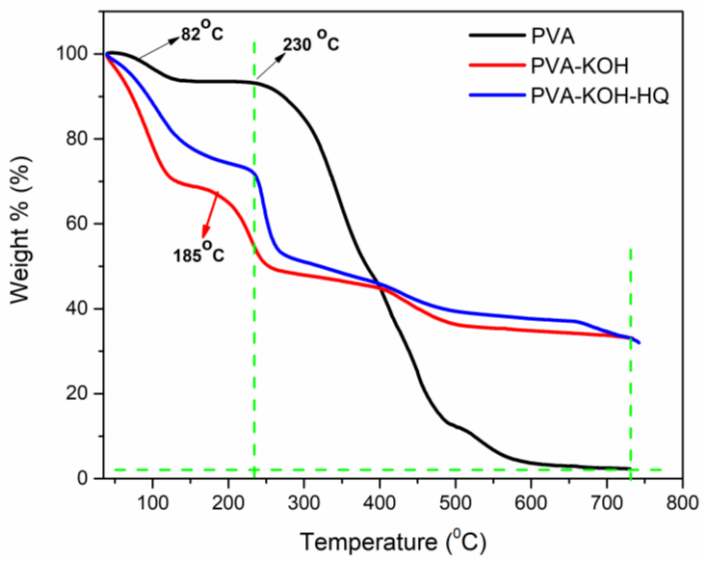

Figure 4: TGA curves of PVA, PVA-KOH and PVA-KOH-HQ based GPE films

6.3.4 Ionic conductivity studies

The impedance plots for the PVA-KOH-HQ based GPE films having PVA-KOH system with different HQ concentrations of 0, 0.1, 0.2, 0.3 and 0.4g are shown in figure 5. The ionic conductivity values, calculated as explained earlier, are observed to increase with the increase in the concentration of HQ in the PVA-KOH system up to the HQ concentration of 0.2 g and then start to decrease with further addition of HQ. Maximum ionic conductivity of 53 mS cm^{-1} is obtained for 0.2 g of HQ content. The HQ acts as a redox mediator and redox shuttle promoter in the electrolyte. At lower HQ concentrations, redox shuttle function of HQ is not active in the system which leads to lesser ionic conductivities at lower concentrations. When the amount of HQ increase to 0.20 g, the redox shuttle function of HQ becomes active and the electrolyte turns in to a quasi-solid state accompanied by the highest

ionic conductivity. The HQ concentrations higher than 0.20 g lead to the aggregation of free ions and the resulting crystallization of HQ in the PVA system hinders the ionic motion and reduces the conductivity of the GPE film [43, 44]. The concentration, 0.2 g of HQ seems to be the optimal HQ amount to deliver maximum ionic conductivity in PVA-KOH-HQ based GPEs films.

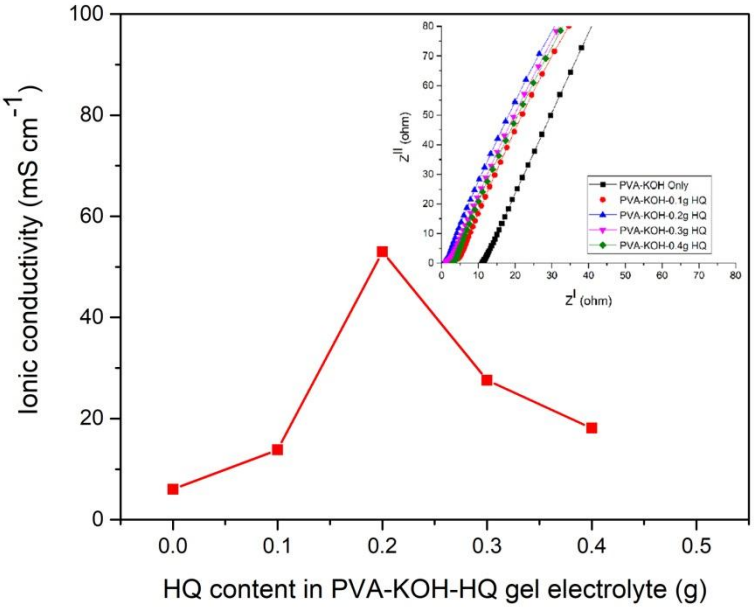

Figure 5: Ionic conductivity of PVA–KOH–HQ based GPE films containing different amounts of HQ. Inset shows the impedance plots of all the GPEs.

6.3.5 Cyclic voltammetry studies

Cyclic voltammetry (CV) performance of the electrolyte helps to determine its operating potential window. The CV studies of PVA-KOH–HQ based GPE films are carried out for 10 cycles at a scan rate of

1 mV s^{-1} in the configuration of SS/GPE film/SS [36] as shown in figure 6. The electrochemical stability of the GPE film in the potential range up to 1 V is clear from the CV curves. An electrochemical stability window of 1V with repeatability is considered ideal for GPE films to be applied as solid electrolytes in supercapacitors.

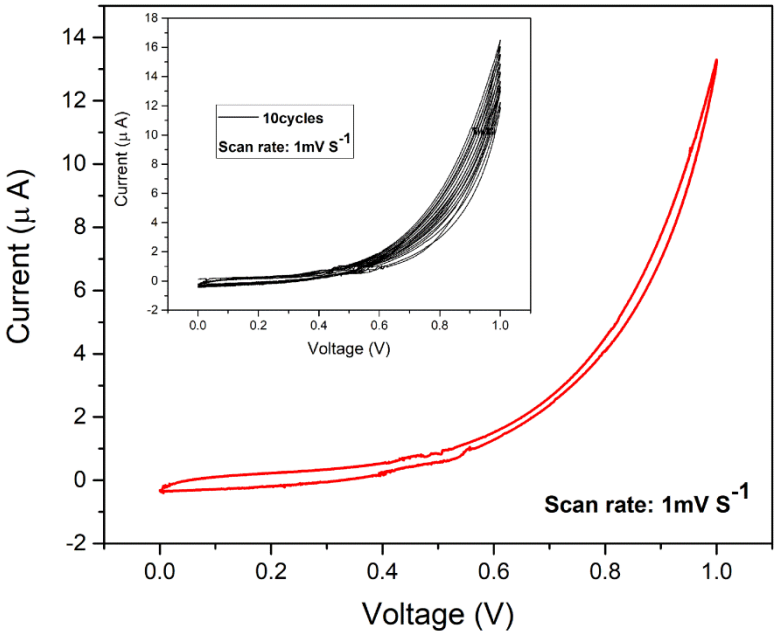

Figure 6: CV curves of the PVA-KOH-HQ based GPE films

6.3.6 Cyclic voltammetry of assembled Supercapacitors

The CV curves of the assembled supercapacitors, based on PVA-KOH and PVA-KOH-HQ based GPE films at a scan rate of 5 mV s^{-1} are shown in figure 7(a). The supercapacitor with PVA-KOH based GPE shows rectangular shaped CV curves with no oxidation-reduction peaks from a Faradic current, over the potential region, as in an ideal electrical

double layer capacitor. The CV curves of the supercapacitor with PVA-KOH-HQ based GPE, having 0.2 g of HQ in the PVA-KOH system, at a scan rate of 5 mV s^{-1} are presented in figure. 7(a). These curves exhibit rectangular curve behaviour along with wide oxidation and reduction waves centred at around 0 V suggesting a combination of electrical double layer capacitance (EDLC) and pseudo-capacitance. Accumulation of charges at the electrode/electrolyte interface contributes towards the EDLC behaviour and the reversible redox reaction from HQ is responsible for the pseudo-capacitance. The redox process at the electrode/electrolyte interface gives rise to pseudo-capacitance for the electrode with the appearance of bumps in the CV curves of the supercapacitor with PVA-KOH-HQ based electrolyte, due to Faradaic processes. The total capacitance observed for the supercapacitor with PVA–KOH-HQ based gel polymer electrolyte should be the sum of the double layer capacitance and the Faradaic pseudo-capacitance [45].

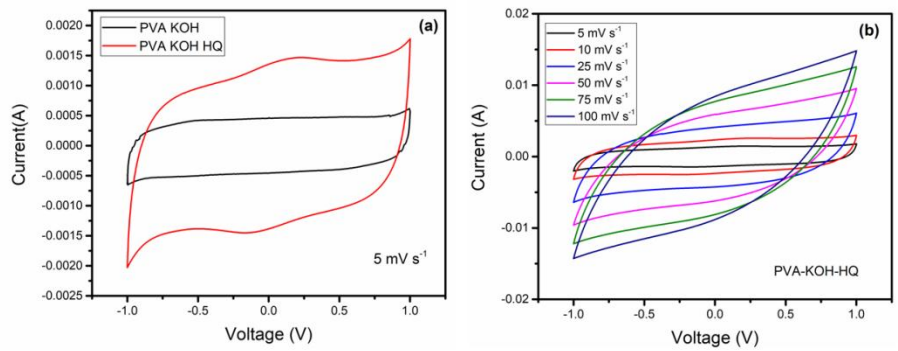

Figure 7: **(a)** CV curves of the supercapacitors with PVA-KOH and PVA-KOH-HQ based GPEs at a scan rate of 5 mV s^{-1}, **(b)** CV curves of the supercapacitor with PVA-KOH-HQ based GPE at scan rates of 5 to 100 mV s^{-1}

The CV curves of the supercapacitor with PVA-KOH-HQ based GPE at different scan rates from 5 mV s^{-1} to 100 mV s^{-1} are shown in figure 7 (b). Over the potential window, the supercapacitor shows pronounced current response. It shows a small deviation in the CV curve at higher scan rate of 100 mV s^{-1}, may be due to incomplete redox reactions as a result of fast ionic charge–discharge process and narrow access of ions on the electrode–electrode interfaces [16]. The shapes of the curves remain close to the rectangular shape at higher scan rates, which suggests the excellent electrochemical stability of the supercapacitor [30].

6.3.7 Galvanostatic charge/discharge (GCD) studies of the assembled supercapacitor

The electrochemical capacitance of materials is evaluated using galvanostatic charge/discharge studies. The GCD curves of the supercapacitors assembled with PVA-KOH and PVA-KOH-HQ based GPEs at a current density of 0.8 A g^{-1} are shown in figure 8 (a). The specific capacitance of the electrode C_s for the supercapacitors with PVA-KOH and PVA-KOH-HQ based GPEs are determined to be 107.06 and 326.53 F g^{-1} respectively at a charge/discharge current density of 0.8 A g^{-1}. Evidently, the C_s of the supercapacitor with PVA-KOH-HQ based GPE is larger than that of the supercapacitor with PVA-KOH based GPE. It is clear that the redox mediator HQ can significantly improve the capacitive property of the supercapacitor.

The compound, HQ is one of the strong electrochemically active organic compounds that is involved in a two electron transfer redox

reaction. During the charging of the supercapacitor, hydroquinone is oxidized into quinone with $2H^+$ and 2 electrons and during the discharge process, quinone is reduced into hydroquinone via the gain of 2 electrons with $2H^+$ at its corresponding oxidation and reduction potentials, as shown in figure 9 [16]. Hydroquinone predominantly exhibits pseudocapacitance at the electrolyte–electrode interface and significantly contributes to the total electrode specific capacitance of the supercapacitor.

The charge/discharge curves of the supercapacitor with PVA-KOH-HQ based GPE at various current densities of 0.4, 0.6, 0.8, 1 and 2 A g^{-1} are shown in figure 8(b) and the corresponding electrode capacitance values are tabulated in Table 1. From the galvanostatic charge/discharge curves at various current densities, the energy density and power density are calculated using the equations given earlier. The energy density and power density of the supercapacitor assembled using PVA-KOH-HQ based GPE are 33.15 Wh kg^{-1} and 689.58 W kg^{-1} respectively, at a current density of 0.8 A g^{-1} and the corresponding values for the supercapacitor with the PVA-KOH based GPE are 5.35 Wh kg^{-1} and 428.6 W kg-1 respectively. The supercapacitor with PVA-KOH-HQ based GPE has excellent electrochemical characteristics of higher energy density and power density than those of the one with PVA-KOH based GPE gel polymer electrolyte based supercapacitor.

Table 1: Electrochemical performance data of the supercapacitor with PVA-KOH-HQ based GPE at different current densities.

Current density ($A\ g^{-1}$)	Specific capacitance, C ($F\ g^{-1}$)	Electrode Specific capacitance Cs=4C ($F\ g^{-1}$)	Energy density ($Wh\ kg^{-1}$)	Power density ($W\ kg^{-1}$)
0.4	90.497	361.99	45.85	384.05
0.6	86.455	345.82	40.212	548.78
0.8	81.63	326.53	33.15	689.58
1	50.942	203.76	15.7	701.85
2	43.478	173.91	7.3	853.8

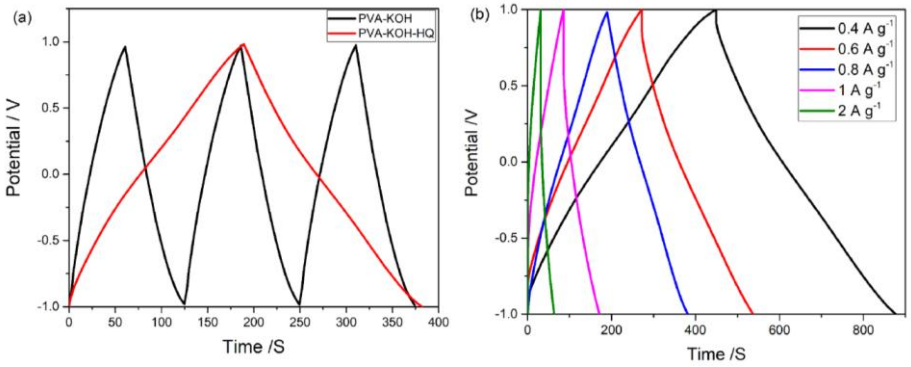

Figure 8: (a) GCD curves of the supercapacitors with PVA-KOH and PVA-KOH-HQ based GPEs at 0.8 A g^{-1} current density, **(b)** GCD curves of the supercapacitor with PVA-KOH-HQ based GPE at current densities from 0.4 to 2 A g^{-1}

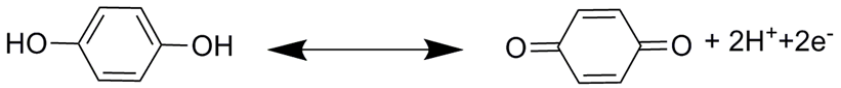

Figure 9: Typical redox process between hydroquinone and quinone [16].

6.3.8 Electrode specific capacitance-current density plot and Ragone plot

The electrode specific capacitance values of the supercapacitor at various current densities are given in figure 10(a). It is observed that the

capacitance slowly decreases as the current density becomes larger. At a current density of 0.4 A g^{-1}, the electrode specific capacitance is 365.38 F g^{-1}. Significantly, its value is retained at 202.24 F g^{-1} at a current density as high as 2 A g^{-1}. The decrease in capacitance at higher current density is attributed to the limited use of the redox reaction in hydroquinone. The Ragone plot represents the energy density versus the power density and such a plot of the supercapacitor with PVA-KOH-HQ based gel polymer electrolyte is shown in figure 10(b).

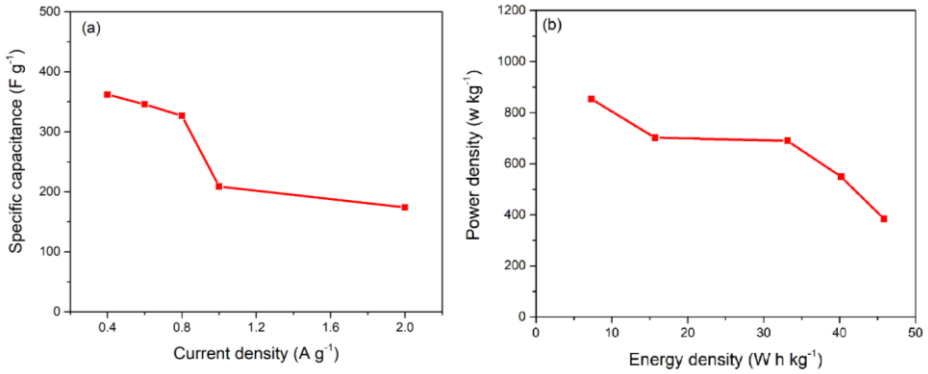

Figure 10: (a) Electrode specific capacitance (C_s) versus current density plot of the supercapacitor with PVA-KOH-HQ based GPE and **(b)** Ragone plot related to energy density and power density of the supercapacitor with PVA-KOH-HQ based GPE

6.3.9 Cycle-life testing

Cyclic durability is an important parameter to decide the application prospects of a supercapacitor device [43]. The C_s variations with 1000 charge–discharge cycles of the supercapacitors with PVA-KOH and PVA-KOH-HQ based GPEs at a current density of 0.8 A g^{-1} are shown in figure. 11. The device with PVA-KOH-HQ based GPE shows excellent capacitance retention of 84.2% of its initial electrode

specific capacitance after 1000 cycles.. The supercapacitor device with PVA-KOH based GPE retains only 48.1% after 1000 charge/discharge cycles indicating their poor cycling stability compared to that of the supercapacitors based on PVA-KOH-HQ based GPEs. By adding HQ to the PVA-KOH system, there is significant improvement in the specific capacitance as well as the stability of the supercapacitor, making the gel polymer electrolyte based on PVA-KOH-HQ, the highly prospective one for designing high power, solid-state supercapacitor devices for the next generation energy storage applications [30].

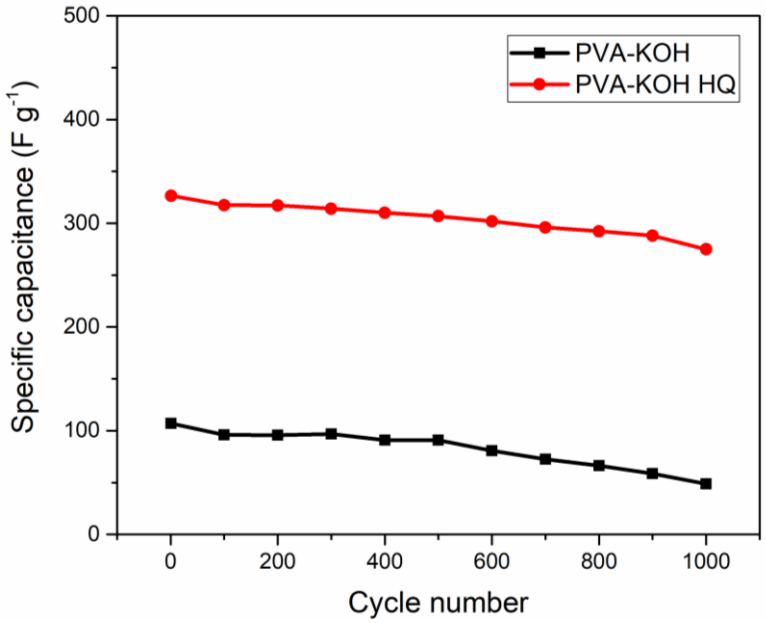

Figure 11: Cycle life of the supercapacitors with PVA-KOH and PVA-KOH-HQ based gel polymer electrolytes.

6.3.10 Self discharge

Self-discharge of the device is very important in energy storage devices for assessing their practical application [11]. Time courses of the open circuit voltage for the supercapacitors with PVA–KOH and PVA–

KOH-HQ based gel polymer electrolytes are shown in figure 12. A rapid self-discharge course within 2 hours is observed for the supercapacitor assembled using the PVA-KOH-HQ based GPE. After two hours, the self-discharge course is decelerated. After 10 hours,the output voltage is observed as ~0.48 V. It is clear that the voltage decay for the device with the HQ based gel polymer electrolyte is lower than that for the device with the PVA-KOH based GPE. This implies that the self-discharge is suppressed [46] by the gel polymer electrolyte containing HQ. The self-discharge performance of the device with the PVA-KOH- HQ based GPE is better than that of the one with PVA–KOH based GPE, indicating the advantages of HQ on improving the supercapacitor performance.

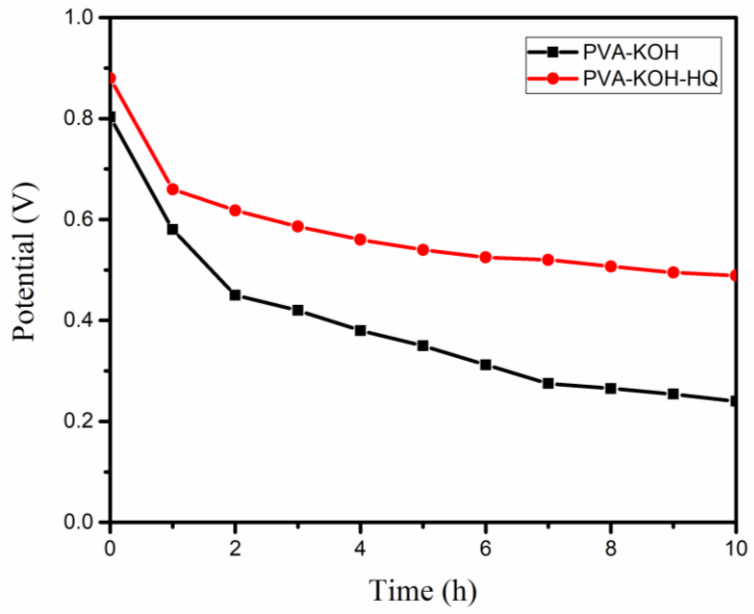

Figure 12: Self discharge curves of the supercapacitors with PVA-KOH and PVA-KOH-HQ based gel polymer electrolytes.

6.4 Conclusions

A solid-state supercapacitor is developed with coconut shell derived, steam activated carbon as electrodes and the redox mediated PVA-KOH-HQ based gel polymer electrolyte serving the purpose of the solid electrolyte and the separator. Presence of the redox mediator 'HQ' in the electrolyte is found to boost the electrochemical performance of the assembled supercapacitors. Ionic conductivity is found to vary with HQ concentration and a maximum conductivity of 53 mS cm^{-1} is found for the GPE films with the HQ concentration of 0.2 g. The GPEs have 1 V electrochemical potential window with repeatability as observed from the cyclic voltammetry analysis. The GCD analysis of the supercapacitors assembled with the PVA-KOH-HQ based GPEs reveal high electrode specific capacitance of 326.53 F g^{-1}, energy density of 33.15 Wh kg^{-1} and power density around 689.58 W kg^{-1} when cycled at a current density of 0.8 A g^{-1} and 84.2% of the initial capacitance is found to be retained after 1000 charge-discharge cycles. From the electrochemical studies, it can be concluded that the presence of the redox mediator HQ in the GPE films can significantly influence the electrochemical performance of the assembled solid-state supercapacitors by improving their pseudo-capacitance behaviour, total specific capacitance and cycling stability. Redox mediators offer high application prospects for improving the performance of energy storage devices and the HQ based GPE films of the present work are highly promising for the development of high power, solid-state supercapacitors with enhanced capacitance, excellent cycling stability and good safety standards for the next generation energy storage applications.

6.5 References

[1] Silvia Roldn, Clara Blanco, Marcos Granda, Rosa Menndez, and Ricardo Santamaria, Towards a Further Generation of High-Energy Carbon-Based Capacitors by Using Redox-Active Electrolytes, Angew. Chem. Int. Ed. 2011, 50, 1699 –1701.

[2] Silvia Roldan, Marcos Granda, Rosa Menendez, Ricardo Santamaría, and Clara Blanco, Mechanisms of Energy Storage in Carbon-Based Supercapacitors Modified with a Quinoid Redox-Active Electrolyte, J. Phys. Chem. C 2011, 115, 17606–17611.

[3] A. Burke, Ultracapacitors: why, how, and where is the technology, J. Power Sources, 91, 2000, 37-50.

[4] Enke Fenga, Guofu Ma*a, Kanjun Sunb, Qian Yanga, Hui Penga, Ziqiang Lei, Toughened redox-active hydrogel as flexible electrolyte and separator applying supercapacitors with superior performance, RSC Adv., 2016, DOI: 10.1039/C6RA14149H.

[5] S. T. Senthilkumar,a R. Kalai Selvan and J. S. Melo, Redox additive/active electrolytes: a novel approach to enhance the performance of supercapacitors, J. Mater. Chem. A, 2013, 1, 12386–12394.

[6] Silvia Roldán∗, Zoraida González, Clara Blanco, Marcos Granda, Rosa Menéndez, Ricardo Santamaría, Redox-active electrolyte for carbon nanotube-based electric double layer capacitors, Electrochimica Acta 56 (2011) 3401–3405.

[7] Anilkumar KM, Manoj M, Jinisha B, Pradeep VS, S. Jayalekshmi, Mn3O4/reduced graphene oxide nanocomposite electrodes with tailored morphology for high power supercapacitor applications, Electrochimica Acta 236 (2017) 424–433.

[8] Cheng Zhong,a Yida Deng,b Wenbin Hu,*ab Jinli Qiao,c Lei Zhangd and Jiujun Zhang, A review of electrolyte materials and compositions for electrochemical supercapacitors, Chem. Soc. Rev., 2015, 44, 7484.

[9] J. Huang, B. G. Sumpter, V. Meunier, Theoretical Model for Nanoporous Carbon Supercapacitors, Angew. Chem. 2008, 120, 530; Angew. Chem. Int. Ed. 2008, 47, 520-524.

[10] [10] Ander González, Eider Goikolea, Jon Andoni Barrena, Roman Mysyk, Review on supercapacitors: Technologies and materials, Renewable and Sustainable Energy Reviews 58(2016)1189–1206.

[11] Haijun Yu, Jihuai Wu∗, Leqing Fan, Kaiqing Xu, Xin Zhong, Youzhen Lin, Jianming Lin, Improvement of the performance for quasi-solid-state supercapacitor by using PVA–KOH–KI polymer gel electrolyte, Electrochimica Acta 56 (2011) 6881– 6886.

[12] Grzegorz Lota, Elzbieta Frackowiak, Striking capacitance of carbon/iodide interface, Electrochemistry Communications 11 (2009) 87–90.

[13] Haijun Yu, Jihuai Wu∗, Leqing Fan, Youzhen Lin, Kaiqing Xu, Ziying Tang, Cunxi Cheng, Shen Tang, Jianming Lin, Miaoliang Huang, Zhang Lan, A novel redox-mediated gel polymer electrolyte for high-performance supercapacitor, Journal of Power Sources 198 (2012) 402– 407.

[14] Anna A. Łatoszynska , Grazyna Zofia Z_ukowska , Iwona A. Rutkowska, Pierre-Louis Taberna , Patrice Simon, Pawel J. Kulesza, Władysław Wieczorek, Non-aqueous gel polymer electrolyte with phosphoric acid ester and its application for quasi solid-state supercapacitors, Journal of Power Sources 274 (2015) 1147e1154.

[15] Le-Qing Fan, Ji Zhong, Ji-Huai Wu, Jian-Ming Lin and Yun-Fang Huang, Improving the energy density of quasi-solid-state electric double-layer capacitors by introducing redox additives into gel polymer electrolytes, J. Mater. Chem. A, 2014, 2, 9011–9014.

[16] S. T. Senthilkumar, R. Kalai Selvan, N. Ponpandian and J. S. Melo, Redox additive aqueous polymer gel electrolyte for an electric double layer capacitor, RSC Adv., 2012, 2, 8937–8940.

[17] Xianfu Wang , Bin Liu , Qiufan Wang , Weifeng Song , Xiaojuan Hou , Di Chen , Yi-bing Cheng , and Guozhen Shen, Three-Dimensional Hierarchical GeSe 2 Nanostructures for High Performance Flexible All-Solid-State Supercapacitors, Adv. Mater. 2013, 25, 1479–1486.

[18] Zhiqiang Niu , Haibo Dong , Bowen Zhu , Jinzhu Li, Huey Hoon Hng , Weiya Zhou, Xiaodong Chen, and Sishen Xie, Highly Stretchable, Integrated Supercapacitors Based on Single-Walled Carbon Nanotube Films with Continuous Reticulate Architecture, Adv. Mater. 2013, 25, 1058–1064.

[19] Shuangyu Liu, Jian Xie, Haibo Li, Ye Wang, Hui Ying Yang, Tiejun Zhu, Shichao Zhang, Gaoshao Cao and Xinbing Zhao, Nitrogen-doped reduced graphene oxide for highperformance flexible all-solid-state microsupercapacitors, J. Mater. Chem. A, 2014, 2, 18125–18131.

[20] Jing Ren , Wenyu Bai , Guozhen Guan , Ye Zhang , and Huisheng Peng, Flexible and Weaveable Capacitor Wire Based on a Carbon Nanocomposite Fiber, Adv. Mater. 2013, 25, 5965–5970.

[21] Lele Peng, Xu Peng, Borui Liu, Changzheng Wu, Yi Xie, and Guihua Yu, Ultrathin Two-Dimensional MnO2/Graphene Hybrid Nanostructures for High-Performance, Flexible Planar Supercapacitors, Nano Lett. 2013, 13, 2151−2157.

[22] Longyan Yuan, Bin Yao, Bin Hu, Kaifu Huo, Wen Chen and Jun Zhou, Polypyrrole-coated paper for flexible solid-state energy storage, Energy Environ. Sci., 2013, 6, 470–476.

[23] Memoria Rosi, Ferry Iskandar, Mikrajuddin Abdullah, and Khairurrijal, Hydrogel-Polymer Electrolytes Based on Polyvinyl Alcohol and Hydroxyethylcellulose for Supercapacitor Applications, Int. J. Electrochem. Sci., 9 (2014) 4251 – 4256.

[24] Qiao Chen, Xinming Li, Xiaobei Zang, Yachang Cao, Yijia He, Peixu Li, Kunlin Wang, Jinquan Wei, Dehai Wu and Hongwei Zhu, Effect of different gel electrolytes on graphenebased solid-state supercapacitors, RSC Adv., 2014, 4, 36253–36256.

[25] Guofu Ma, Miaomiao Dong, Kanjun Sun, Enke Feng, Hui Peng and Ziqiang Lei, A redox mediator doped gel polymer as an electrolyte and separator for a high performance solid state supercapacitor, J. Mater. Chem. A, 2015, 3, 4035–4041.

[26] Silvia Roldán, Marcos Granda, Rosa Menéndez, Ricardo Santamaría, Clara Blanco, Supercapacitor modified with methylene blue as redox active electrolyte, Electrochimica Acta 83 (2012) 241– 246.

[27] Jihuai Wu, Haijun Yu, Leqing Fan, Genggeng Luo, Jianming Lin and Miaoliang Huang, A simple and high-effective electrolyte mediated with p-phenylenediamine for supercapacitor, J. Mater. Chem., 2012, 22, 19025–19030.

[28] Libin Chen, Yanru Chen, Jifeng Wu, Jianwei Wang, Hua Bai and Lei Li, Electrochemical supercapacitor with polymeric active electrolyte, J. Mater. Chem. A, 2014, 2, 10526–10531.

[29] Libin Chen, Hua Bai, Zhifeng Huang and Lei Li, Mechanism investigation and suppression of self-discharge in active electrolyte enhanced supercapacitors, Energy Environ. Sci., 2014, 7, 1750–1759.

[30] Guofu Ma, Jiajia Li, Kanjun Sun, Hui Peng, Jingjing Mu, Ziqiang Lei, High performance solid-state supercapacitor with PVA-KOH-K3[Fe(CN)6] gel polymer as electrolyte and separator, Journal of Power Sources 256 (2014) 281-287.

[31] Cheng Zhou and Jinping Liu, Carbon nanotube network film directly grown on carbon cloth for high performance solid state flexible supercapacitors, Nanotechnology 25 (2014) 035402 (8pp).

[32] Yuxi Xu , Zhaoyang Lin , Xiaoqing Huang , Yang Wang , Yu Huang , and Xiangfeng Duan, Functionalized Graphene Hydrogel-Based High- Performance Supercapacitors, Adv. Mater. 2013, 25, 5779–5784.

[33] Guoji Huang, ChengyiHou, YuanlongShao, BingjieZhu, Baoping Jia, Hongzhi Wang, Qinghong Zhang, Yaogang Li, High-performance all-solid-state yarn supercapacitors based on porous grapheme ribbons, Nano Energy(2015) 12, 26–32.

[34] Hong-Fei Ju, Wei-Li Song and Li-Zhen Fan, Rational design of graphene/porous carbon aerogels for high-performance flexible all-solid state supercapacitors, J. Mater. Chem. A, 2014, 2, 10895–10903.

[35] C. Muhamed Ashraf, K. M. Anilkumar, B. Jinisha, M. Manoj, V. S. Pradeep, S. Jayalekshmi, AcidWashed, Steam Activated, Coconut Shell Derived Carbon for High Power Supercapacitor Applications, Journal of The Electrochemical Society, 165 (5) A900-A909 (2018).

[36] B. Jinisha , K. M. Anilkumar, M. Manoj, A. Abhilash, V. S. Pradeep, S. Jayalekshmi, Poly (ethylene oxide) (PEO)-based, sodium ion-conducting, solid polymer electrolyte films, dispersed with Al2O3 filler, for applications in sodium ion cells, Ionics https://doi.org/10.1007/s11581-017-2332-2, 2017.

[37] R. Kötz, M. Carlen, Principles and applications of electrochemical capacitors, Electrochim. Acta 45 (2000) 2483-2498.

[38] C. Meng, C. Liu, L. Chen, C. Hu, S. Fan, Highly Flexible and All-Solid-State Paperlike Polymer Supercapacitors Nano Lett. 10 (2010) 4025-4031.

[39] MANAS MANDAL, DEBASIS GHOSH, KRISHNA CHATTOPADHYAY, and CHAPAL KUMAR DAS, A Novel Asymmetric Supercapacitor Designed with Mn3O4@Multi-wall Carbon Nanotube Nanocomposite and Reduced Graphene Oxide Electrodes, Journal of ELECTRONIC MATERIALS, Vol. 45, No. 7, 2016, DOI: 10.1007/s11664-016-4493-6.

[40] Mengjin Jiang, Jiadeng Zhu, Chen Chen, Yao Lu, Yeqian Ge, Xiangwu Zhang, Poly(vinyl Alcohol) Borate Gel Polymer Electrolytes Prepared by Electrodeposition and Their Application in Electrochemical Supercapacitors, ACS Appl. Mater. Interfaces 2016, 8, 3473−3481.

[41] Chun-Chen Yang, Chemical composition and XRD analyses for alkaline composite PVA polymer electrolyte, Materials Letters 58 (2003) 33– 38.

[42] Lidan Fan, Juan Chen, Gang Qin, Libo Wang, Xiaoyi Hu, Zhongshuo Shen, Preparation of PVA-KOH-Halloysite Nanotube Alkaline Solid Polymer Electrolyte and its Application in Ni-MH Battery, Int. J. Electrochem. Sci., 12 (2017) 5142 – 5156.

[43] Haijun Yu, Jihuai Wu, Leqing Fan, Youzhen Lin, Kaiqing Xu, Ziying Tang, Cunxi Cheng, Shen Tang, Jianming Lin, Miaoliang Huang, Zhang Lan, A novel redox-mediated gel polymer electrolyte for high-performance supercapacitor, Journal of Power Sources 198 (2012) 402– 407.

[44] P. Jannasch, Polymer 42 (2001) 8629-8635.

[45] B. E. Conway, V. Birss, J. Wojtowic, The role and utilization of pseudocapacitance for energy storage by supercapacitors, J. Power Sources 66 (1997) 1-14.

[46] Hajime Wada, Kumiko Yoshikawa, Shinji Nohara, Naoji Furukawa, Hiroshi Inoue, Nozomu Sugoh, Hideharu Iwasaki, Chiaki Iwakura, Electrochemical characteristics of new electric double layer capacitor with acidic polymer hydrogel electrolyte, Journal of Power Sources 159 (2006) 1464–1467.

Chapter 7

Summary, conclusions and scope for further studies

A summary of the results of the work presented in the thesis and the conclusions arrived at are dealt with, in this chapter. The scope for further investigations based on the present studies is also highlighted.

7.1 Summary and conclusions

The work presented in the thesis is centred on the studies on solid and gel polymer electrolytes (SPEs and GPEs) for developing the next generation all solid state rechargeable batteries and supercapacitors. The prime objective of the work is to evaluate the electrochemical properties of SPEs and GPEs to assess their application prospects in rechargeable cells and supercapacitors and to understand in detail the lithium transport mechanism. Safety is another important criterion to be addressed in energy storage systems, since conventional liquid electrolytes have many inherent problems related to safety issues. The possibilities of leakage of the liquid electrolytes and short circuits inside the cells during operation are the main concerns to be eliminated. Solid polymer electrolytes are considered as excellent alternatives to their liquid counterparts and their applications in electrochemical cells enhance the safety aspects and offer flexibility in the design of the cell geometry.

The possibility of having safe, durable and liquid free cells is one of the main advantages of using solid electrolytes. However, the solid type and the gel type polymer electrolytes face limitations due to lesser ionic conductivity in comparison with conventional liquid electrolytes. The prime objective of the work presented in the thesis is to propose strategies for the identification of potential materials for developing solid polymer electrolytes with enhanced ionic conductivity for applications in emerging energy storage devices such as all solid state lithium and sodium based cells, and supercapacitors. The highlight of the present studies is the development of SPE films based on the PEO/PVP polymer blend, treated with $LiNO_3$, with ionic conductivity around $1.13x10^{-3}$ S/cm, which is close to that of liquid electrolytes. These SPE films are free standing and highly flexible and have excellent thermal stability above 400 ^oC. They can be of potential applications in the development of all solid state Li ion cells, using these SPEs serving as the solid electrolyte and the separator, with high flexibility in the shape and the size of the cells. Solid state lithium ion half cells with open circuit voltages of 3V and 5V, assembled using these SPEs show promising performance characteristics. Solid supercapacitors have also been assembled using the gel polymer electrolyte film based on the PVA-KOH-HQ system, serving as the electrolyte and the separator and activated carbon as the electrodes.

The work presented in the thesis starts with the studies on the SPE films based on the polymer blend of PEO and PVdF, treated with $LiNO_3$ as the lithium source. The simple technique of solution casting is used to obtain free standing, highly flexible and transparent SPE films

with moderate Li ion conductivity, good thermal stability and appreciable electrochemical activity suitable for applications in all solid state Li ion cells. The XRD studies and the FTIR spectroscopic analysis confirm the lowering of crystalline nature with higher amount of lithium nitrate in the polymer blend and the complex formation of lithium nitrate with the polymer blend. The smooth and porous nature of the SPE film surface enhances the mobility of ion transport and the maximum ionic conductivity of 8.245 $x10^{-5}$ S cm^{-1} is obtained with 10 weight % of lithium nitrate in the polymer blend. These SPE films are electrochemically stable up to 4V versus Li. The present investigations have unveiled that the PEO-PVdF-$LiNO_3$ based SPE films are interesting materials with good application prospects in the field of solid state devices and their promising electrochemical properties are connected with their complex amorphous nanostructure.

The second study introduces the unique type of SPE films based on lithium enriched PEO-PVP polymer blend. The SPE films based on the PEO-PVP blend, treated with $LiNO_3$ as the lithium source are also grown as free standing, transparent and highly flexible films by solution casting method. In comparison with the previous work, PVP is used instead of PVdF to make the polymer blend with the semi-crystalline and rigid polymer, PEO. The amorphous nature of PVP is expected to improve the flexible nature of the PEO-PVP blend system, which in turn can facilitate better Li ion transport through the resulting SPE film.As mentioned earlier, these SPE films are found to exhibit excellent thermal stability above 400 °C, maximum room temperature ionic conductivity around 1.13×10^{-3} S cm^{-1}, wide electrochemical stability

window above 4.8V and are endowed with excellent electrochemical characteristics. These flexible and free standing SPE films with room temperature ionic conductivity close to that of liquid electrolytes and laudable electrochemical characteristics offer high application prospectus in the design of all solid state Li-ion cells.

The next study deals with the assembling of two solid state Li ion cells with the PEO-PVP-$LiNO_3$ based solid polymer electrolyte film serving as both the electrolyte and the separator. Cells have been assembled with two different cathode materials, $LiFePO_4$ and $LiNi_{0.5}Mn_{1.5}O_4$ to give open circuit voltages of 3V and 5 V respectively, using Li metal foil as the anode. The cathode materials are synthesized by sol-gel technique and are characterised structurally and morphologically using the XRD and the FE-SEM techniques. The performance of the half-cells assembled using $LiFePO_4$ and $LiNi_{0.5}Mn_{1.5}O_4$ cathodes and the SPE film is assessed electrochemically using the CV and the GCD techniques. Although the initial discharge capacity values and the nature of the CV curves are promising, the capacity fading with increase in the number of charge-discharge cycles is large. There are many challenges to be addressed to achieve good capacity retention over larger number of cycles. The synthesis conditions of the cathode materials have to be optimised to get particle size in the 10-20 nm range and homogeneous particle size distribution to achieve improvement in the cell performance. As an initial attempt, the present results are promising which offer ample scope for developing high voltage, all solid state Li ion cells.

The next part of the research work deals with the studies on the solid polymer electrolyte (SPE) films, based on the polymer blend of PEO and the plasticizers EC and PC and complexed with $NaNO_3$, and modified with the addition of the nano-filler material Al_2O_3. These free standing, flexible and transparent SPE films, obtained by solution casting technique have good thermal stability upto 400° C as seen from the thermal studies. The XRD studies establish the reduced crystalline nature of these SPE films, due to the complex formation with the sodium salt and the presence of the plasticizers and the filler material.. Easier ion transport is promoted by the enhanced amorphous nature of the SPE films which in turn leads to high Na ion conductivity. The complex formation between the PEO based polymer blend and $NaNO_3$ can be ascertained on the basis of the FTIR spectroscopy studies. The FESEM analysis gives clear evidence for the smoother and porous surface morphology of the SPE films. The most fascinating aspect of the present studies is regarding the marvellous effect of the Al_2O_3 filler, in enhancing the ionic conductivity of the SPE films substantially and bringing it to around 1.86×10^{-4} S cm^{-1}. The high room temperature ionic conductivity and the electrochemical stability window up to 4V, coupled with the excellent thermal stability of these SPE films are suitable for developing all solid state Na ion cells, capable of stable operation at temperatures much above room temperature.

The last part of the research work deals with the assembling of solid-state supercapacitors with activated carbon as electrodes and the redox mediated poly (vinyl alcohol)-pottassium hydroxide-hydroquinone (PVA-KOH-HQ) gel polymer electrolyte film serving as the electrolyte

and the separator. Maximum ionic conductivity of 53 mS cm^{-1} has been obtained for these GPE films with HQ concentration of 0.2g. The 1 V electrochemical potential window with repeatability is another important property of these GPE films. Solid state supercapacitors assembled using activated carbon as electrodes and the GPE film serving the purpose of the electrolyte and the separator are found to deliver high electrode specific capacitance of 326.53 F g^{-1}, energy density of 33.15 Wh kg^{-1} and power density of 689.58 W kg^{-1} when cycled at a current density of 0.8 A g^{-1}.Another remarkable result is the observation that 84.2% of the initial capacitance is retained after subjecting these solid-state supercapacitors to 1000 charge-discharge cycles. It can be concluded from the electrochemical analysis that the presence of the redox mediator HQ in the GPE films can significantly influence the electrochemical performance of the solid-state supercapacitors by enhancing their ionic conductivity and the pseudocapacitance. Redox mediators have high application prospects in improving the performance of energy storage devices. The GPE films of the present work can be considered as interesting candidates for the development of all solid state supercapacitors with enhanced capacitance, excellent cycling stability and good safety standards.

7.2 Future prospects

The results of the present investigations offer plenty of scope for further studies to improve the performance of the materials and devices developed in the present work.

1) Identification and development of nanostructured cathode materials to design all solid state Li ion half cells with good capacity retention over large number charge-discharge cycles.
2) Focussing more on the practical application of the three types of the SPE films developed, attempts have been initiated for assembling all solid state, Li ion and sodium ion full cells using cost effective and eco-friendly cathodes and suitable anode materials.
3) Development of different electrode materials based on metal oxides and conducting polymers and GPE films for designing high power solid- state supercapacitors.